

University of Alberta

The role of Programmed Death-1 (PD-1) expression in the negative
selection of T lymphocytes

by

Julia Catherine Parkman

A thesis submitted to the Faculty of Graduate Studies and Research
in partial fulfillment of the requirements for the degree of

Master of Science

in

Immunology

Medical Microbiology and Immunology

©Julia Catherine Parkman

Spring 2011

Edmonton, Alberta

Permission is hereby granted to the University of Alberta Libraries to reproduce single copies of this thesis and to lend or sell such copies for private, scholarly or scientific research purposes only. Where the thesis is converted to, or otherwise made available in digital form, the University of Alberta will advise potential users of the thesis of these terms.

The author reserves all other publication and other rights in association with the copyright in the thesis and, except as herein before provided, neither the thesis nor any substantial portion thereof may be printed or otherwise reproduced in any material form whatsoever without the author's prior written permission.

Examining Committee

Troy A. Baldwin, Medical Microbiology and Immunology

Hanne L. Ostergaard, Medical Microbiology and Immunology

Colin C. Anderson, Surgery

Robert Ingham, Medical Microbiology and Immunology

Abstract

The immune system must be able to mount a response against pathogens and transformed cells while remaining tolerant to healthy host tissue. A key process for ensuring this self-tolerance is the negative selection of self-reactive thymocytes. Expression of Programmed Death-1 (PD-1), a co-inhibitory member of the CD28 family associated with dampened peripheral immune responses, was found to be upregulated in 20-40% of thymocytes undergoing negative selection in the HY^{cd4} model of thymic development. Although analysis of gene and protein expression directly *ex vivo* indicates that PD-1⁻ and PD-1⁺ thymocytes are equally apoptotic, PD-1⁺ thymocytes appear to be protected from apoptosis in an *in vitro* stimulation assay. Analysis of HY^{cd4}PD-1^{-/-} mice indicates that thymocytes receive a higher intensity signal in the absence of PD-1. Future work utilizing HY^{cd4}PD-1^{-/-} mice will increase our understanding of the role of PD-1 in thymic negative selection.

Acknowledgements

I would like to thank my supervisor, Dr. Troy Baldwin, for his support over the past few years. I also want to thank my committee members, Dr. Hanne Ostergaard and Dr. Colin Anderson, for their guidance and encouragement. Additionally, I wish to acknowledge the technical and emotional support I received from the members of the Baldwin Lab: Nancy Hu, Alyssa Sader, Dominic Golec, Stephanie Nicol, Alex Suen, and Bing Zhang. I would also like to thank Dr. Robert Ingham for his helpful suggestions and Dorothy Kratochwil-Otto for technical assistance. Finally, I want to thank Dr. Judy Gnarpe, the rest of the staff and students in MMI, and my family and friends for their encouragement.

Table of Contents

Chapter 1: Introduction.....	1
Early T cell development.....	2
Entering the thymus.....	2
Progressing through DN1-DN4: across the thymus and back.....	8
DN1.....	9
DN2.....	10
DN3.....	11
DN4.....	12
DP.....	12
Differential MAPK signaling in positive and negative selection.....	13
Positive selection.....	14
CD4/CD8 commitment decision.....	15
CD4SP and CD8SP.....	19
Exiting the thymus.....	20
Negative selection.....	21
The roles of different thymic APCs in negative selection.....	24
mTECs.....	24
cTECs.....	25
DCs.....	25
Models of negative selection.....	27

Programmed Death-1 (PD-1).....	32
Chapter 2: Materials and Methods.....	37
Mice.....	37
Flow cytometry.....	37
Cell surface staining.....	37
Intracellular staining.....	38
Cell Sorting.....	39
pERK staining.....	39
Quantitative reverse-transcriptase PCR.....	40
Western Blot.....	41
Generation of bone marrow-derived DCs.....	42
<i>In vitro</i> stimulation assay.....	42
Bone marrow chimeras.....	43
T cell depletion.....	43
HY ^{cd4} PD-1 ^{-/-} mixed BM chimeras.....	43
Restriction of high antigen-presentation to cTECs.....	44
Restriction of antigen-presentation to hematopoietically derived cells.....	44
Statistical analysis.....	44
Chapter 3: Results.....	45
Characterization of the HY ^{cd4} model of thymic selection.....	45

Thymus.....	45
Spleen.....	50
PD-1 is upregulated in the HY ^{cd4} M model of negative selection.....	55
Comparison of gene expression profiles of PD-1 ⁺ and PD-1 ⁻ thymocytes examined directly <i>ex vivo</i>	59
Expression of proteins associated with apoptosis in PD-1 ⁺ and PD-1 ⁻ thymocytes examined directly <i>ex vivo</i>	74
<i>In vitro</i> stimulation of PD-1 ⁻ and PD-1 ⁺ thymocytes.....	79
Evaluation of factors that may protect PD-1 ⁺ thymocytes from apoptosis.....	91
Cbl-2.....	91
Egr-2.....	94
Dgk α	94
pERK.....	96
Characterization of HY ^{cd4} PD-1 deficient mice.....	98
Thymus	98
Spleen.....	110
<i>In vitro</i> stimulation of thymocytes from PD-1 deficient mice.....	114
HY ^{cd4} PD-1 ^{-/-} mixed BM chimeras.....	116
Characterization of chimeras in which high-affinity antigen presentation is restriction to either hematopoietically derived cells or TECs.....	119

Chapter 4: Discussion.....	124
Peripheral T3.70 ⁺ T cells in the HY ^{cd4} male and female mouse.....	124
Gene expression profiles of PD-1 ⁻ and PD-1 ⁺ thymocytes.....	127
Mechanism of negative selection of PD-1 ⁺ thymocytes.....	129
HY ^{cd4} PD-1 deficient mice.....	132
Antigen-presentation restricted chimeras.....	133
Literature Cited.....	135
Appendix I.....	164
Appendix II.....	186

List of Tables

Table 1-1: Phenotypes of progenitor cells at different stages of
differentiation.....6

List of Figures

Figure 1-1: Movement of thymocytes within the thymus.....	4
Figure 1-2: The kinetic signaling model of CD4/CD8 lineage commitment.....	18
Figure 1-3: Bim and Nur77 are mediators of clonal deletion.....	23
Figure 1-4: Many TCR-transgenic mice express an inappropriately timed TCR α chain.....	29
Figure 1-5: Generation of the HY ^{cd4} model.....	31
Figure 1-6: PD-1 is an inhibitor receptor containing an ITIM and an ITSM in its cytoplasmic tail.....	35
Figure 3-1: The HY ^{cd4} model of thymic selection: thymus.....	48
Figure 3-2: The HY ^{cd4} model of thymic selection: spleen.....	52
Figure 3-3: Relative proportions of naïve, effector memory, and central memory splenic T cells in the HY ^{cd4} model.....	54
Figure 3-4: PD-1 expression in HY ^{cd4} F and M thymocytes.....	57
Figure 3-5: Cell sorting prior to RNA extraction.....	61
Figure 3-6: Comparison of Bim, Nur77, Gadd45 β , and zfp52 gene expression between T3.70 ⁺ CD69 ⁻ HY ^{cd4} D ^{b/-} DP, T3.70 ⁺ CD69 ⁺ HY ^{cd4} F DP, T3.70 ⁺ CD69 ⁺ HY ^{cd4} M DP, T3.70 ⁺ HY ^{cd4} M DP PD-1 ⁻ , T3.70 ⁺ HY ^{cd4} M DP PD-1 ⁺ , and T3.70 ⁺ CD69 ⁺ HY ^{cd4} F SP8 populations.....	67
Figure 3-7: Comparison of 2610019F03Rik, Runx3, CCR7, and KLF2 gene expression between T3.70 ⁺ CD69 ⁻ HY ^{cd4} D ^{b/-}	

DP, T3.70 ⁺ CD69 ⁺ HY ^{cd4} F DP, T3.70 ⁺ CD69 ⁺ HY ^{cd4} M	
DP, T3.70 ⁺ HY ^{cd4} M DP PD-1 ⁻ ,T3.70 ⁺ HY ^{cd4} M	
DP PD-1 ⁺ , and T3.70 ⁺ CD69 ⁺ HY ^{cd4} F SP8 populations.....	71
Figure 3-8: Expression of Bim, Nur77, and Bcl-2.....	76
Figure 3-9: Levels of cleaved caspase 3.....	78
Figure 3-10: Phenotyping of B6 splenocytes.....	80
Figure 3-11: <i>In vitro</i> simulation of HY ^{cd4} M and HY ^{cd4} F thymocytes	
with B6 splenocytes pulsed at indicated concentrations of smcy.....	82
Figure 3-12: DCs generated from BM are of myeloid lineage and	
express PD-L1 and PD-L2.....	86
Figure 3-13: Phenotyping of BM-derived DCs.....	87
Figure 3-14: <i>In vitro</i> simulation of HY ^{cd4} M and HY ^{cd4} F thymocytes	
with BM-derived DCs at indicated concentrations of smcy.....	89
Figure 3-15: No difference in Cbl-b expression between PD-1 ⁻ and PD-1 ⁺	
thymocytes.....	93
Figure 3-16: No difference in Egr-2 or Dgk α expression between PD-1 ⁻	
and PD-1 ⁺ thymocytes.....	95
Figure 3-17: No difference in pERK expression between PD-1 ⁻ and PD-1 ⁺	
thymocytes.....	97
Figure 3-18: PD-1 deficiency does not impair negative selection.....	100
Figure 3-19: T3.70 ⁺ HY ^{cd4} M DP thymocytes express slightly	
higher levels of activation markers.....	102
Figure 3-20: T3.70 ⁺ HY ^{cd4} M DP PD-1 ⁻ thymocytes still express	

low levels of PD-1.....	104
Figure 3-21: Similar levels of pro-apoptotic proteins in PD-1 sufficient and PD-1 deficient DP thymocytes.....	107
Figure 3-22: Similar levels of cleaved caspase 3 in PD-1 sufficient and PD-1 deficient DP thymocytes.....	109
Figure 3-23: Similar numbers of T3.70 ⁺ CD8 ⁺ T cells in spleens of PD-1 deficient and sufficient mice.....	111
Figure 3-24: Similar proportions of naïve, effector memory, and central memory T3.70 ⁺ CD8 ⁺ T cells in HY ^{cd4} M and HY ^{cd4} M PD-1 ^{-/-} spleens.....	113
Figure 3-25: <i>In vitro</i> simulation of thymocytes from PD-1 sufficient and deficient mice with BM-derived DCs at indicated concentrations of smcy.....	115
Figure 3-26: Low frequency HY ^{cd4} PD-1 ^{-/-} mixed BM chimeras.....	117
Figure 3-27: Restriction of male antigen presentation to thymic epithelial cells or to hematopoietically derived cells.....	121
Figure 4-1: NFAT signaling is associated with anergy induction.....	131

List of Abbreviations

AIDS = acquired immunodeficiency syndrome

AIRE = autoimmune regulator

APC = antigen presenting cell

B6 = C57BL/6

Bcl-2 = B cell lymphoma 2

BCR = B cell receptor

BH3 = Bcl-2 homology-3

Bim = Bcl-2-interacting mediator of cell death

BM = bone marrow

BrdU = 5-bromo-2-deoxyuridine

Cbl-b = Casitas B-cell lymphoma-b

CCL / CXCL = chemokine ligand

CCR = chemokine receptor

CD = cluster of differentiation

cDC = cortical dendritic cell

CFSE = carboxyfluorescein diacetate succinimidyl ester

CLP = common lymphoid progenitors

CMJ = cortical-medullary junction

cTEC = cortical thymic epithelial cell

DC = dendritic cell

Dgk α = diacylglycerol kinase alpha

Dll4 = Delta-like 4

DN = double negative

DP = double positive

Egr-2 = early growth response gene

ELPs= Early lymphoid progenitors

ERK = extracellular signal-regulated kinase

ETPs = Early thymic progenitors

FACS = Fluorescence-activated cell sorting

FBS = fetal bovine serum

FADD = Fas/APO-1-associated death domain

Flt3= fms-like tyrosine kinase receptor-3

Gadd45 β = growth arrest and DNA damage 45 beta

GATA-3 = GATA-binding protein 3

GM-CSF= granulocyte-macrophage colony-stimulating factor

GPCR= G α i protein coupled receptor

HBSS = Hank's Balanced Salt Solution

HRP = horseradish peroxidase

HSA = heat shock antigen

HSCs = hematopoietic stem cells

ICAM-1= Intercellular adhesion molecule

IL= Interleukin

ITIM = immunoreceptor tyrosine based inhibitory motif

ITSM = immunoreceptor tyrosine based switch motif

JNK = Jun N-terminal kinase

KLF2 = Kruppel-like factor 2

LN = lymph node

MAPK = Mitogen-activated protein kinase

MFI = mean fluorescence intensity

MHC = Major Histocompatibility Complex

MORT1 = mediator of receptor-induced toxicity-1

MPPs= multipotent progenitors

mTEC = medullary thymic epithelial cell

NFAT = nuclear factor of activated T cells

NK = nature killer cell

PBS = phosphate buffered saline

pERK = phosphorylated extracellular signal-regulated kinase

PMA = phorbol 12-myristate 13-acetate

PMC = perimedullary cortex

PD-1 = Programmed Death 1

PKC θ = protein kinase C theta

PSGL-1 = P-selectin glycoprotein-1

RAG = recombination-activating gene

RT = room temperature

RTE = recent thymic emigrants

RT-PCR = reverse transcriptase polymerase chain reaction

Runx = runt-related transcription factor

Sirp α = signal regulatory protein alpha

SCF = stem cell factor

SCZ= subcapsular zone

SCID = severe combined immunodeficiency

S1P= sphingosine 1-phosphate

SP = single positive

SNP = single nucleotide polymorphism

STAT5 = signal transducer and activator of transcription 5

TCR = T cell receptor

TEC = thymic epithelial cell

ThPOK= T-helper inducing POZ/Kruppel-like factor

TRA = tissue restricted antigen

V(D)J = variable (diversity) joining

VCAM-1 = vascular cell adhesion molecule 1

ZAP-70 = zeta-chain-associated protein kinase 70

Zfp52 = zinc finger protein 52

Chapter 1: Introduction

The human body must constantly fight off pathogens such as bacteria and viruses, as well as cancer. A robust immune system is essential for protection against these threats to health. The importance of a functioning immune system is illustrated by the frequency and severity of disease that occurs in individuals with either a genetic immunodeficiency, such as severe combined immunodeficiency (SCID), or acquired immunodeficiency, such as acquired immunodeficiency syndrome (AIDS) (1, 2). Co-operation is important in the immune system. The mammalian immune system can be broadly divided into an innate arm and an adaptive arm. The innate immune system reacts first to an infection; within the first few days it works to control the pathogen while alerting cells involved in the adaptive immune response (3). The innate system consists of physical and chemical barriers to infection and also has a cellular component. Phagocytes such as neutrophils, macrophages, and dendritic cells (DCs) are adept at engulfing foreign material and presenting it to adaptive immune cells (3), while Natural Killer (NK) cells target self-cells with decreased expression of Major Histocompatibility Complex (MHC) Class I resulting from viral infection, or altered-self cells expressing molecules induced by stress or transformation (4). The adaptive branch of the immune system is different from the innate branch in that it is specific and exhibits memory (3). The adaptive immune system involves B and T lymphocytes (also known as B and T cells) that recognize antigen via their clonal antigen receptors, the B cell receptor (BCR) or T cell receptor (TCR), respectively

(3). T cells recognize this antigen in the context of MHC on antigen presenting cells (APCs), and with additional co-stimulation from cell surface proteins, are activated and proceed to fight the infection (3).

Progenitors of both B cells and T cells originate in the bone marrow (BM) (3). B cell maturation continues in the bone marrow while T cell progenitors migrate to the thymus where T cell maturation takes place (3). It is essential that T cells recognize antigen in the context of MHC and can distinguish between healthy host cells and pathogen infected or transformed cells. These important characteristics are accomplished through positive and negative selection during T cell development in the thymus.

Early T cell development

Entering the thymus

The thymus continually produces T cells throughout life but does not contain a resident stem cell population (5). Therefore, thymocyte progenitors must be recruited from the blood. T cell progenitors migrate from the BM through the blood to the thymus. The thymus consists of an inner medulla and an outer cortex and the area between the medulla and cortex is known as the cortical-medullary junction (CMJ) (**Fig 1-1**). By injecting carboxyfluorescein diacetate succinimidyl

ester (CFSE) labeled, lineage negative bone marrow cells into non-irradiated recipients, it was established that thymocytes progenitors enter the CMJ (6).

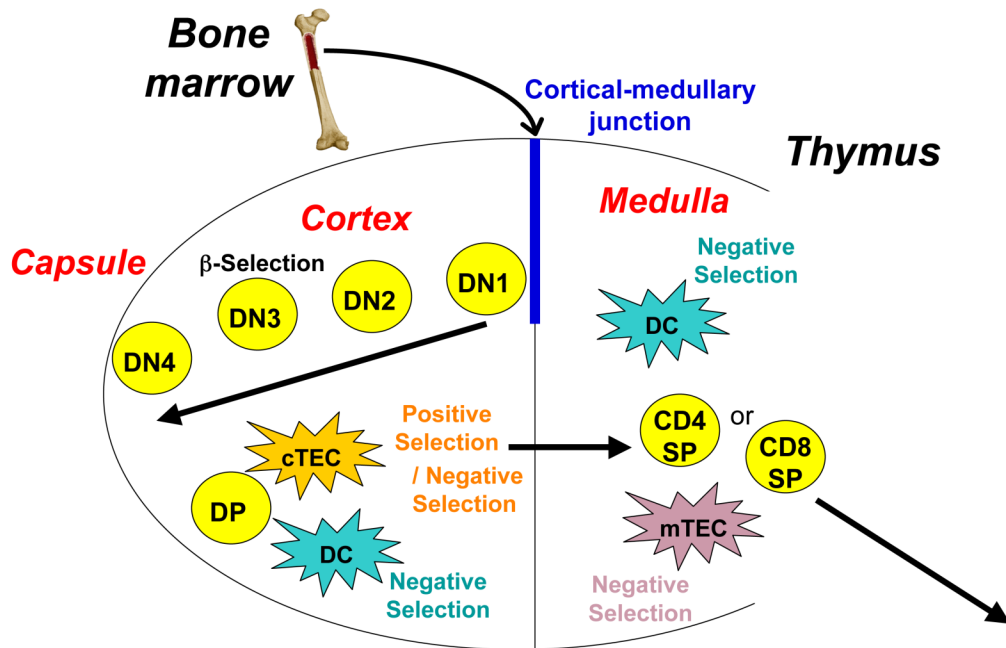


Figure 1-1: Movement of thymocytes within the thymus. T cell progenitors enter the thymus at the cortical-medullary junction (CMJ). They then migrate towards the capsule as they mature from (double negative) (DN)1 to DN4. At the DN4 stage the thymocytes move back through the cortex and enter the medulla. Both positive selection, which is mediated by radioresistant cortical thymic epithelial cells (cTECs), and negative selection, which may be mediated by cTECs, medullary thymic epithelial cells (mTECs), or dendritic cells, can occur at the DP stage. Following positive selection the thymocyte commits to either the CD4 helper lineage or the CD8 cytotoxic lineage, and the single positive (SP) thymocyte follows a sphingosine-1-phosphate (S1P) gradient out of the thymus.

The exact progenitor cell type settling the thymus is controversial. All blood cell lines are derived from self-renewing hematopoietic stem cells (HSCs), which develop into multipotent progenitors (MPPs) (7). These MPPs can give rise to all blood cell lines but lack the ability to self-renew (**Table 1-1**). Early lymphoid progenitors (ELPs) develop from MPPs and can develop into common lymphoid progenitors (CLPs) and the further differentiated CLP-2 (7). To determine the progenitor cell type that seeds the thymus, progenitor cells at different stages of development were injected into nonirradiated mice. Using this type of protocol it was found that CLPs and a subset of cells classified as MPPs (that were later reclassified as ELPs) can enter the thymus whereas HSCs cannot (8). Although previous studies (9, 10) using irradiated recipients showed that HSCs can seed the thymus, this recruitment was likely not physiological as side effects of irradiation include vascular damage and increased expression of cytokines and chemokines (11). Thus, it is currently thought that ELPs, CLPs, and CLP-2s are the cell types that can home to the thymus.

Table 1-1: Phenotypes of progenitor cells at different stages of differentiation.

Cell type	Phenotype	Ability to seed thymus?
Hematopoietic stem cell (HSC)	Flt3 ⁻ Lin ⁻ Sca-1 ⁺ Kit ⁺	No
Multipotent progenitor (MPP)	Flt3 ^{low} Lin ⁻ Sca-1 ⁺ Kit ⁺	No
Early lymphoid progenitor (ELP)	Flt3 ^{hi} Lin ⁻ Sca-1 ⁺ Kit ⁺	Yes
Common lymphoid progenitor (CLP) and CLP-2	Flt3 ⁺ Lin ⁻ IL7R ^{hi} Sca-1 ^{low} Kit ^{low}	Yes

The molecules and signals involved in progenitor recruitment from the blood are still being elucidated although many potential factors have been identified including selectins, integrins, chemokines, and CD44. Selectins are C-type lectins that bind glycoproteins and glycolipids, and it is thought that progenitors utilize selectin-mediated interactions to enter the thymus similar to what is observed with T cells entering other tissues (12). In support of this hypothesis, immunofluorescence staining has revealed that P-selectin is expressed by endothelial and perivascular cells in the thymus, while flow cytometry staining with a P-selectin immunoglobulin fusion protein showed that its ligand, P-selectin glycoprotein-1 (PSGL-1), is found on thymic progenitors (13). Additionally, in mice deficient in either P-selectin or PSGL-1, or following the administration of anti-P-selectin blocking antibodies, a decrease in thymic homing is observed (13, 14). Integrins have also been reported to be involved in thymic entry. Anti- α 4, anti- α 6, and anti- β 2 blocking antibodies decrease homing to the thymus (14, 15). In addition, α 4 β 1/ β 7 ligands, including VCAM-1, as well as the ligand for α L β 2, ICAM-1, are found on endothelial cells and antibodies blocking these ligands decrease progenitor homing to the thymus (14, 16). Many chemokine receptors have been implicated in homing. The cells that first enter the thymus after sub-lethal irradiation have increased expression of CXCR4 and CCR5, and it has been shown that CXCR4 and CCR5 deficiency results in decreased homing (17). A blocking anti-CCL25 antibody also decreases homing, indicating that CCR9/CCL25 interactions are important for recruitment (14). Although CCR9 deficiency alone does not appear to affect thymic homing, a defect was observed

when CCR9^{-/-} BM was compared to wildtype BM in a mixed BM chimera experiment (18). It has also been shown that CCR7^{-/-}CCR9^{-/-} mice exhibit severe defects in homing, indicating that CCR7 and CCR9 can compensate for each other (19, 20). Since integrins are activated by Gαi protein coupled receptor (GPCR) signaling, and chemokine receptors are GPCRs, it is unclear if the role of chemokines is to allow integrin binding or if they are directly involved in recruitment from the blood (21). Finally, it has been demonstrated that anti-CD44 blocking antibodies decrease homing to thymus (22). Therefore, there appears to be a number of different cell surface receptors and ligands that are important for progenitor entry into the thymus, but it is unclear whether they all operate at the same time or under certain experimental conditions.

Progressing through DN1-DN4: across the thymus and back

Thymus-settling progenitors lack both the CD4 and CD8 co-receptors and are therefore referred to as double negative (DN) thymocytes. DN thymocytes can be further divided into four development stages based on cell surface markers and their location in the thymus: DN1 (CD44⁺CD25⁻), DN2 (CD44⁺CD25⁺), DN3 (CD44⁻CD25⁺), and DN4 (CD44⁻CD25⁻) (23). In general, thymocytes begin their development at the CMJ, move out towards the capsule and then back towards the medulla. Both interactions with stromal cells and chemokine gradients are important for directing migration. Interestingly, while mutations in chemokines or their receptors lead to changes in localization within the thymus, thymic development appears to occur normally. This may be due to

chemokine/chemokine receptor redundancy, as sometimes defects become apparent through competition experiments (18, 24, 25). Alternatively, a recent study examining gene expression of thymic stromal cells did not find distinct expression profiles of chemokines (or any other genes) in the central cortex, suggesting that the central cortex may not provide specific signals to developing thymocytes (26).

DN1

DN1 thymocytes proliferate, further commit to the T lineage, and migrate towards the capsule. The DN1 stage is an extremely heterogeneous cell population and can be further divided into five sub-stages (DN1a – DN1e) based on expression of CD117 (c-kit) and CD24 (27). The true early thymic progenitors (ETPs) are considered to be the DN1a cells, which are CD117⁺ and CD24⁻ (27). DN1 cells undergo proliferation before being asynchronously released from the perimedullary cortex (PMC) region to continue their development (28). It is currently unclear which molecules are important for DN1 proliferation, however, stem cell factor and other cytokines are likely important. Mice deficient in both stem cell factor and the common cytokine receptor gamma chain have significantly decreased DN1 thymocyte numbers (29).

While DN1 thymocytes continue their commitment to the T cell lineage, they still retain the ability to differentiate into non-T lineage cells, including B cells, DCs, and NK cells. Notch signaling throughout the DN stage is required to restrict

lineage potential and ensure T cell lineage commitment (30). Notch1 expressed on DN thymocytes interacts with Delta-like 4 (Dll4) on thymic stromal cells. When Dll4 is absent T cell development is impaired and an increased presence of B cells in the thymus is observed (31, 32).

It has been estimated that DN1s reside in the PMC for approximately ten days (28). Chemokines have been shown to be important molecules for the trafficking of DN1 thymocytes from the PMC towards the capsule. Two chemokine/chemokine receptor pairs implicated in this migration include CCL19 and its receptor CCR7 and CXCL12 and its receptor CXCR4. CCL19 is expressed on stromal cells in the CMJ, cortex, and medulla, while CXCL12 is only expressed on cortical stromal cells. CCR7 is expressed in late DN1 stage and CXCR4 is expressed on DN1-DN4 and on DP thymocytes (25, 33). Mutations in CXCR4 or CCR7 (or their ligands), results in a DN1 developmental block and the accumulation of DN1 thymocytes in the PMC (24, 25, 33). Collectively, these data provide strong support for the role of CCR7 and CXCR4 in directing migration of DN1 towards the capsule.

DN2

DN1 cells become DN2 cells ($CD24^+CD25^+CD44^+CD117^+$) as they enter the inner cortex. DN2 cells continue to proliferate with the help of interleukin (IL)-7 and stem cell factor (SCF). The DN2 stage is relatively transient and has been shown to last for about two days (28). Expression of recombination-activating

gene (RAG) -1 and RAG-2 is upregulated at the DN2 stage (34). RAG-1 and RAG-2 are part of the variable (diversity) joining (V(D)J) recombinase, the enzyme complex which mediates recombination of TCR α , β , γ , and δ loci. Recombination of the TCR γ , TCR δ , and TCR β loci begins at the DN2 stage and is completed at the DN3 stage (35, 36). It has been demonstrated that IL-7 signaling allows the access to the TCR γ gene locus (37). Although DN2 cells still have the potential to develop into other lineages, such as NK and DC, continued signaling through Notch inhibits B cell potential and promotes progenitor survival (30). DN2 cells continue to migrate towards the capsule across VCAM-1⁺ cortical epithelial cells. It has been shown that DN2 and DN3 thymocytes utilize $\alpha_4\beta_1$ integrin binding to VCAM-1 in a co-incubation assay (38). Therefore, while a transient stage of development, the DN2 stage is important since this is when rearrangement of the TCR loci begins and continued T-lineage restriction occurs.

DN3

DN3 thymocytes (CD24⁺CD25⁺CD27^{lo}CD44^{lo}CD117^{lo}) are located in the outer cortex and reside there for about two days (28). During this time, the cells continue to migrate along VCAM1⁺ stromal cells towards the capsule, proliferate, complete TCR β gene rearrangement, and irreversibly commit to the T cell lineage, either $\alpha\beta$ or $\gamma\delta$. Although the signals that direct DN3 cells to continue to migrate towards the capsule are not clear, it is thought that CCL25/CCR9 and CXCL12/CXCR4 interactions may be important (25, 39). At the DN3 stage, $\alpha\beta$ -committed thymocytes must pass their first major developmental checkpoint - β -

selection. β -selection is mediated by the pre-TCR which consists of a TCR β chain and an invariant pTCR α chain. preTCR α signaling does not require ligand engagement but rather appears to result from homodimerization (40, 41). Successful β -selection leads to thymocyte survival, extensive proliferation, allelic exclusion at the TCR β locus, initiation of rearrangement at the TCR α chain locus, and induction of CD4 and CD8 expression. Mechanisms underlying $\alpha\beta$ versus $\gamma\delta$ commitment are still unclear although it appears that $\gamma\delta$ T cell lineage commitment is associated with stronger TCR signals. It was shown that TCR $\gamma\delta^+$ DN3 cells can develop into both $\alpha\beta$ and $\gamma\delta$ T cells, but that they only develop into $\gamma\delta$ T cells if a strong signaling is received through the TCR (42).

DN4

DN4 thymocytes (CD4^{lo}CD8^{lo}CD25⁻CD44^{lo}) reside in the subcapsular zone (SCZ) for about one day or less and then rapidly transit to the CD4⁺CD8⁺ DP stage (28). The thymocytes now begin to migrate back through the cortex towards the medulla.

DP

At this stage, which lasts 1 to 2 days, the cell leaves the cell cycle, TCR α chain recombination continues, and the thymocytes continue to migrate inward towards the medulla (43). Following successful rearrangement of the TCR α chain, DP thymocytes express a mature, functional $\alpha\beta$ TCR. There are three possible outcomes for a DP thymocyte: death by neglect, positive selection, or negative

selection. The fate of the DP has been demonstrated to be determined by the strength of the interaction of the TCR on the thymocyte with self-MHC/peptide (44). If the DP thymocyte does not express a functional TCR or if the TCR has no affinity for self-MHC/peptide, the DP will die due to a lack of TCR signaling. This is known as death by neglect and it is the fate of the majority of DP thymocytes (45). If there is a low affinity interaction between TCR and self-MHC/peptide, the thymocyte will undergo positive selection. Approximately 5-10% of thymocytes successfully undergo positive selection (46). Positive selection is associated with TCR signaling mediated cell survival as well as induction of CCR7. TCR signaling in positive selection results in upregulation of the Egr-2 transcription factor and then upregulation of Bcl-2 (47). CCR7 expression directs the thymocytes to the medulla where there is an abundance of CCR7 ligands (48, 49). Thus, positive selection prevents the export of thymocytes that do not express a functional TCR or cannot interact with self-MHC. If there is a high affinity interaction between the TCR and self-MHC/peptide, the thymocyte will be negatively selected, preventing the release of self-reactive T cells into the periphery, where they could attack host tissues. It has been estimated that 5-10% thymocytes undergo negative selection (46).

Differential MAPK signaling in positive and negative selection

One of the long-standing questions that remains unanswered in the field of thymocyte development is how a DP thymocyte discriminates between positive and negative selecting ligands. While affinity appears to be important, the

differential signal transduction induced by the different ligands is unclear. However, the mitogen-activated protein kinase (MAPK) pathway appears to play a central role in this binary fate decision. Positive selection is associated with mild, but sustained extracellular signal-regulated kinase (ERK) activation, while negative selection is associated with a burst of ERK activation, as well as activation of Jun N-terminal kinase (JNK) and p38. Treatment with U0126, an inhibitor of ERK signaling, causes defects in positive selection, while negative selection appears unaffected (50). Conversely, treatment with SB203580, an inhibitor of p38, leads to a defect in negative selection but positive selection appears unaffected (51). In addition, thymocytes expressing a dominant negative JNK1 and thymocytes deficient in JNK2 exhibit defects in negative selection (52, 53).

Positive selection

Positive selection is mediated by peptide/MHC expressed on cortical thymic epithelial cells (cTECs). It was first discovered that positive selection conferred MHC restriction by examining BM chimeras in which the host and donor had different MHC haplotypes. It was shown that T cells recognized antigen only when presented with the MHC of the same haplotype of the radioresistant thymic epithelial cells (54). The thymic epithelial cells that were mediating positive selection were determined to be the cTECs since positive selection was prevented when MHC Class II was absent on cTECs, but expressed on mTECs, DCs, and B cells (55, 56). Also, cathepsin L, an endosomal protease important in generating

peptides for positive selection of MHC Class II restricted thymocytes (57), is expressed in cTECs but not in DCs (58). In addition, a proteasome subunit unique to cTECs was recently identified and it was found that its presence is necessary to produce optimal numbers of CD8⁺ T cells (59, 60), further supporting cTECs as the predominant cell type inducing positive selection.

CD4/CD8 commitment decision

Following positive selection thymocytes are instructed to adopt the CD4 or CD8 lineage based on the specificity of the TCR for MHC Class I or MHC Class II. Different models have been developed to explain the process of lineage commitment (61). The classical models of lineage decision all predict that positive selection and lineage commitment happen simultaneously and by the same TCR signals. One of the earlier models, the stochastic selection model, states that during positive selection transcription of either the CD4 or CD8 co-receptor is randomly stopped (61). However, experiments showed that lineage commitment efficiency was far above what would be predicted based on random choice (62). Another model is the strength-of-signal instructional model. This model is based upon the finding that more of the src family kinase Lck associates with CD4 than CD8 (63). In this model, DP thymocytes receive stronger signals through TCR and CD4 ligation of MHC Class II and weaker signals through TCR and CD8 ligation of MHC Class I, and it is the strength of signal that determines lineage commitment (64). The duration of signal instructional model is an updated version of the strength of signal model. This model hypothesizes that a short-lived

signal produces CD8⁺ T cells, while a long-lived signals produces CD4⁺ T cells (65).

The newest model, the kinetic signaling model, in combination with transcriptional regulation, differs from the classical models described above in that positive selection and lineage commitment do not occur simultaneously (61) (**Fig 1-2**). In this model positive selection happens first, then lineage choice follows. As in the duration of signal instructional model, lineage choice is determined by TCR signal duration. However, in the kinetic signaling model, members of the common cytokine receptor gamma-chain family, such as IL-7, evaluate the signal (66). Transcription of CD4 occurs unless a silencer element stops transcription (67, 68). In contrast, CD8 transcription requires enhancer elements such as E8III, which is active in DPs (69), and E8I, which is active in CD8SPs (70). E8III is suppressed by TCR signals during positive selection resulting in down-regulation of CD8 and transition to the CD4⁺CD8^{lo} phenotype (71). At the CD4⁺CD8^{lo} intermediate stage, continued TCR signaling will promote expression of transcription factors necessary for CD4 commitment. However, according to this model, if TCR signaling is diminished, there is increased IL-7 signaling. E8I is activated in response to IL-7 signaling through STAT5, which leads to a phenomenon called co-receptor reversal in which CD4 gene expression is terminated and CD8 gene expression is initiated, and this leads to the generation of CD8SPs (66, 72). Thus, according to this model CD8 differentiation is IL-7 dependent, while CD4 differentiation is IL-7 independent.

However, TCR signaling generally increases responsiveness to IL-7 (73). In addition, IL-7R knockout mice, do not exhibit gross defects in lineage commitment (74).

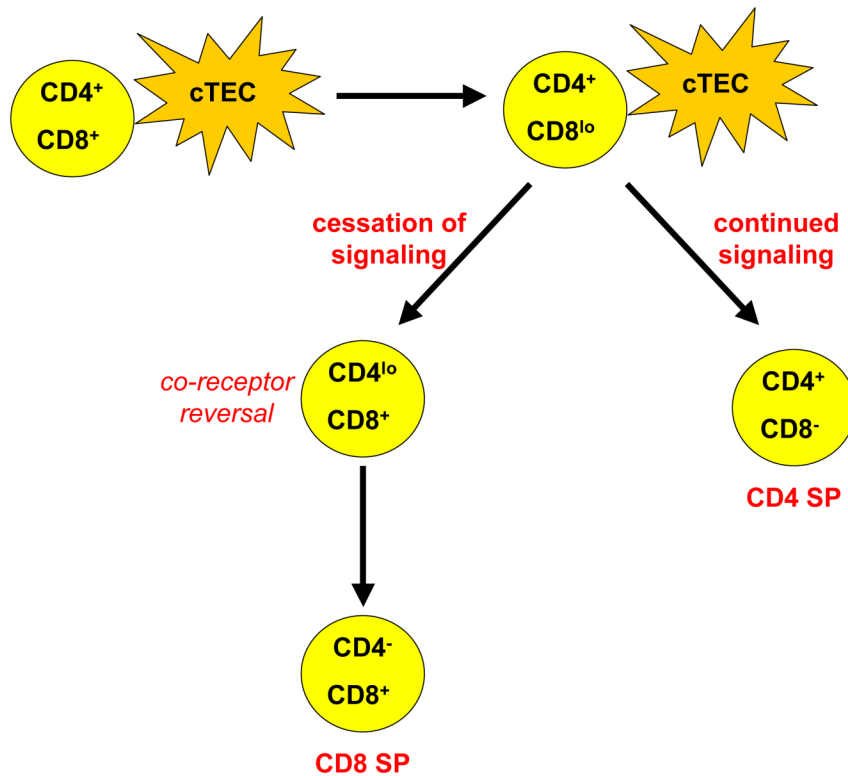


Figure 1-2: The kinetic signaling model of CD4/CD8 lineage commitment.

Signaling through the TCR during positive selection stops CD8 gene transcription, resulting in a thymocyte that is now CD4⁺CD8^{lo}. If this thymocyte is MHC Class II restricted, TCR signaling will continue and the thymocyte will develop into a CD4SP. However, if this thymocyte is MHC Class I restricted, TCR signaling decreases, co-receptor reversal is induced, and the thymocyte will develop into a CD8SP.

Despite these issues, a number of molecular details that support the kinetic signal model of lineage commitment have recently been elucidated. Three proteins appear to be critical for lineage commitment: GATA-binding protein 3 (GATA-3), T-helper inducing POZ/Kruppel-like factor (ThPOK), and runt-related transcription factor 3 (Runx3). GATA-3 is a zinc finger protein that is expressed following TCR signaling at the DP stage (75). It has been shown that GATA-3 binds to ThPOK to increase ThPOK expression (76). In the absence of GATA-3, CD4 T cell differentiation is blocked allowing some MHC Class II-restricted thymocytes to develop into CD8⁺ cells (76), and overexpression of GATA-3 blocks CD8 development (77). ThPOK is a zinc finger protein that is only expressed in CD4⁺ cells (78, 79). A mutation in the ThPOK gene results in mice that lack T helper cells and, in addition, when ThPOK is over-expressed, mostly CD4 cells are produced (78, 79). Runx3 is a transcription factor that is expressed by CD8SPs (80). Runx3 binds to the CD4 silencer element (80) as well as binding to the E8I enhancer element (81). It also binds to the gene that encodes ThPOK to repress ThPOK expression (82). Runx deficiency results in increased CD4SPs, while overexpression results in increased CD8SPs (83, 84). Thus, collectively, lineage commitment appears to be determined by the mutually antagonist actions of ThPOK and Runx3.

CD4SP and CD8SP

Following positive selection and lineage commitment, mature CD4SP and CD8SP thymocytes are generated. CD4SP and CD8SP cells are CD24⁺CD62^{lo}CD69⁺Qa2⁻

and are found in the outer medulla. In addition to occurring at the DP stage, negative selection of self-reactive thymocytes may also occur at the SP stage in the medulla. SP cells upregulate CCR7 after positive selection, which directs migration from the cortex to the medulla (49). TCR signaling increases expression of CCR7 on SP cells through the ERK pathway (85). CCL19 and CCL21, the ligands for CCR7 are found on mTECs and induce migration of SP cells to the medulla (49). CCR7 deficient thymocytes do not enter the medulla although SP thymocytes still develop somewhat normally in the cortex, indicating that the medulla is not necessary for DP to SP development (48). Interestingly, these SP cells that cannot traffic to the medulla are not tolerant to self (48), suggesting that the medulla is necessary for negative selection.

Exiting the thymus

Following a relative short residence time in the medulla (4-5 days), thymocytes emigrate from the thymus and populate the peripheral lymphoid organs (86). Recent thymic emigrants (RTE) display an heat shock antigen (HSA)^{lo}CD69⁻CD62L^{hi}Qa-2^{hi} phenotype (87). Sphingosine-1-phosphate receptor 1 (S1P1), a G-protein coupled receptor, has been found to regulate T cell emigration from the thymus as well as other lymphoid organs and lymph nodes (LNs) (88). The current model suggests that mature thymocytes expressing S1P1 migrate along a S1P concentration gradient that is created by the action of S1Plyase (89). S1P concentrations are high in the blood, but low in tissue, resulting in the movement of mature SP thymocytes from the thymus to the blood. Interestingly, CD69

expression inhibits S1P1 expression; therefore thymocytes can respond better to S1P if they are CD69⁻ (90). Furthermore, it has been shown that transgenic mice that overexpress CD69 have decreased egress (91). Expression of S1P1 is directly regulated by Kruppel-like factor 2 (KLF2), a zinc-finger transcription factor (92). There is a KLF2-binding site upstream of the transcription start site of the S1PR1 gene and chromatin immunoprecipitation assays have shown that KLF2 binds in this region (92). Taken together, thymocytes emigration appears to be controlled at multiple levels and includes both cell intrinsic and extrinsic factors.

Negative selection

Negative selection is the process by which potentially self-reactive thymocytes are either removed from the T cell repertoire or are altered so that they are no longer self-reactive. Negative selection occurs when T cells react to self-peptide MHC in a high affinity manner (44). There are three main mechanisms of thymic negative selection: clonal deletion, anergy, and receptor editing. Clonal deletion is the apoptosis of self-reactive thymocytes and is thought to be the most common mechanism of negative selection. The first experiment to demonstrate clonal deletion utilized an antibody specific for TCR V β 17a, which binds the MHC Class II protein IE. It was discovered that in mice that express IE, there are almost no V β 17a⁺ peripheral T cells or mature thymocytes, while immature thymocytes with this TCR are present (93). While the molecular mechanisms underlying

clonal deletion are not clear, it was recently determined that clonal deletion does not require the extrinsic apoptosis pathway since apoptosis was unaffected when a dominant negative form of Fas/APO-1-associated death domain (FADD)/mediator of receptor-induced toxicity-1 (MORT1) was transgenically expressed in thymocytes (94). However, the pro-apoptotic protein Bim, which induces apoptosis through interaction with other Bcl-2 family members at the mitochondria, was shown to be important for clonal deletion (95) (**Fig 1-3**). Additionally, the orphan nuclear steroid receptor Nur77 is induced after TCR stimulation and has also been identified as an important mediator of clonal deletion. A dominant negative form of Nur77 inhibits negative selection and overexpression of Nur77 leads to increased thymocyte apoptosis (94). It is currently unclear if Nur77 mediates clonal deletion as a transcription factor or by translocating to the mitochondria and interacting with Bcl-2 (96-98). Therefore, Bim and Nur77 appear to be two of the key molecules involved in clonal deletion.

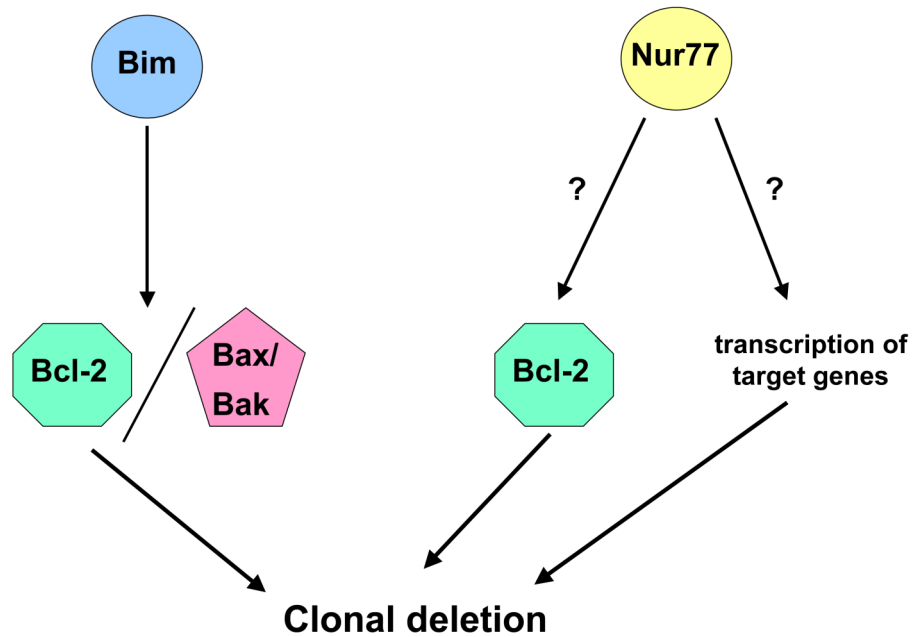


Figure 1-3: Bim and Nur77 are mediators of clonal deletion. Bim and Nur77 have been demonstrated to be important for clonal deletion of self-reactive thymocytes. Bim mediates clonal deletion through interaction with Bcl-2 family members. It has been suggested that Nur77 induces apoptosis by acting as a transcription factor and/or associating with Bcl-2.

As mentioned above, there are also non-apoptotic mechanisms of negative selection. For example, receptor editing, or the additional rearrangement at the TCR α locus to create an $\alpha\beta$ -TCR that is no longer self-reactive, has been demonstrated to occur the OT-1 model of negative selection (99). Anergy, a state of non-responsiveness to antigen has also been described (100, 101). We recently showed that although apoptosis is impaired in HY^{cd4}Bim^{-/-} mice, negative selection remains intact as there is no increase in the numbers of SP8 cells (102), further suggesting the existence of non-apoptotic negative selection mechanisms.

The roles of different thymic APCs in negative selection

mTECs

It is generally accepted that the medulla is an important site of negative selection in the thymus. For example, it has been shown that to become tolerant, it is necessary for thymocytes to enter the medulla as CCR7 deficient mice develop autoimmune disease (48). The medulla is home to a large number of DCs as well as mTECs, both being cell types capable of inducing negative selection. mTECs are able to express tissue-restricted antigens (TRAs) due to expression of the autoimmune regulator (AIRE), a transcription factor which allows for ectopic expression of tissue specific antigens (103). AIRE-deficient mice and humans with AIRE mutations develop autoimmunity to various organs (103, 104).

cTECs

While cortical thymic epithelial cells are essential for positive selection, some experiments have shown that cTECs are not capable of mediating negative selection. For example, when MHC Class I expression was restricted to cTECs, normal positive selection of CD8⁺ T cells occurred, but mature T cells from these mice lysed syngeneic targets as efficiently as they lysed allogeneic targets (105). In contrast, it has also been shown that in numerous situations cTECs can mediate negative selection (106-111). Interestingly, Mayerova and Hogquist found that when high affinity self antigen is only expressed on cTECS the mechanism of negative selection is clonal deletion in the 2C and HY models, but receptor editing in the OT-1 model (108). In addition, McCaughtry et al found that although cTECs are inefficient at inducing apoptosis, they do prevent an increase in SPs, indicating that negative selection is still occurring (112). However, it is important to note that whether or not cTECs can induce negative selection, in part, depends on whether they express the negatively selecting ligand that the thymocyte recognizes (107).

DCs

DCs are the professional APCs in the thymus. DCs have long been recognized as being inducers of negative selection, including the classical BM chimera experiments where T cells from recipient mice were found to be tolerant of cells derived from the BM donor (113). They express high levels of MHC Class I and II as well as the co-stimulatory molecules B7-1 and B7-2. DCs are generally

thought to be the most important APC for inducing clonal deletion, by both presenting antigen directly to developing thymocytes, and by presenting TRA expressed by mTECs to thymocytes through cross-presentation (114). It is important to note that there are three different populations of DCs in the thymus: plasmacytoid DCs, myeloid DCs, and lymphoid DCs (115). Lymphoid DCs ($CD11c^+$ signal regulatory protein alpha ($Sirp\alpha$) $^-CD11b^-CD8\alpha^{hi}$) develop from a common T cell/DC precursor, are the most abundant type of DC in the thymus, and are thought to be the most important type of thymic DC for mediating negative selection (115). Both plasmacytoid ($CD11c^+Sirp\alpha^{low}B220^+CD8\alpha^{-/low}$), and myeloid ($CD11c^+Sirp\alpha^+CD11b^+CD8\alpha^{-/low}$) DCs migrate from the blood to the thymus, and it has been suggested that they may be involved in inducing tolerance to TRAs (116).

Although the medulla contains a greater density of DCs, there are DCs present in the cortex as well (117). It has been shown that in the $HY^{cd4}M$ mouse, apoptotic thymocytes are found only in the cortex, near DCs (112). In addition, clonal deletion was intact in $HY^{cd4}CCR7^{-/-}$ mice, indicating that it is not necessary for thymocytes to migrate to the medulla to be deleted in this model (112). This is not actually in conflict with reports of the medulla being important for clonal deletion (48), because in this case the majority of T cells are specific for male antigen, which is expressed ubiquitously and therefore will be expressed in the cortex. In contrast, wildtype mice or TCR transgenics specific for a TRA may need to traffic to the medulla to be exposed to TRAs. Taken together, it appears that a paradigm

is emerging where the important factor determining whether a cell type can induce negative selection is its expression of the high affinity antigen, and not necessary lineage or location.

Models of Negative Selection

There are many systems available to study negative selection, each with its advantages and disadvantages. One of the earliest models of negative selection was *in vitro* stimulation of isolated thymocytes with anti-CD3 or peptide (118, 119). *In vitro* stimulation is a relatively inexpensive system, and it allows control over the amount of stimulation delivered and the timing of stimulation. However, this is an artificial system, and thymocytes are stressed when removed from the thymic environment, which could result in changes in gene expression.

Additionally, the APCs used are not usually thymically derived. *In vivo* injection of peptide may have increased physiological relevance, although it also has drawbacks. It has been shown that much of the deletion that occurs at the DP stage following *in vivo* injection is a side effect of the activation of peripheral T cells (120, 121).

TCR transgenic mice that express a cognate antigen, either endogenously or transgenically, are often used as models of negative selection as they allow for a significant population of T cells that will respond to self-antigen and also are easy to identify. However, unlike in wildtype mice where the TCR β chain is expressed with the preTCR α chain at DN3 and the TCR α chain is not expressed on the

surface until the DP stage, many TCR transgenic mice express both the TCR α and TCR β chains at the DN2 stage (122) (**Fig 1-4**). This effectively enables the DN2 cells of the transgenic mouse to recognize antigen in the same manner as DP cells. DN and DP cells are different in many aspects including gene expression (123) and proliferation capacity (124). Therefore, studying selection events, particularly negative selection, in TCR transgenic mice has been suggested to result in selection artifacts. The importance of these differences between DN and DP cells is apparent in the altered T cell repertoire of TCR transgenic mice. For example, in the HY mouse model, there is an increased percentage of thymic and peripheral DN cells and many of these cells have a mature phenotype and behave like mature $\gamma\delta$ T cells (122). In addition, $\alpha\beta$ TCR DN cells have decreased expression of CD5, are resistant to cyclosporine A treatment, and express CD8 $\alpha\alpha$ following TCR stimulation (125). Additionally, deletion occurs at the DN to DP transition in the traditional HY male mouse, while deletion likely occurs at the DP to SP transition in wildtype mice (126). To overcome these artifacts resulting from premature TCR expression, a more physiological mouse model system, called HY^{cd4} was developed (122).

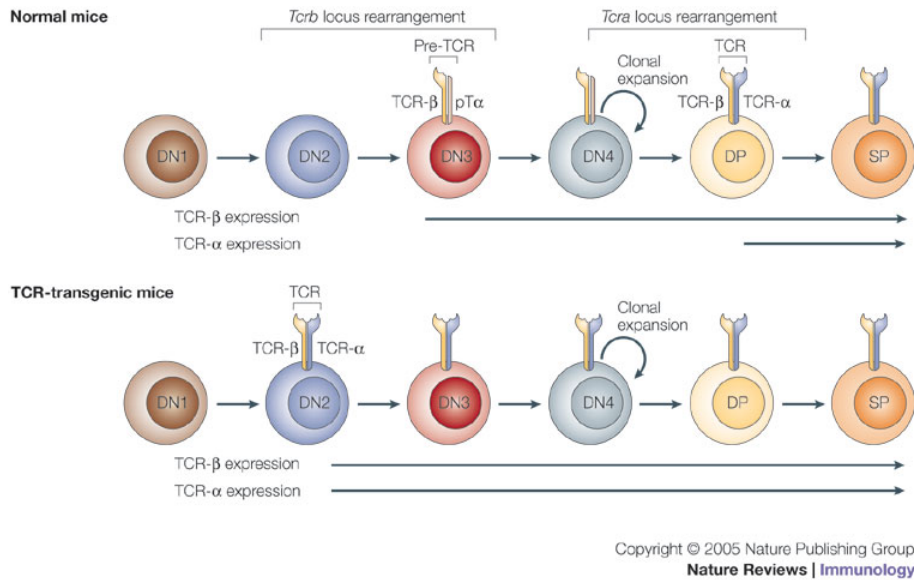


Figure 1-4: Many TCR-transgenic mice express an inappropriately timed TCR α chain. Wildtype mice express a pre-TCR at the DN3 stage and a full $\alpha\beta$ -TCR at the DP stage. TCR-transgenic mice that express a full $\alpha\beta$ -TCR at the DN2 stage instead of at the DP stage result in a non-physiological model of negative selection. *From Hogquist, K. A. et al. 2005. Nature Reviews Immunology 5, 772-782.*

The HY^{cd4} mouse was created using a system where the HY TCR α chain is under the control of the CD4 promoter-enhancer (**Fig 1-5**). A transcriptional and translational STOP cassette flanked by loxP sites was inserted upstream of the HY TCR α chain cDNA to create a conditional HY TCR α expressing mouse. When this conditional HY TCR α mouse is crossed with a CD4-Cre mouse, which initiates Cre expression at the DP stage of development, this STOP cassette is removed through recombination allowing transcription of the HY TCR α chain cDNA at the DP stage. Finally, introduction of the HY TCR β chain results in the triple transgenic HY^{cd4} mouse. The HY TCR consists of V α 17 and V β 8.2 and is specific for male antigen (smcy 738-764: KCSRNRQYL) in the context of H-2D^b. The HY TCR expressing cells can be identified using the monoclonal antibody T3.70 which recognizes V α 17. Thus the HY^{cd4}D^{b-/-} mouse is a model of non-selection as it lacks D^b, which is the restriction element for the HY TCR. The HY^{cd4} female (F) mouse is a model of positive selection because the high affinity HY antigen is not present but an unidentified low affinity peptide capable of inducing positive selection is present. The HY^{cd4} male (M) mouse is a model of negative selection because the high affinity HY antigen is present. In HY^{cd4} male mice, deletion occurs at the DP to SP transition (122).

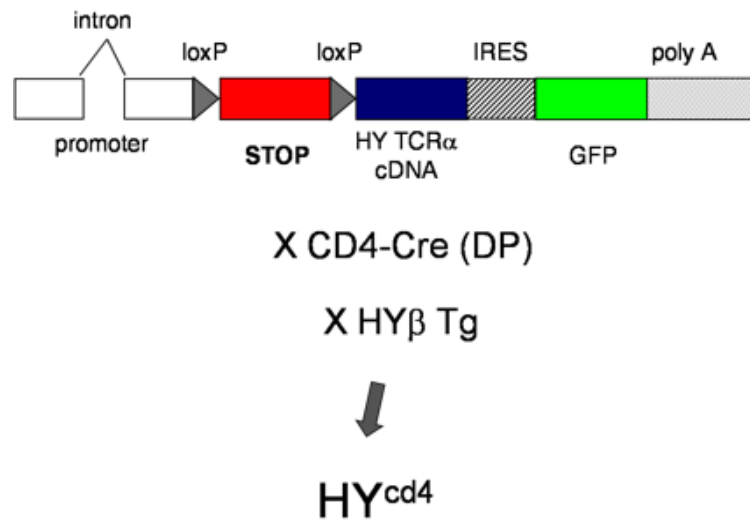


Figure 1-5: Generation of the HY^{cd4} model. HY TCR α chain cDNA was placed under the control of the CD4 promoter-enhancer. A STOP cassette flanked by loxP sites upstream of the HY TCR α cDNA places transcription of HY TCR α chain dependent on Cre-mediated recombination. When this conditional HY TCR α chain expressing mouse is crossed with a CD4-Cre mouse, transcription of HY TCR α chain cDNA is initiated at the DP stage of thymocyte development. A third cross with an HY TCR β transgenic mouse results the HY^{cd4} mouse.

To identify genes induced in negative selection, a gene array was performed using the HY^{cd4} model (127). Both Bim and Nur77 were found to be upregulated in negative selection over positive selection, as expected given their roles in clonal deletion. Another gene identified as being specifically induced in negative selection was programmed death -1 (PD-1). Other microarray studies have also identified PD-1 as being upregulated in negative selection (128, 129).

Programmed Death-1 (PD-1)

Programmed Death-1 (PD-1) is an inhibitory member of the CD28 family of co-receptors and is expressed on thymocytes and T cells, B cells, and myeloid cells (130-132). The role of PD-1 in the thymus is currently unclear. PD-1 interactions are known to be involved in anergy and T cell exhaustion in the periphery (133). PD-1 deficient mice develop spontaneous autoimmunity disease. Interestingly, the type of autoimmunity is strain-specific. For example C57BL/6 mice develop arthritis glomerulonephritis (134), while BALB/c mice develop dilated cardiomyopathy (135). It has also been shown that a single nucleotide polymorphism (SNP) in *pdccl1*, the gene that encodes PD-1, is associated with autoimmune diseases in humans such as systemic lupus erythematosus (136), rheumatoid arthritis (137), and type 1 diabetes (138). This SNP is a guanine to adenine substitution in the fourth intron of *pdccl1*. This substitution inhibits

binding of runt-related transcription factor 1 (RUNX1) to an enhancer, which likely results in decreased transcription of *pdccl1* (136).

PD-1 has been shown to bind two ligands: PD-L1 (B7-H1) and PD-L2 (B7-DC). Interestingly, there is differential expression of these ligands. PD-L1 is expressed on T cells, B cells, macrophages, and DCs, while PD-L2 is found on activated macrophages and DCs (131, 139, 140). PD-L1 is also expressed by endothelial cells in the heart, β cells in the pancreas, and the placenta (131). This suggests that PD-L1 may be important in peripheral tolerance. It has been shown that PD-L1, but not PD-L2, is important for peripheral tolerance (141). Both PD-L1 and PD-L2 are found in the thymus. Interestingly, the ligands are spatially segregated with PD-L1 in the cortex and the medulla and PD-L2 in the medulla (131).

It is not clear how PD-1 signals but PD-1 does have an immunoreceptor tyrosine based inhibitory motif (ITIM) and an immunoreceptor tyrosine based switch motif (ITSM) in its cytoplasmic domain (132) (**Fig 1-6**). The ITIM has the consensus sequence I/VxYxxL/V, while the ITSM has the consensus sequence TxYxxI/V (142). The ITSM was first identified in signaling lymphocyte activating molecule (SLAM) (143). In SLAM, Src homology 2-domain containing molecule 1A (SH2D1A) can bind to the ITSM and its presence determines which phosphatases can then bind (143). Interestingly, the ITSM has been shown to transduce both activating and inhibitory signals in SLAM (142). Less is known about the role of the ITSM in PD-1 although it appears to be important for signal transduction.

Signaling through PD-1 has been examined by creating chimeric molecules with the cytoplasmic domain of PD-1 and the extracellular domain of Fc γ RIIB (144) or CD28 (145). Signaling was examined in murine B cells (144) and human CD4⁺ T cells (145). Both groups found that SHP-2, a protein tyrosine phosphatase, was recruited (144, 145), and one of the groups found that SHP-1 was also recruited (145). Both SHP-2 and SHP-1 dephosphorylate downstream signaling molecules. Mutating the ITIM motif had no observable effect while the ITSM was necessary for inhibition of signaling (144, 145).

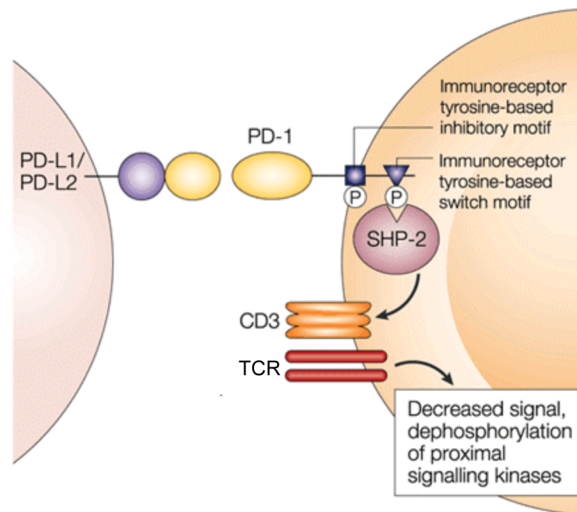


Figure 1-6: PD-1 is an inhibitor receptor containing an ITIM and an ITSM in its cytoplasmic tail. Signaling through PD-1 recruits SHP-2 to its ITSM. SHP-2 dephosphorylates downstream signaling molecules. *Modified from Sharpe, A.H., and G. J. Freeman. 2002. Nature Reviews Immunology 2: 116-126.*

PD-1 has been implicated in thymic selection events but its role in positive and/or negative selection is unclear. Keir and colleagues transgenically overexpressed PD-1 on DP thymocytes and found that when PD-1 was stimulated with an agonistic antibody there were decreased levels of ERK activation and Bcl-2, indicating that PD-1 interactions inhibit positive selection (146). However, PD-1 was found to be upregulated in a gene array using the OT-1 model of positive selection, implying that it is associated with positive selection events (147), although it is important to note that the OT-1 TCR interacts with antigen at a relatively high affinity for positive selection (148). In addition, PD-1^{-/-} mice in a 2C model of positive selection have decreased DP numbers indicating that PD-1 deficiency inhibits positive selection (149), while no change was observed in negative selection in 2C PD-1^{-/-} mice (134).

Part of the conflicting observations about the role of PD-1 in positive and negative selection may be due to the use different transgenic models that may not exhibit appropriately timed expression of the TCR α chain. Given the role of PD-1 as a negative regulator of T cell activation in the periphery, the association of PD-1 deficiency or mutation with autoimmune disease, the presence of PD-L1 and PD-L2 in the thymus, and that PD-1 was found to be upregulated in the HY^{cd4}M mouse, we hypothesize that it is involved in negative selection, possibly in an anergic or non-apoptotic mechanism. The objective of this study is to use the physiologically relevant HY^{cd4} model to determine the role of PD-1 in thymocyte development.

Chapter 2: Materials and Methods

Mice

C57BL/6 (B6) mice were obtained from the National Cancer Institute, Jackson Laboratories, or Taconic. HY^{cd4} mice have been previously described (122). HY^{cd4}PD-1^{-/-} mice were generated by breeding HY^{cd4} mice with PD-1^{-/-} mice (150), supplied by Dr. Tasuku Honjo (Kyoto University). All mice were bred and maintained in our colony at the University of Alberta, treated in accordance with protocols approved by the University of Alberta Animal Care and Use Committee and used between 4 and 12 weeks of age for experiments.

Flow cytometry

Cell surface staining

Thymus, lymph node (LN), and spleen were harvested from euthanized mice and a single cell suspension was created by gentle grinding through a wire mesh screen into Hank's Balanced Salt Solution (HBSS) (Thermo Scientific). LN and spleen cells were incubated with Fc block (supernatant from 24G.2 hybridoma) at 1/100 for 10 min and then washed once with FACS buffer (phosphate buffered saline (PBS), 1% fetal bovine serum (FBS), 0.02% sodium azide (pH 7.2)) prior to staining. All antibody staining was performed at 1/200 dilution in FACS buffer except for anti-MHC Class II (1/500 dilution) and anti-Bcl-2 (staining was performed as per manufacture's instructions). Antibodies were added to cells

resuspended in FACS buffer and the cells were incubated on ice for 30 min then washed twice with FACS buffer. The following antibodies were purchased from ebioscience: CD4 (RM4-5), CD8 (53-6.7), TCRb (H57-597), HY-TCR (T3.70), CD2 (RM2-5), CD5 (53-7.3), CD69 (H1.2F3), PD-1 (J43), PD-L1 (M1H5), PD-L2 (TY25), CD24 (M1/69), MHC Class I (34-1-25), MHC Class II (M5/114.15.2), CD80 (16-10A1), CD86 (GL1), CD40 (HM40-3), CD44 (IM7), CD62L (MEL-14), CD172a/Sirp α (P84), CD11c (N418), CD11b (M1/70), and CD19 (eBio1D3). Anti-mouse polyclonal and streptavidin-conjugated antibodies were also purchased from ebioscience. Cell events were collected using a FACS Canto II™ (BD Biosciences) and FlowJo software was used for data analysis.

Intracellular staining

Cell-surface staining was completed prior to intracellular staining except when staining for Bim. For cleaved caspase-3, Bim, Bcl-2, and Cbl-b staining, cells were fixed with the BD Cytofix/Cytoperm™ Fixation/Permeabilization Kit and then stained with the appropriate antibodies. Anti-cleaved caspase 3 (D175) was purchased from Cell Signaling Technology. Anti-Bim_{S/EL/L} (10B12) was purchased from Alexis Biochemicals. Bcl-2 was detected using the PE Hamster Anti-Mouse Bcl-2 Set from BD Pharmingen. Cbl-b (C-20) and normal goat IgG was purchased from Santa Cruz Biotechnology. Anti-goat, rat, mouse, and rabbit IgG was purchased from invitrogen. Nur77 (12.14) was purchased from ebioscience and staining was performed using the ebioscience Foxp3 Staining Buffer Set as per manufacture's instructions. Cell events were collected using a

FACS Canto II™ (BD Biosciences) and FlowJo software was used for data analysis.

Cell Sorting

Cells were stained for cell surface antigens at 2×10^7 cells/mL in FACS buffer.

HY^{cd4}D^{b/-} T3.70⁺CD4⁺CD8⁺CD69⁻, HY^{cd4}F T3.70⁺CD4⁺CD8⁺CD69⁺, HY^{cd4}F

T3.70⁺CD8⁺CD69⁺, HY^{cd4}M T3.70⁺CD4⁺CD8⁺CD69⁺, HY^{cd4}M

T3.70⁺CD4⁺CD8⁺PD-1⁺, and HY^{cd4}M T3.70⁺CD4⁺CD8⁺PD-1⁻ thymocytes were purified on the FACS Aria.

pERK staining

T3.70⁺CD4⁺CD8⁺PD-1⁻ and T3.70⁺CD4⁺CD8⁺PD-1⁺ thymocytes were purified

using the FACS Aria. Sorted cells were washed in RP10 (RPMI + 10% FBS +

5mM HEPES + 50U(mg)/mL penicillin/streptomycin + 2mM L-glutamine +

50μM 2-mercaptoethanol + 50μg/mL gentamicin sulfate) and rested at 37 °C for

approximately 1.5h. DCs were pulsed with 1μM smcy peptide for 30 min at 37 °C.

Thymocytes and DCs were mixed at a 1:1 ratio in a 96 well plate. 50ng/mL (PMA

phorbol 12-myristate 13-acetate) and 1μM ionomycin were added to some wells

as a positive control for stimulation. The plate was spun down at 1,000 RPM for 1

min and incubated at 37 °C for 20 min. Cells were harvested, fixed in BD

Fix/Lyse Buffer at 37 °C for 10 min, washed with PBS, permeabilized with 80%

methanol, incubated on ice for 30 min and washed with FACS buffer. Cells were

incubated with Fc block, then phospho-specific anti-ERK1/2 (BD Biosciences) or

isotype IgG (BD Biosciences) for 30 min, then washed and incubated with biotin-anti-mouse for 30 min, then washed and incubated with SA PE Cy7 for 30 min. Cell events were collected using a FACS Canto II™ (BD Biosciences) and FlowJo software was used for data analysis.

Quantitative reverse-transcriptase PCR

Total RNA was isolated using the Qiagen RNeasy Mini kit and cDNA was synthesized using the SuperScript III first-strand cDNA synthesis kit (Invitrogen). Quantitative RT-PCR was performed using the Power SYBR Green kit (Applied Biosystems) and the 7900 HT Fast real-time PCR system (Applied Biosystems). Relative gene expression levels were determined via the $\Delta\Delta$ cycle threshold (C_T) method with $HY^{cd4}D^{b-/-} CD4^+CD8^+CD69^-$ as the reference population and β -actin as the reference gene. The following primer sequences were used. β -actin: forward: 5'CTAAGGCCAACCGTGAA AAG-3', reverse: 5'-ACCAGAGGCAT ACAGGGACA-3', Bim: forward: 5'-CGGTCCT CCAGTGGGTATTT-3, reverse: 5'-AGGACTTGGGGTTTGTGTTG-3', Nur77: forward: 5'-GGCATGG TGAAGGAAGTTGT-3', reverse: 5'-TGAGGGAAGTGAGAA GATTGGT-3', Gadd45 β : forward: 5'-GAGACCTGCACTGCCTCCT-3', reverse: 5'-CATTGG TTATTGCCT CTGCTC-3', Zfp52: forward: 5' – GGAATGCCTGGACTCTGC TC – 3', reverse: 5' – TCCTTTTCAGTCCTCACAGGTT – 3', 2610019F03Rik: forward: 5'- AAGTCTCAGAGGTTGGAAAGAAG -3', reverse: 5' – CAGCTC TTCTCTTAGTCGTTGGT – 3', Runx3: forward: 5'-ACCGTGTTACCAACC CTAC-3', reverse: 5'-GCCTTGGTCTGGTCTTCTA TCT-3', CCR7: forward: 5'

– CAGGGAAACCCAGGAAAAAC – 3', reverse: 5' – CCTCATCTTGGCAGA
AGCAC – 3', KLF2: forward: 5' – CGTGTTGGACT TCAT CCTCTC – 3',
reverse: 5' – CGGCTCCGGGTAGTAGAAG – 3', Cbl-b: forward: 5'-TCTCAT
TCAGAAAGGCATCGT-3', reverse: 5'- CGGGAGTGGT TTGTCTTGTT-3',
Egr-2: forward: 5'-TTGACCAGATGAACGGAGTG-3', reverse: 5'- TGGAGA
ATTTGCCCATGTAAG-3', Dgka: forward: 5'-CATATCCTGCCTCCGTGTTC
-3', reverse: 5'-ACTAGAAGGGGGTGGGTGTT-3'.

Western Blot

Purified T3.70⁺CD4⁺CD8⁺PD-1⁺ and T3.70⁺CD4⁺CD8⁺PD-1⁻ thymocytes were lysed in 1% Triton X-100 in PBS, and 15µg of protein of each was loaded into an 8% resolving SDS-PAGE gel. The gel ran at 150V and was then transferred to an Immobilon P membrane overnight at 30V. The membrane was blocked for 8h in 5% skim milk. The membrane was blotted with anti-Cbl-b antibody (C-20, Santa Cruz Biotechnology) diluted 1:1 000 in 5% skim milk overnight at 4 °C. The blot was washed 5 times for 5min each in TBS-T (TBS + 0.1% Tween 20) and then blotted with horseradish peroxidase (HRP)-conjugated bovine-anti-goat antibody (Jackson ImmunoResearch) diluted 1:5 000 in 5% skim milk for 2h at room temperature. The blot was washed 5 times for 5 min each in TBS-T then developed using SuperSignal® West Pico Chemiluminescent Substrate (ThermoScientific) and a Kodak M35A X-OMAT Processor. The membrane was incubated in a 55 °C water bath with stripping buffer (0.1M β-mercaptoethanol, Tris pH 6.8, 2% SDS) for 30 min and then re-probed as described above with

anti-ERK2 antibody (C14, Santa Cruz Biotechnology) at 1:2000 and HRP-conjugated goat-anti-rabbit antibody (Jackson ImmunoResearch) at 1:10 000.

Generation of BM-derived DCs

BM-derived DCs were generated as previously described (151) with some modifications. Briefly, the tibia, femur, and humerus were harvested and cleaned of tissue and muscle. The ends of the bones were cut off and the marrow was flushed out with sterile Easy-Sep Media (PBS, 2% FBS, 2mM EDTA). Cells were filtered through a 70 μ M BD Falcon™ cell strainer, were spun down at 1600 RPM for 10 min, resuspended at 1×10^6 cells/mL in RP10 with 10ng/mL granulocyte-macrophage colony-stimulating factor (GM-CSF) and cultured in 24 well plates. 1mL RP10 + 10ng/mL GM-CSF was added at day 2 and 1mL of media was changed on day 4, 6, and 8, if applicable. Cells were used between day 6 and day 9. Cells were harvested by washing in cold Versene (0.5mM EDTA in PBS). In some instances DCs were stimulated overnight with 10 μ g/mL anti CD40 (ebioscience).

***In vitro* stimulation assay**

B6 female splenocytes or BM-derived DCs were used as APCs. 4×10^5 B6 female splenocytes or BM-derived DCs in RP10 (ThermoScientific) were added to a 96 well plate. Serial dilutions of smcy (PROIMMUNE) were added to each of the wells (0nM, 1nM, 10nM, 100nM, 1 μ M, and 10 μ M). Functional grade purified PD-L1 blocking antibody was added in some experiments at a final concentration

of 10 μ g/mL or 30 μ g/mL. The plate was then incubated at 37 °C for 10 min. Then 1.6 X 10⁶ thymocytes were added to each well. As a positive control, 50ng/mL PMA and 1 μ M ionomycin were added to one well of thymocytes. Cells were incubated for 3h at 37 °C, harvested, and examined by flow cytometry.

Bone marrow chimeras

T cell depletion

The EasySep FITC Selection Kit was used. BM was harvested from tibia, femur, and humerus, and resuspended at 1.0 X 10⁸ cells/mL. The cells were then incubated with Fc block for 5 min at room temperature (RT), followed by FITC-conjugated anti-Thy1.2 (ebioscience) for 15 min at RT and washed once in Easy Sep media. The cells were incubated with the FITC selection cocktail for 15 min at RT, incubated with magnetic nanoparticles for 10 min at RT, and finally placed in the magnet for 10 min. After 10 min, the non-adherent cells were collected and resuspended at a concentration of 5 X 10⁷/mL.

HY^{cd4}PD-1^{-/-} mixed BM chimeras

T cell depleted HY^{cd4}PD-1^{-/-} female bone marrow (BM) was mixed with either B6 female or male T cell depleted BM at a 1:50 ratio and 1 X10⁷ total BM cells was injected into lethally irradiated (1000 Gy) female or male B6 mice, respectively. Mice were given water with 15 μ g/mL polymixin B sulfate and 40 μ g/mL neomycin sulfate until used.

Restriction of high affinity antigen-presentation to thymic epithelial cells

1 X 10⁷ cells of T cell depleted HY^{cd4}F D^{b/-} BM was injected into lethally irradiated (1500Gy) B6 male recipient mice. Days one and two before irradiation the recipients were injected with 200µg anti-NK1.1 antibody. Mice were given water with 15µg/mL polymixin B sulfate and 40µg/mL neomycin sulfate for one month after reconstitution.

Restriction of antigen-presentation to hematopoietically derived cells

1 X 10⁷ cells of T cell depleted HY^{cd4}M BM was injected into lethally irradiated (1500Gy) B6 female recipient mice. The first and second days after reconstitution, 2µg of anti-CD8 antibody was injected into each recipient. Mice were given water with 15µg/mL polymixin B sulfate and 40µg/mL neomycin sulfate for one month after reconstitution.

Statistical analysis

Prism (GraphPad Software) was used to determine mean, standard deviation, and *p* values. A two-tailed unpaired *t* test with a 95% confidence interval was used to calculate *p* values.

Chapter 3: Results

Characterization of the HY^{cd4} model of thymic selection

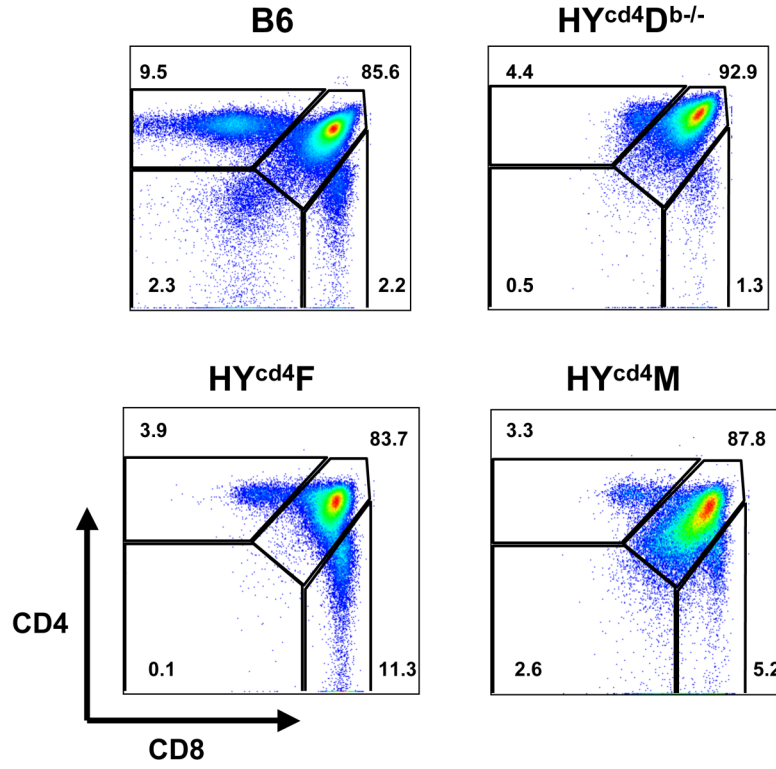
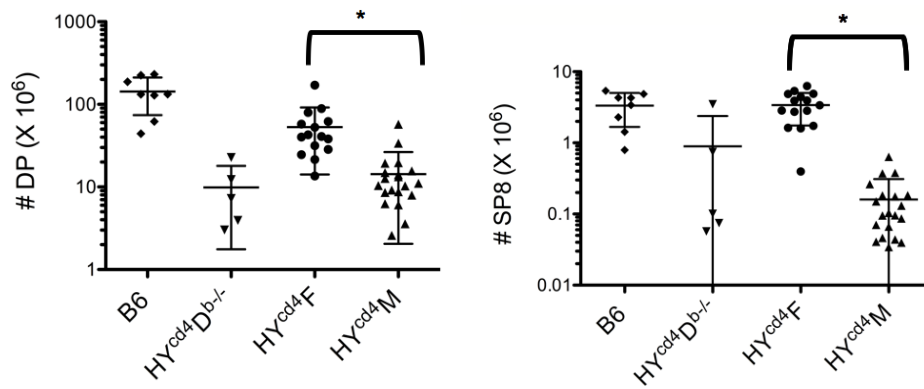
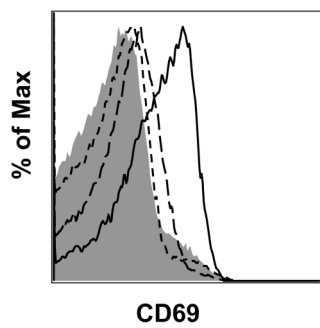
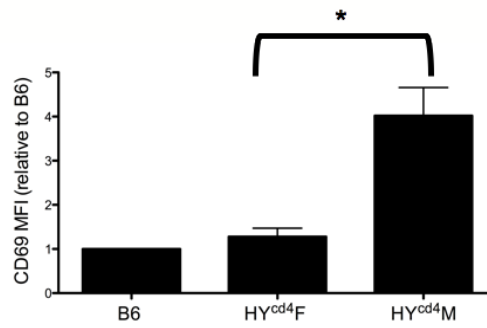
Thymus

In a wildtype, non-TCR transgenic mouse, all four populations of thymocytes are present: CD4⁻CD8⁻ (DN), CD4⁺CD8⁺ (DP), CD4⁺CD8⁻ (SP4), and CD4⁻CD8⁺ (CD8). The majority of the cells are DP, there is a slightly higher proportion of SP4 thymocytes compared SP8 thymocytes and there are few DN cells (**Fig 3-1A**). The CD4/CD8 plot of the T3.70⁺ thymocytes from HY^{cd4}D^{b-/-} mice shows an increased proportion of DP thymocytes and a decreased proportion of SP4 and SP8 thymocytes compared to wildtype (B6) mice, indicating that DP thymocytes are prevented from being positively selected and developing into SP cells (**Fig 3-1A**). There are few SP4 cells because the HY-TCR is MHC Class I restricted. The lower number of SP8 cells is because the mice lack D^b, which is the restriction element for the HY-TCR. The SP8 cells that are present are likely being positively selected on an endogenous TCR α chain as the model does not involve features to prevent selection on endogenous TCR α chains, such as RAG^{-/-} or TCR α ^{-/-}. In fact, SP cells selected on endogenous TCR α chains are a possibility for all HY^{cd4} mice in all experiments. The CD4⁺CD8⁻ cells express higher levels of CD8 than the CD4⁺CD8⁻ cells in the B6 mouse and are likely not true CD4SPs. Although they could be selected on MHC Class II, based on the kinetic signalling model, it is possible that many of these cells have temporarily downregulated

CD8 in the process of becoming CD4⁻CD8⁺ (66). This can be said of all the CD4⁺CD8⁻ cells in this MHC Class I directed model. Of the T3.70⁺ thymocytes in HY^{cd4}F mice, there are a lower percentage of DP cells and an increased percentage of SP8 cells compared to both wildtype and HY^{cd4}D^{b-/-} mice. This suggests that the DPs are being positively selected and developing into SP8s (**Fig 3-1A**). The thymic profile of the T3.70⁺ thymocytes of HY^{cd4}M mice have an increased proportion of DP compared to both wildtype and HY^{cd4}F mice, and a lower proportion of SP8 compared to HY^{cd4}F mice, indicating that that negative selection is preventing the development of DPs to SP8s (**Fig 3-1A**). When absolute numbers of antigen-specific thymocytes are calculated there are significantly more male-specific DP thymocytes in the female over the male (p=0.0002), confirming that negative selection occurs at the DP to SP8 transition in the HY^{cd4} model (**Fig 3-1B**). In addition, the female has a higher number of male-specific SP8 thymocytes than both the D^{b-/-} and male due to non-selection and negative selection, respectively (p=0.0075 and p<0.0001, respectively) (**Fig 3-1B**).

Surface expression of CD69 is an indicator of antigen encounter. Comparison of CD69 expression on T3.70⁺ DP thymocytes confirms that the HY^{cd4}D^{b-/-}, HY^{cd4}F, and HY^{cd4}M mice illustrate non-selection, positive selection, and negative selection, respectively (**Fig 3-1C,D**). B6 DPs and T3.70⁺ HY^{cd4}D^{b-/-} DPs exhibit the lowest levels of CD69 expression, T3.70⁺ HY^{cd4}F DPs express slightly higher levels of CD69, and T3.70⁺ HY^{cd4}M DPs express the highest levels of CD69.

These CD69 profiles indicate that T3.70⁺ HY^{cd4}D^{b-/-} DPs are receiving little signal, T3.70⁺ HY^{cd4}F DPs are receiving a low affinity signal, while T3.70⁺ HY^{cd4}M DPs are receiving a high affinity signal, which is consistent with non-selection, positive selection and negative selection, respectively (**Fig 3-1C,D**). Negative selection in T3.70⁺ HY^{cd4}M DP thymocytes was further confirmed by examining levels of activated (cleaved) caspase 3, a downstream indicator of apoptosis. An increased percentage of T3.70⁺HY^{cd4}M DPs contain cleaved caspase 3 compared to B6 DPs and T3.70⁺HY^{cd4}F DPs, indicating that a higher proportion is undergoing apoptosis (**Fig 3-1E**). Intriguingly, there appears to be an additional population of very low levels of cleaved caspase 3 in the T3.70⁺HY^{cd4}F DPs (**Fig 3-1E**). Collectively, these data confirm published data (122) demonstrating that the HY^{cd4}D^{b-/-} is a model of non-selection, the HY^{cd4}F is a model of positive selection, and the HY^{cd4}M is a model of negative selection.

A**B****C****D**

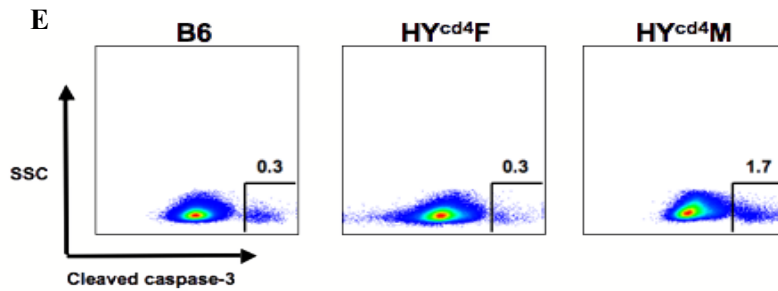


Figure 3-1: The HY^{cd4} model of thymic selection: thymus. A) CD4/CD8 thymic profiles of total thymocytes (B6) or T3.70⁺ thymocytes for indicated mouse. B) Absolute numbers of total (B6) or T3.70⁺ DP (top), * indicates p=0.0002, and CD8SP (bottom), * indicates p=0.0001 thymocytes. n=8 for B6, n=5 for HY^{cd4}D^{b/-}, n=15 for HY^{cd4}F, n=20 for HY^{cd4}M. C) CD69 surface expression on total DP (B6) or T3.70⁺DP for indicated mouse. B6 = shaded, HY^{cd4}D^{b/-} = short dashed line, HY^{cd4}F = long dashed line, HY^{cd4}M = solid black line. D) Compilation of MFI of CD69 surface expression relative to B6. * indicates p=0.0034, n=5 for all mice. E) Representative levels of cleaved caspase 3 in total DP (B6) or T3.70⁺ DP for indicated mouse.

Spleen

The B6 spleen contains CD4⁺ and CD8⁺ T cells, as well as CD4⁻CD8⁻ cells, which likely includes B cells, macrophages, and DCs to name but a few. As expected, the majority of T3.70⁺ cells in the female are CD8⁺ T cells (**Fig 3-2B**).

Unexpectedly, there is a large population of T3.70⁺ CD8⁺ T cells in the male; however, it should be noted that these cells have decreased expression of CD8 (**Fig 3-2A,B**). A compilation of absolute numbers reveals that there are a greater number of T3.70⁺ CD8⁺ T cells in the male compared to the female ($p=0.0042$) (**Fig 3-2C**). The large number of T3.70⁺ T cells in the male may be derived from a few T cells that escaped negative selection. T3.70⁺ T cells that enter the periphery in the male will be bombarded by their high-affinity antigen and may undergo extensive proliferation. A similar population is found in the periphery of the traditional HY male mice (152), and these cells have been shown to proliferate in response to IL-2 and IL-15, and to produce pro-inflammatory cytokines (153, 154). However, it is important to note that it is not known if these cells are functional in the HY^{cd4}M mice. HY^{cd4}M mice do not display overt autoimmune disease and so an alternative explanation is that these CD8⁺T cells may be anergic. The paucity of T3.70⁺ CD8⁺ splenocytes in HY^{cd4}F mice is somewhat surprising. Since the ligand that the HY-TCR recognizes in female mice is not yet known, it is possible that the expression of this ligand in the periphery is minimal. As antigen encounter is important for homeostatic proliferation, this could account for the low numbers of T3.70⁺ CD8⁺ T cells in the female (155, 156). In addition, examination of CD5 expression levels has

shown that the HY-TCR has low affinity for its unknown ligand in the HY^{cd4}F, making it less likely to undergo homeostatic proliferation (148).

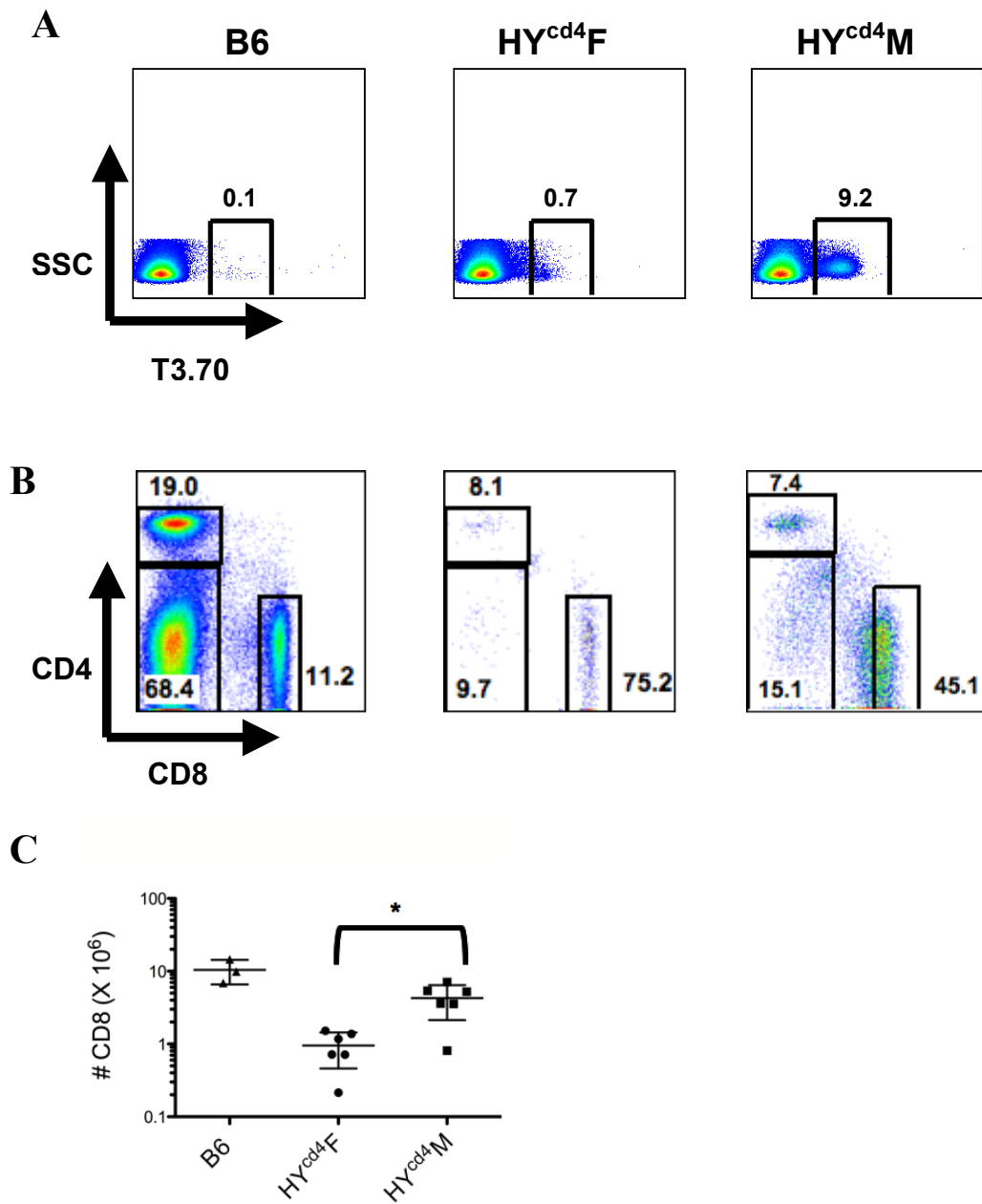


Figure 3-2: The HY^{cd4} model of thymic selection: spleen. A) Percent of T3.70⁺ splenocytes for the indicated mouse. B) CD4/CD8 profiles of total splenocytes (B6) or T3.70⁺ splenocytes for the indicated mouse. C) Absolute numbers of total CD8⁺ (B6) or T3.70⁺ CD8⁺ splenocytes. * indicates p=0.0042, n=3 for B6, n=6 for HY^{cd4}F, n=6 for HY^{cd4}M.

Expression of CD44 and CD62L can be used to identify naïve and memory T cells. CD44 is upregulated in response to high affinity and CD62L expression facilitates entry into the lymph nodes. Naïve cells are CD44⁻CD62L⁺, effector memory cells are CD44⁺CD62L⁻, and central memory cells are CD44⁺CD62L⁺ (157). Representative flow cytometry plots and calculations of absolute cell numbers show that, as expected, the majority of CD8⁺ T cells in B6 mice, as well as the T3.70⁺ CD8⁺T cells in HY^{cd4}F mice are naïve (**Fig 3-3**). The CD8⁺ T cells in wildtype mice are composed of a polyclonal repertoire, consisting of T cells with many different specificities. Thus, it would be expected that a large number of T cells would not have seen their specific antigen. As discussed above, CD44 expression is induced by high affinity antigen, in this case male antigen, which is absent in the female. The majority of T3.70⁺ CD8⁺ T cells in HY^{cd4}M mice have an activated phenotype as indicated by CD44 surface expression, and a high proportion of these cells are central memory T cells. This is expected as the T3.70⁺ CD8⁺T cells in the male are a monoclonal population and their antigen is abundant. Thus, in HY^{cd4}F, the cells are mainly naïve, while in HY^{cd4}M they are activated. It is unclear why there is a large population of T3.70⁺ cells in the male, but it is likely due to the escape of some T3.70⁺ thymocytes from negative selection in the thymus.

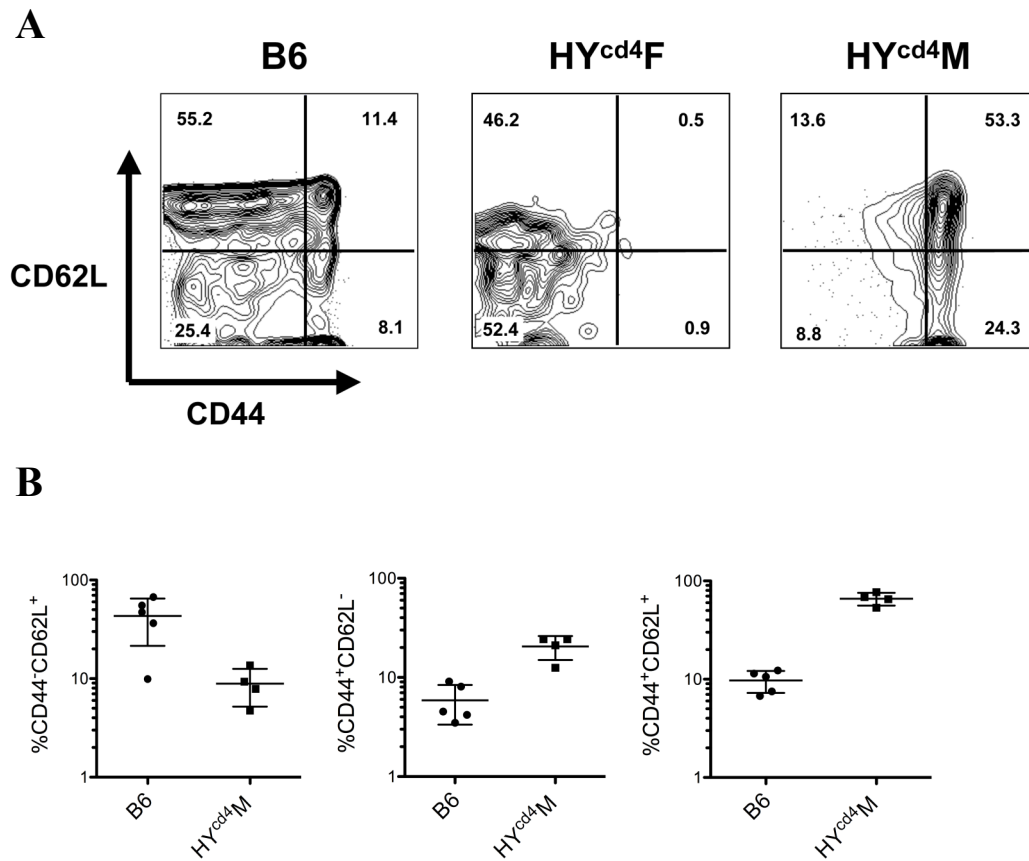
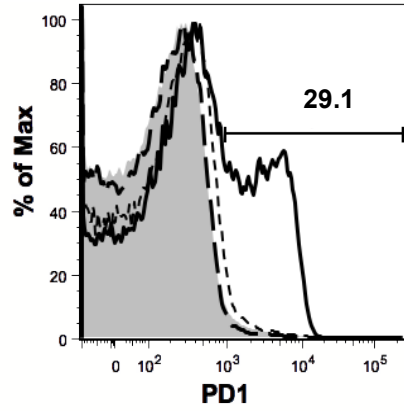
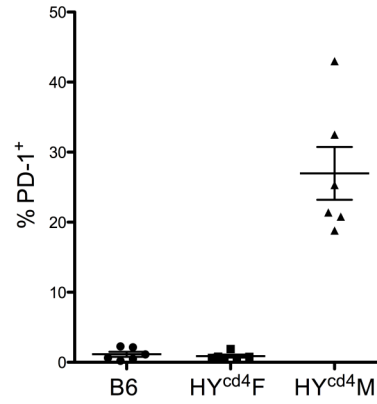
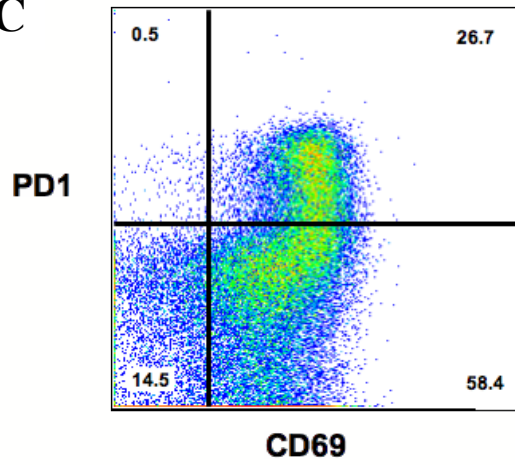
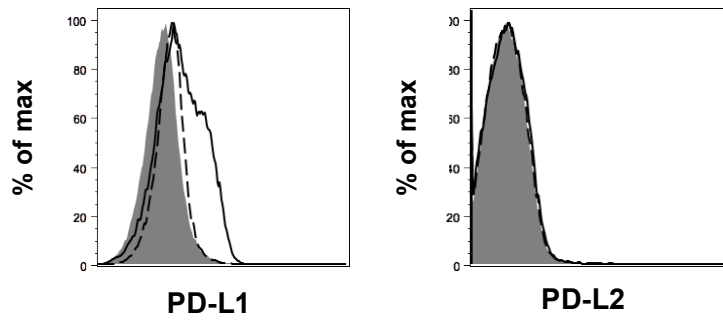


Figure 3-3: Relative proportions of naïve, effector memory, and central memory splenic T cells in the HY^{cd4} model: A) CD62L by CD44 plots of total CD8⁺ splenocytes (B6) or T3.70⁺ CD8⁺ splenocytes for indicated mouse. B) Proportion of naïve (CD44⁻CD62L⁺), effector memory (CD44⁺CD62L⁻), and central memory (CD44⁺CD62L⁺) CD8⁺ T cells (B6) or T3.70⁺ CD8⁺ T cells (HY^{cd4}M). n=5 for B6, n=4 for HY^{cd4}M.

Programmed Death 1 (PD-1) is upregulated in the HY^{cd4}M model of negative selection

A gene array was previously performed on HY^{cd4}D^{b-/-}, HY^{cd4}F, and HY^{cd4}M mice to identify genes that are differentially regulated in positive and negative selection (127). One of the genes found to be upregulated in negative selection but not in positive or non-selection was Programmed Death 1 (PD-1). PD-1 is a co-inhibitory member of the CD28 family and is associated with anergy in the periphery (130, 158). Flow cytometry was performed on T3.70⁺ HY^{cd4}D^{b-/-}, HY^{cd4}F, and HY^{cd4}M DP thymocytes, as well as on B6 DP thymocytes, to confirm that PD-1 is upregulated in negative selection, but not positive selection or non-selection, at the protein level. PD-1 expression was only observed in T3.70⁺ HY^{cd4}M thymocytes, confirming the microarray results (**Fig 3-4A**). The percentage of T3.70⁺ HY^{cd4}M DP thymocytes expressing PD-1 varies from between 20-40% (**Fig 3-4B**). Interestingly, the vast majority of T3.70⁺PD-1⁺ DP thymocytes from HY^{cd4}M mice are also CD69⁺, indicating that PD-1 expression is restricted to those cells that have encountered high affinity antigen (**Fig 3-4C**). Additionally, PD-L1 is expressed on T3.70⁺ HY^{cd4}M DPs (**Fig 3-4D**). Interestingly, PD-L1 expression has been reported on DN and SP thymocytes but not DP thymocytes (139). PD-L2 is not expressed on any of the DP thymocyte populations (**Fig 3-4D**), which is consistent with published data (139). PD-1 is not expressed on peripheral CD8⁺ T cells in any of the mice (**Fig 3-4E**). This was somewhat surprising as PD-1 expression on peripheral T cells has been previously

reported (159), and as well, PD-1 is expressed on DP thymocytes in HY^{cd4}M mice (Fig 3-4A).

A**B****C****D**

E

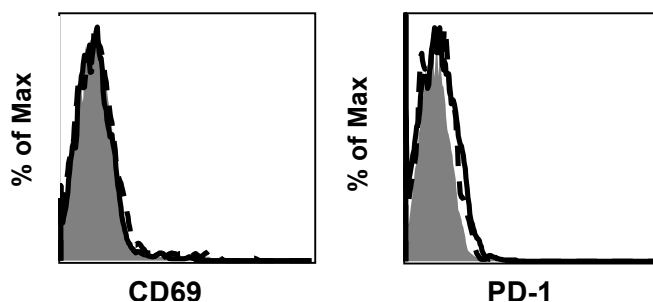


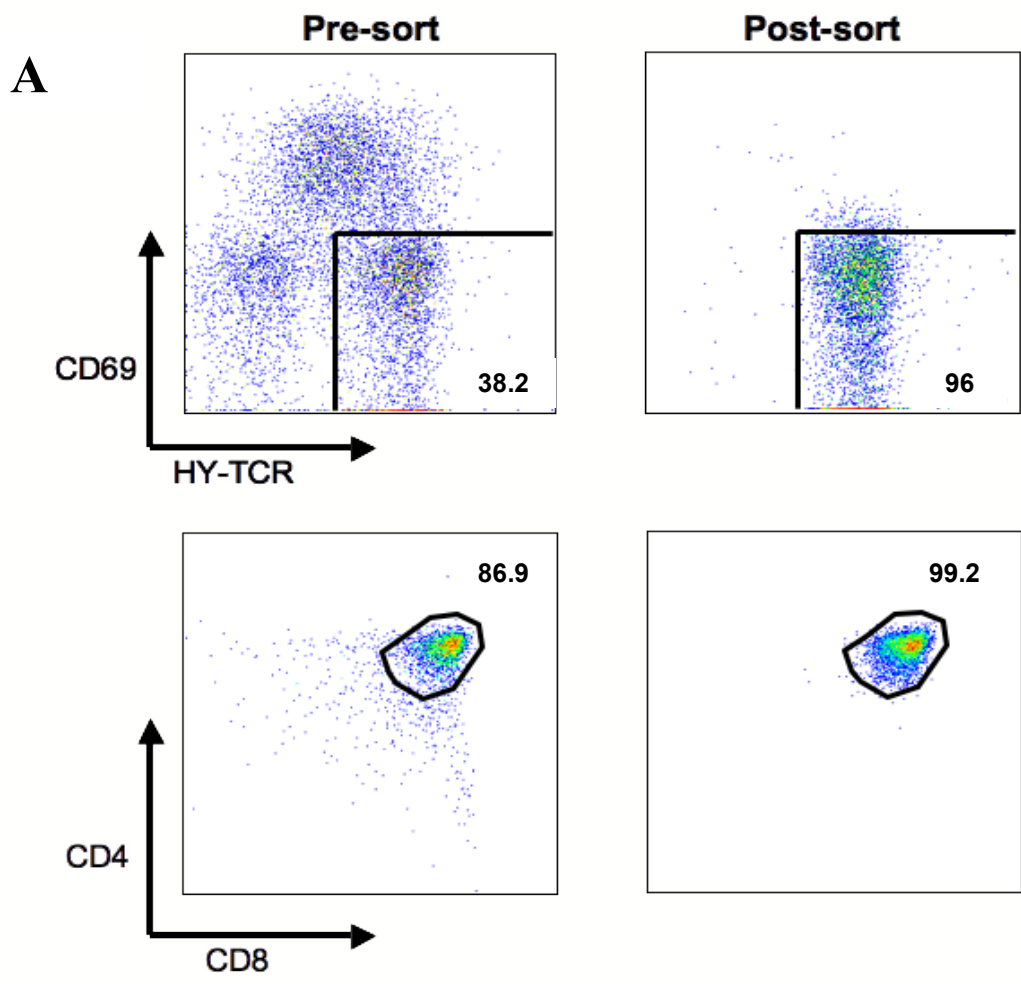
Figure 3-4: PD-1 expression in HY^{cd4} F and M thymocytes. A) PD-1 expression on total thymocytes (B6) or T3.70⁺ thymocytes for the indicated mouse. B) Compilation of percent PD-1⁺ of total (B6) or T3.70⁺ DP thymocytes, n=6 for all mice. C) PD-1 and CD69 expression on T3.70⁺ HY^{cd4}M DPs. D) PD-L1 and PD-L2 expression on total thymocytes (B6) or T3.70⁺ thymocytes for indicated mouse. E) CD69 and PD-1 expression on total CD8⁺ splenocytes (B6) or T3.70⁺ CD8⁺ splenocytes for indicated mouse. B6 = shaded, HY^{cd4}D^{b/-} = short dashed line, HY^{cd4}F = long dashed line, HY^{cd4}M = solid black line (for A) D) and E)).

Comparison of gene expression profiles of PD-1⁺ and PD-1⁻ thymocytes examined directly *ex vivo*

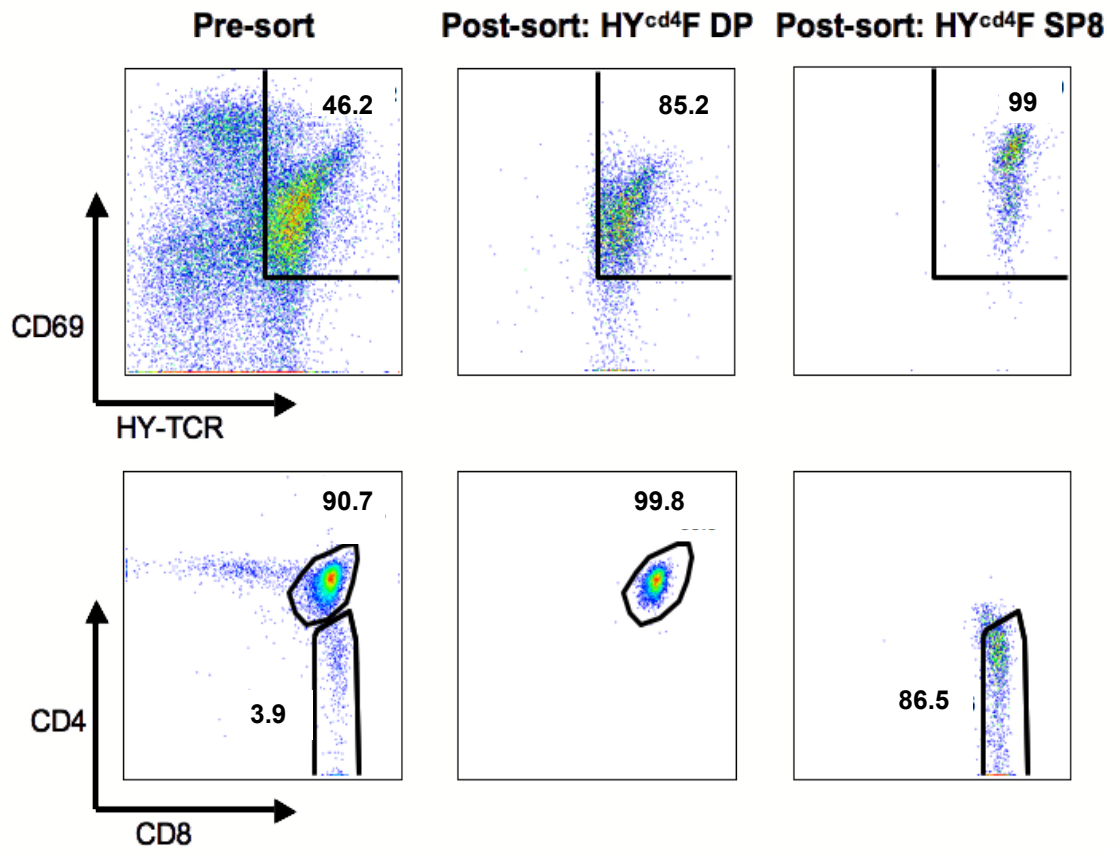
Based on the expression of PD-1 on HY^{cd4}M DP thymocytes, the presence of PD-L1 and PD-L2 in the thymus, the involvement of PD-1 interactions in anergy in the periphery, and the discovery that PD-1⁺ cells can survive 72h after high affinity antigen encounter (112), it was hypothesized that PD-1 expression on DP thymocytes induces anergy as a mechanism of negative selection instead of clonal deletion.

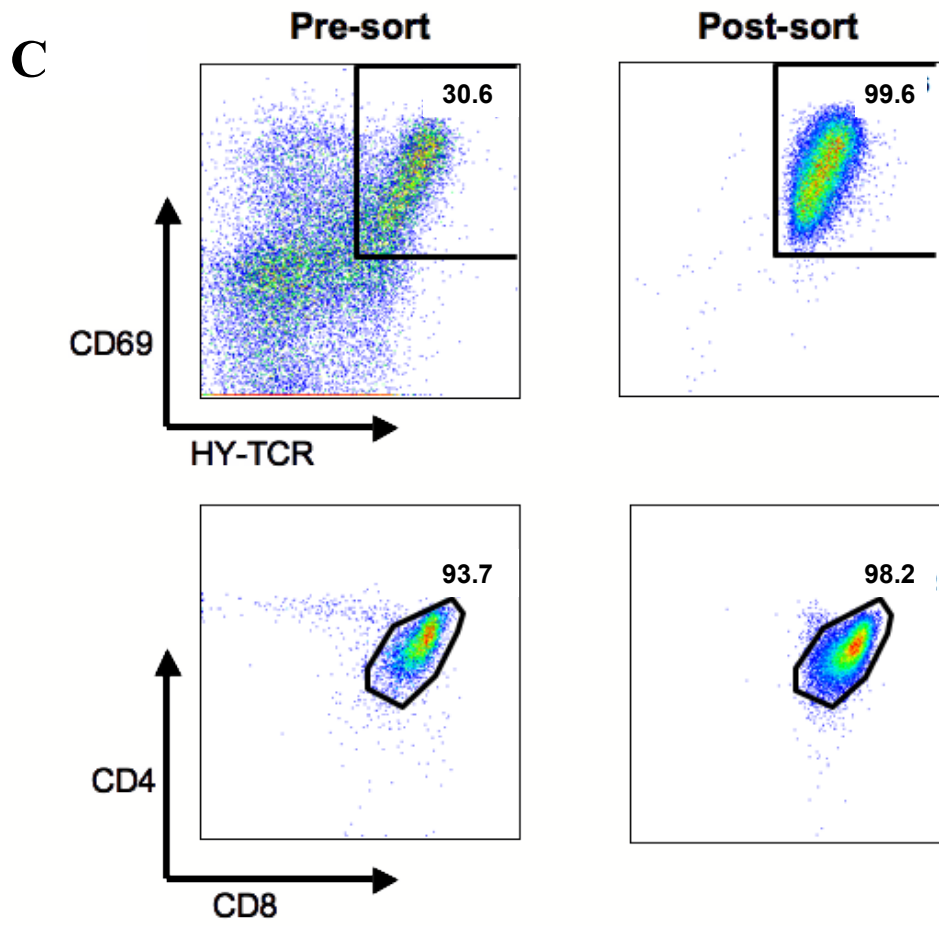
To determine if PD-1⁻ and PD-1⁺ thymocytes have different abilities to undergo apoptosis, quantitative real time PCR (qRT-PCR) was performed on different cell populations to evaluate the relative expression of various genes associated with clonal deletion. The following populations were sorted to a high level of purity and RNA was extracted. T3.70⁺ CD69⁻ HY^{cd4}D^{b/-} DP (**Fig 3-5A**, 95.2% pure), T3.70⁺ CD69⁺ HY^{cd4}F DP (**Fig 3-5B**, 85.0% pure), T3.70⁺ CD69⁺ HY^{cd4}F SP8 (**Fig 3-5B**, 85.6% pure), T3.70⁺ CD69⁺ HY^{cd4}M DP (**Fig 3-5C**, 97.8% pure), T3.70⁺HY^{cd4}M DP PD-1⁻ (**Fig 3-5D**, 89.4% pure), and T3.70⁺HY^{cd4}M DP PD-1⁺ (**Fig 3-5D**, 87.5% pure). Quantitative RT-PCR was performed to compare the mRNA expression of genes of interest between the populations. Relative expression was calculated based on the $\Delta\Delta C_t$ method with T3.70⁺ CD69⁻ HY^{cd4}D^{b/-} DP as the baseline population and β -actin as the reference gene. All

qRT-PCR and flow cytometry results are compared with the previously mentioned microarray results (127), when applicable.



B





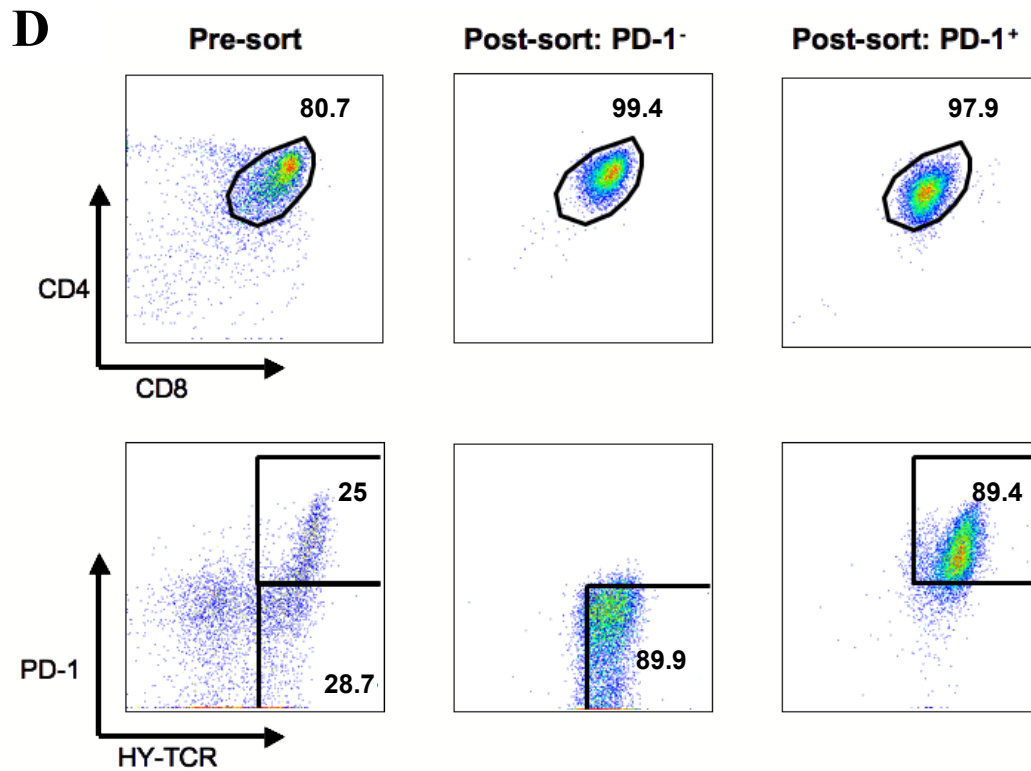
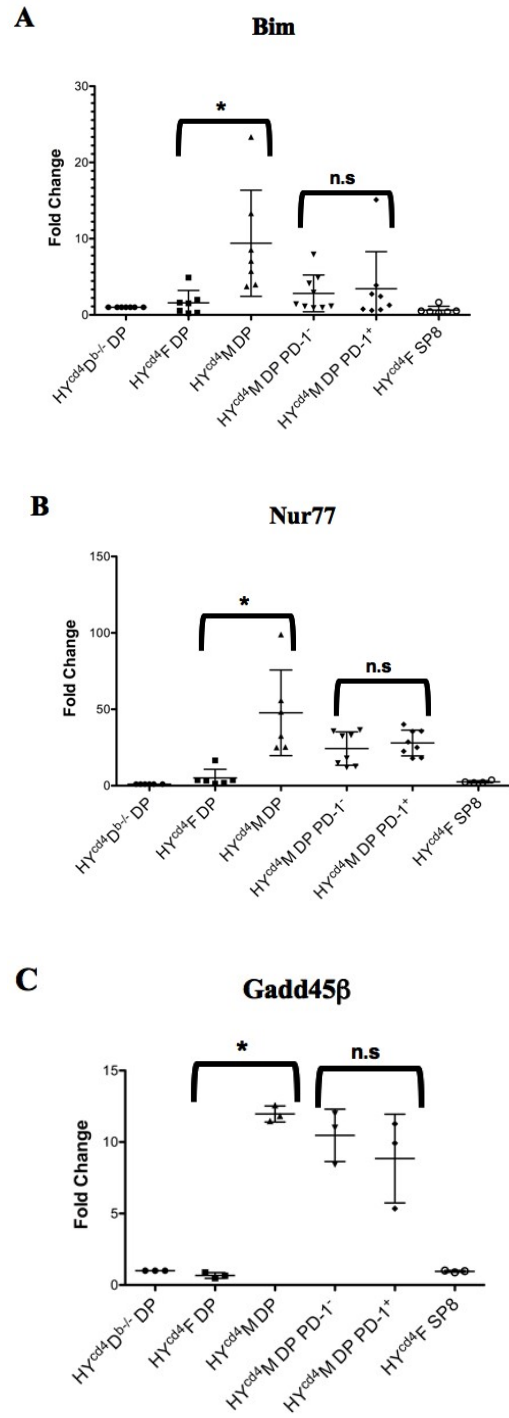


Figure 3-5: Cell sorting prior to RNA extraction. A) $T3.70^+CD69^-HY^{cd4}D^{b/-}$ DP (95.2% pure). B) $T3.70^+CD69^+HY^{cd4}F$ DP (85.0% pure), and $T3.70^+CD69^+HY^{cd4}F$ SP8 (85.6% pure). C) $T3.70^+CD69^+HY^{cd4}M$ DP (97.8% pure). D) $T3.70^+HY^{cd4}M$ DP PD-1⁻ (89.4% pure), and $T3.70^+HY^{cd4}M$ DP PD-1⁺ (87.5% pure).

Bim (bcl2l11) is a pro-apoptotic member of the Bcl2 family and is essential for clonal deletion (95). Bim was found to be upregulated 5.57 fold in negative selection over non-selection and 3.92 fold in negative selection over positive selection in the microarray. As expected, Bim expression is not increased in the T3.70⁺ CD69⁺HY^{cd4}F DP population, while it is highly upregulated in the T3.70⁺ CD69⁺ HY^{cd4}M DP population (p=0.0135) (**Fig 3-6A**). Bim is expressed almost equally between the T3.70⁺HY^{cd4}M DP PD-1⁻ and T3.70⁺HY^{cd4}M DP PD-1⁺ populations, with slightly higher (but non-significant) expression in T3.70⁺HY^{cd4}M DP PD-1⁺ thymocytes (p=0.7410). Bim is not induced in the T3.70⁺ CD69⁺ HY^{cd4}F SP8 population, indicating that Bim upregulation is specific to negative selection. A similar trend was observed with Nur77 (Nr4a1), a steroid orphan nuclear receptor that is associated with clonal deletion (160). Nur77 was upregulated 16.06 fold in negative selection over non-selection and 11.29 fold in negative selection over positive selection in the microarray. As with Bim, the RT-PCR data recapitulated the microarray results: Nur77 expression is induced to higher levels in the T3.70⁺ CD69⁺ HY^{cd4}M DP population than the T3.70⁺CD69⁺HY^{cd4}F DP population (p=0.0045) and the T3.70⁺CD69⁺HY^{cd4}F SP8 population, while its levels are similar between T3.70⁺HY^{cd4}M DP PD-1⁻ and T3.70⁺HY^{cd4}M DP PD-1⁺ thymocytes (p=0.4719) (**Fig 3-6B**). Growth arrest and DNA damage (Gadd) 45 β has been associated with negative selection in previously published gene arrays (128, 161), although it just barely missed the cut-off in the microarray mentioned above (127). Gadd45 β is highly upregulated in T3.70⁺CD69⁺ HY^{cd4}M DP thymocytes over T3.70⁺CD69⁺HY^{cd4}F DP

thymocytes ($p < 0.0001$) and is not induced in the $T3.70^+CD69^+HY^{cd4}F$ SP8 thymocytes (**Fig 3-6C**). The expression of *Gadd45 β* is similar between $T3.70^+HY^{cd4}M$ DP PD-1⁻ and $T3.70^+HY^{cd4}M$ DP PD-1⁺ thymocytes, with it being slightly higher in the $T3.70^+HY^{cd4}M$ DP PD-1⁻ population ($p = 0.4789$). Another gene found to be upregulated in negative selection by the microarray was zinc finger protein (*zfp*) 52. Expression of *zfp52* was 7.8 fold higher in negative selection over positive selection and 6.7 fold higher in negative selection over non-selection. As with the genes described above, expression of *zfp52* is upregulated in the $T3.70^+CD69^+HY^{cd4}M$ DP population over the $T3.70^+CD69^+HY^{cd4}F$ DP population ($p = 0.0045$) and the $T3.70^+CD69^+HY^{cd4}F$ SP8 population, but is expressed at similar levels between the $T3.70^+HY^{cd4}M$ DP PD-1⁻ and $T3.70^+HY^{cd4}M$ DP PD-1⁺ populations ($p = 0.3804$) (**Fig 3-6D**).



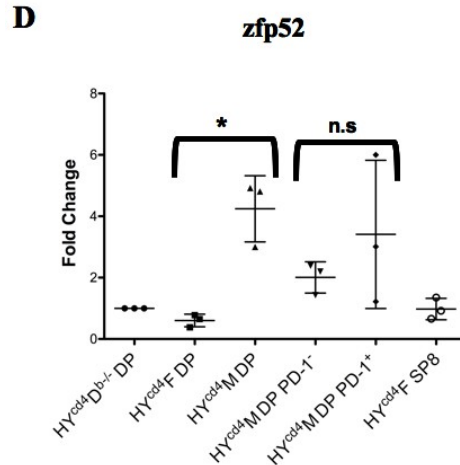


Figure 3-6: Comparison of Bim, Nur77, Gadd45 β , and zfp52 gene expression between T3.70⁺CD69⁻ HY^{cd4}D^{b/-} DP, T3.70⁺CD69⁺ HY^{cd4}F DP, T3.70⁺CD69⁺ HY^{cd4}M DP, T3.70⁺HY^{cd4}M DP PD-1⁻, T3.70⁺HY^{cd4}M DP PD-1⁺, and T3.70⁺CD69⁺ HY^{cd4}F SP8 populations. The $\Delta\Delta C_t$ method was used to calculate fold change with β -actin as the reference gene and T3.70⁺CD69⁻ HY^{cd4}D^{b/-} DP as the reference population. A) Bim, * indicates p=0.0135, n=7 for T3.70⁺CD69⁻ HY^{cd4}D^{b/-} DP, T3.70⁺CD69⁺ HY^{cd4}F DP, and T3.70⁺CD69⁺ HY^{cd4}M DP, n=9 for T3.70⁺HY^{cd4}M DP PD-1⁻, n=8 for T3.70⁺HY^{cd4}M DP PD-1⁺, n=6 for T3.70⁺CD69⁺ HY^{cd4}F SP8. B) Nur77, * indicates p=0.0045, n=6 for T3.70⁺CD69⁻ HY^{cd4}D^{b/-} DP, T3.70⁺CD69⁺ HY^{cd4}F DP, and T3.70⁺CD69⁺ HY^{cd4}M DP, n=8 for T3.70⁺HY^{cd4}M DP PD-1⁻ and T3.70⁺HY^{cd4}M DP PD-1⁺, n=4 for T3.70⁺CD69⁺ HY^{cd4}F SP8. C) Gadd45 β , * indicates p<0.0001, n=3 for all populations. D) zfp52, * indicates p=0.0045, n=3 for all populations. At least two biological replicates were used for the T3.70⁺HY^{cd4}M DP PD-1⁻ and T3.70⁺HY^{cd4}M DP PD-1⁺ populations. n.s.= not statistically significant.

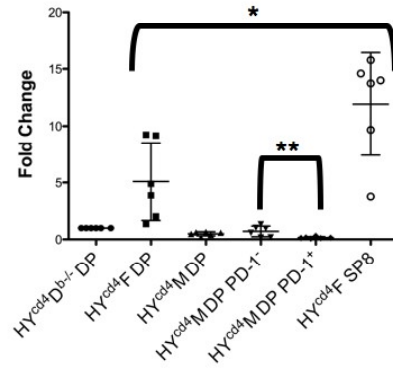
To determine whether PD-1 expression was altering the fate of $\text{HY}^{\text{cd4}}\text{M DP}$ thymocytes (ie. allowing them to become positively selected), the expression of genes associated with positive selection were examined. The expression of 2610019F03Rik, a relatively unknown gene that was upregulated in positive selection over negative selection in the microarray, and expression of Runx3, a factor important in lineage commitment to the CD8^+ cytotoxic T cell line (whose expression was unchanged in the microarray in DP thymocytes undergoing positive or negative selection) were analysed in $\text{HY}^{\text{cd4}}\text{M PD-1}^+$ and PD-1^- DP thymocytes. In the microarray, 2610019F03Rik was upregulated 11.8 fold and 4.1 fold in positive selection over negative and non-selection, respectively. 2610019F03Rik was found to be upregulated in both $\text{T3.70}^+\text{CD69}^+\text{HY}^{\text{cd4}}\text{F DP}$ thymocytes and $\text{T3.70}^+\text{CD69}^+\text{HY}^{\text{cd4}}\text{F SP8}$ thymocytes over $\text{T3.70}^+\text{CD69}^- \text{HY}^{\text{cd4}}\text{D}^{\text{b/-}}$ DP thymocytes, with higher expression in the $\text{T3.70}^+\text{CD69}^+\text{HY}^{\text{cd4}}\text{F SP8}$ population ($p=0.0144$), as expected (**Fig 3-7A**). 2610019F03Rik is downregulated in $\text{T3.70}^+\text{CD69}^+\text{HY}^{\text{cd4}}\text{M DP}$ thymocytes compared to $\text{T3.70}^+\text{CD69}^- \text{HY}^{\text{cd4}}\text{D}^{\text{b/-}}$ DP thymocytes, and interestingly, 2610019F03Rik is not downregulated as extensively in the $\text{T3.70}^+\text{HY}^{\text{cd4}}\text{M DP PD-1}^-$ population compared to the $\text{T3.70}^+\text{HY}^{\text{cd4}}\text{M DP PD-1}^+$ population ($p=0.0188$). Runx3 facilitates CD8 commitment by antagonizing ThPOK and repressing CD4 genes (81, 82). Although Runx3 was not upregulated in positive selection over negative and non-selection in the microarray, as expected, Runx3 expression was increased in the $\text{T3.70}^+\text{CD69}^+\text{HY}^{\text{cd4}}\text{F SP8}$ population over both the $\text{T3.70}^+\text{CD69}^+\text{HY}^{\text{cd4}}\text{F DP}$ population ($p=0.0096$) and the $\text{T3.70}^+\text{CD69}^+\text{HY}^{\text{cd4}}\text{M DP}$ population (**Fig 3-**

7B). Neither the T3.70⁺CD69⁺HY^{cd4}F DP population nor the T3.70⁺CD69⁺HY^{cd4}M DP population has increased expression of Runx3 compared to the T3.70⁺CD69⁻HY^{cd4}D^{b/-} DP population. However, as with the above genes, expression of Runx3 is similar between T3.70⁺HY^{cd4}M DP PD-1⁻ and T3.70⁺HY^{cd4}M DP PD-1⁺ thymocytes (p=0.1720).

CCR7, a chemokine receptor important in thymocyte migration from the cortex to the medulla (49), has increased expression in the T3.70⁺CD69⁺HY^{cd4}F SP8 population over the T3.70⁺CD69⁺HY^{cd4}F DP population (p=0.0063), as expected (**Fig 3-7C**). CCR7 is only slightly upregulated in T3.70⁺CD69⁺HY^{cd4}F DP thymocytes over T3.70⁺CD69⁻HY^{cd4}D^{b/-} DP thymocytes and its expression is slightly downregulated in T3.70⁺CD69⁺HY^{cd4}M DP thymocytes. CCR7 expression levels are similar between T3.70⁺HY^{cd4}M DP PD-1⁻ and T3.70⁺HY^{cd4}M DP PD-1⁺ thymocytes (p=0.4386), indicating that PD-1⁻ and PD-1⁺ thymocytes have the same ability to migrate to the medulla following positive selection. Kruppel-like factor 2 (KLF2) is a transcription factor that is important for thymic egress (92). There was no significant increase in expression of KLF2 in the T3.70⁺CD69⁺HY^{cd4}F SP8 population over the T3.70⁺CD69⁺HY^{cd4}F DP population (p=0.3305) (**Fig 3-7D**). This could be because KLF2 may be expressed transiently, just as the thymocytes exit the thymus. As with many of the other genes examined, there was no difference in KLF2 expression between the T3.70⁺HY^{cd4}M DP PD-1⁻ and T3.70⁺HY^{cd4}M DP PD-1⁺ populations.

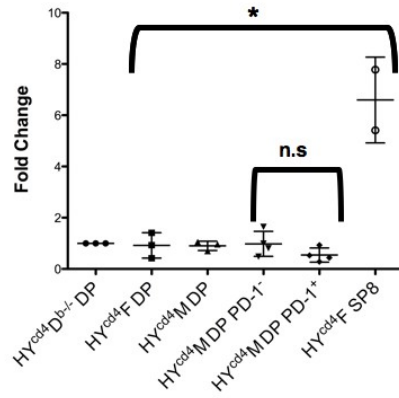
A

2610019F03Rik



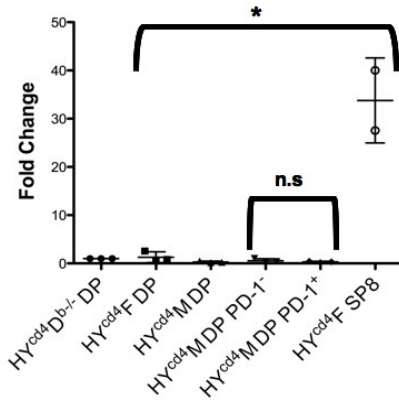
B

Runx3



C

CCR7



D

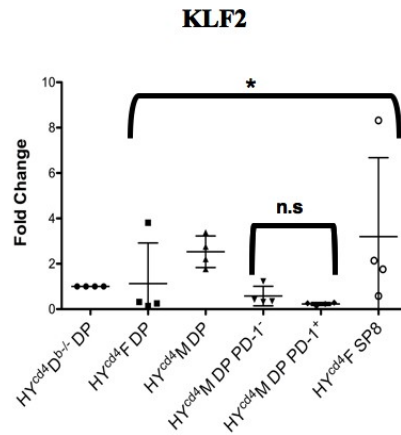


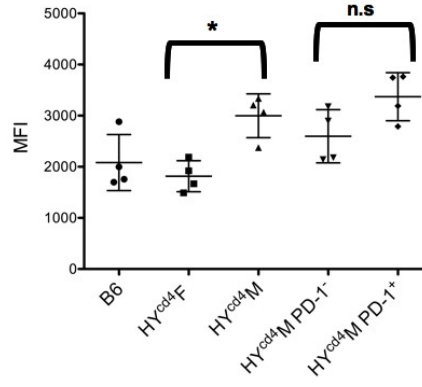
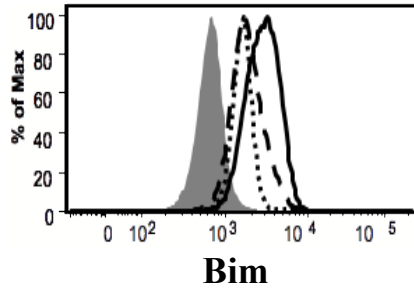
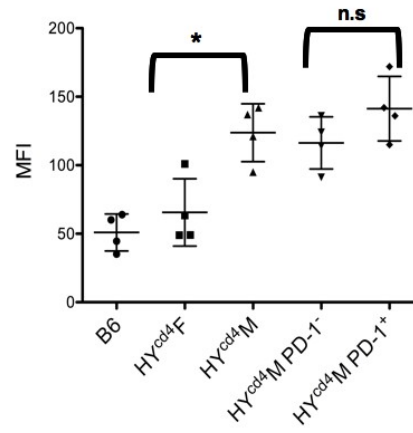
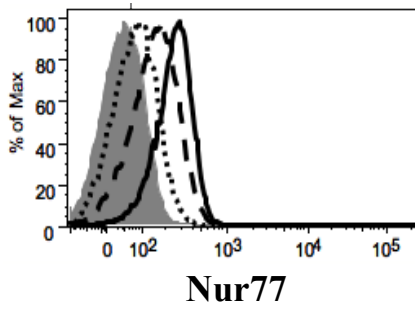
Figure 3-7: Comparison of 2610019F03Rik, Runx3, CCR7, and KLF2 gene expression between T3.70⁺CD69⁻HY^{cd4}D^{b/-} DP, T3.70⁺CD69⁺HY^{cd4}F DP, T3.70⁺CD69⁺HY^{cd4}M DP, T3.70⁺HY^{cd4}M DP PD-1⁻, T3.70⁺HY^{cd4}M DP PD-1⁺, and T3.70⁺CD69⁺HY^{cd4}F SP8 populations. The $\Delta\Delta\text{Ct}$ method was used to calculate fold change with β -actin as the reference gene and T3.70⁺CD69⁻HY^{cd4}D^{b/-} DP as the reference population. A) 2610019F03Rik, * indicates p=0.0144, ** indicates p=0.0188, n=6 for all populations, B) Runx3, * indicates p=0.0096, n=3 for T3.70⁺CD69⁻HY^{cd4}D^{b/-} DP, T3.70⁺CD69⁺HY^{cd4}F DP, and T3.70⁺CD69⁺HY^{cd4}M DP, n=4 for T3.70⁺HY^{cd4}M DP PD-1⁻ and T3.70⁺HY^{cd4}M DP PD-1⁺, n=2 for T3.70⁺CD69⁺HY^{cd4}F SP8. C) CCR7, * indicates p=0.0063, n=3 for all populations except T3.70⁺CD69⁺HY^{cd4}F SP8, where n=2. D) KLF2, n=4 for all populations. At least two biological replicates were used for the T3.70⁺HY^{cd4}M DP PD-1⁻ and T3.70⁺HY^{cd4}M DP PD-1⁺ populations. n.s.= not statistically significant.

Taken together, the gene expression profiles described above indicate that expression of apoptotic genes associated with negative selection are upregulated in T3.70⁺CD69⁺HY^{cd4}M DP thymocytes over T3.70⁺CD69⁺HY^{cd4}F DP thymocytes, T3.70⁺CD69⁺HY^{cd4}F SP8 thymocytes and T3.70⁺CD69⁻HY^{cd4}D^{b-/-} DP thymocytes. The expression level of these genes in T3.70⁺HY^{cd4}M DP PD-1⁻ and T3.70⁺HY^{cd4}M DP PD-1⁺ thymocytes are not different indicating that PD-1 expression does not affect expression of genes associated with clonal deletion. In addition, Runx3 expression levels indicate that lineage commitment to the CD8⁺ T cell lineage is not different in HY^{cd4}M PD-1⁺ or PD-1⁻ DP thymocytes. The expression profile of 2610019F03Rik indicates that this gene may be involved in positive selection. However, while the increased downregulation of 2610019F03Rik in PD-1⁺ thymocytes over PD-1⁻ thymocytes is interesting, further characterization of this gene is necessary before conclusions can be made about the significance of its expression pattern during negative selection. In addition, the RT-PCR results also indicate that T3.70⁺CD69⁺HY^{cd4}F SP8 thymocytes have increased ability to enter the medulla, and that PD-1⁻ and PD-1⁺ thymocytes have similar expression of motility and thymic egress genes.

Expression of proteins associated with apoptosis in PD-1⁺ and PD-1⁻ thymocytes examined directly *ex vivo*

Flow cytometry was performed on a selection of the genes examined by RT-PCR to confirm their expression at the protein level. Similar to the RT-PCR results, both Bim and Nur77 expression was significantly increased in T3.70⁺HY^{cd4}M DP thymocytes over T3.70⁺HY^{cd4}F DP thymocytes (p=0.0041 and p=0.0115, respectively) (**Fig 3-8A,B**). Also, similar to the RT-PCR results, T3.70⁺HY^{cd4}M DP PD-1⁻ and T3.70⁺HY^{cd4}M DP PD-1⁺ thymocytes expressed similar amounts of Bim and Nur77 (p=0.0692 and p=0.1501). Interestingly, expression of Bcl-2, an anti-apoptotic protein, was found to be upregulated in the in T3.70⁺HY^{cd4}M DP thymocytes over T3.70⁺HY^{cd4}F DP thymocytes (p=0.0303) (**Fig 3-8C**). This was also seen in the microarray: Bcl-2 was upregulated 2.98 fold in negative selection over non-selection and 3.56 fold in negative selection over positive selection (127). Furthermore, Bcl-2 is upregulated in T3.70⁺HY^{cd4}M DP PD-1⁺ thymocytes over T3.70⁺HY^{cd4}M DP PD-1⁻ thymocytes (p=0.0095). Taken together, it appears as though PD-1⁻ and PD-1⁺ thymocytes have a similar expression profile of pro-apoptotic genes while PD-1⁺ thymocytes have increased levels of Bcl-2. Since a comparison of gene expression is not a specific indicator of clonal deletion, the levels of cleaved caspase 3 were compared between PD-1⁻ and PD-1⁺ thymocytes as a more downstream and direct indicator of apoptosis. As previously published, levels of cleaved caspase 3 are similar between B6 DPs and T3.70⁺HY^{cd4}F DPs, while they are increased in T3.70⁺HY^{cd4}M DPs (p=0.0021) (102) (**Fig 3-9A,B**).

While there is a modest increase in the percentage of PD-1⁻ cells expressing cleaved caspase 3 compared to PD-1⁺ cells, the difference is not statistically significant (p=0.5552). Therefore, it appears that T3.70⁺HY^{cd4}M DP PD-1⁻ and T3.70⁺HY^{cd4}M DP PD-1⁺ thymocytes undergo similar amounts of apoptosis.

A**B**

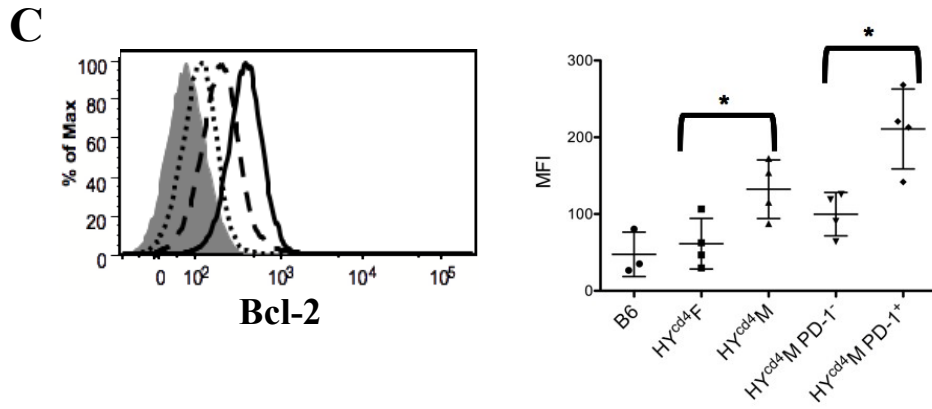


Figure 3-8: Expression of Bim, Nur77, and Bcl-2. Expression of Bim (A), Nur77 (B), and Bcl-2 (C) in total thymocytes (B6) or T3.70⁺ thymocytes for the indicated mouse (top) as determined by flow cytometry. Compilations of Bim (A), Nur77 (B), and Bcl-2 (C) MFIs of total (B6) or T3.70⁺ DP thymocytes for indicated mouse (bottom). B6 = shaded, HY^{cd4}F = short dashed line, HY^{cd4}M PD-1⁻ = long dashed line, HY^{cd4}M PD-1⁺ = solid black line.

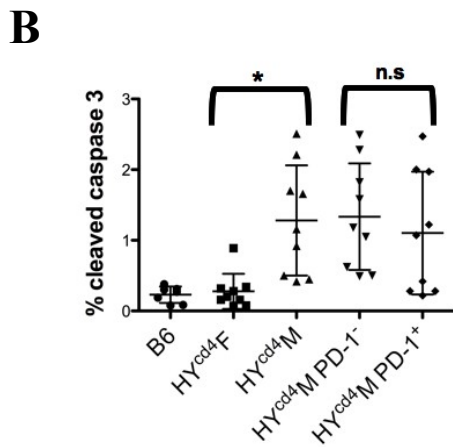
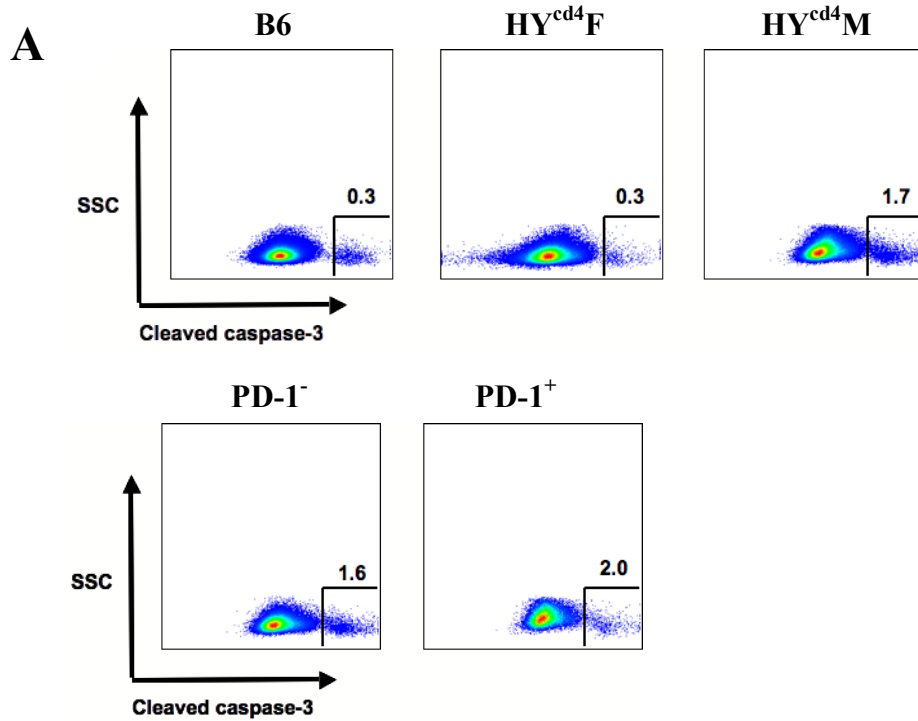


Figure 3-9: Levels of cleaved caspase 3. A) Levels of cleaved caspase 3 in total DP (B6) or T3.70⁺ DP (HY^{cd4}F, HY^{cd4}M, HY^{cd4}M PD-1⁻, and HY^{cd4}M PD-1⁺), as indicated, as determined by flow cytometry. B) Compilation of levels of cleaved caspase 3 in populations described in (A), * indicates p=0.0021, n=7 for B6, n=9 for HY^{cd4}F, HY^{cd4}M, HY^{cd4}M PD-1⁻, and HY^{cd4}M PD-1⁺.

***In vitro* stimulation of PD-1⁻ and PD-1⁺ thymocytes**

Examination of thymocytes directly *ex vivo* can be problematic for many reasons. It is difficult to control the timing of exposure to antigen-presenting cells (APCs) or the type of APC encountered by the thymocyte. Thus, we developed an *in vitro* stimulation assay where the ratio of thymocytes to antigen-presenting cells, the concentration of male peptide, and the time of exposure can be controlled to further study the fate of PD-1⁻ versus PD-1⁺ thymocytes after high-affinity antigen encounter.

HY^{cd4}M and HY^{cd4}F thymocytes were incubated with smcy-pulsed B6 splenocytes for 3h, after which, levels of cleaved caspase 3, relative to the levels of cleaved caspase 3 with no smcy, were examined. Prior to conducting the stimulation experiments, we examined the phenotype of the B6 splenocytes to determine the dominant type of APC(s), as well as the expression of PD-1 ligands, PD-L1 and PD-L2. A representative analysis of the composition of B6 splenocytes is depicted in **Fig 3-10**. After gating on the TCRβ⁻ population, the splenocytes consisted of approximately 47.2% B cells as indicated by CD19 expression, 10.9% DCs as indicated by CD11c expression, and 2% macrophages as indicated by absence of CD11c and expression of CD11b (**Fig 3-10**). The B cells, DCs, and macrophages all expressed PD-L1 but expressed very little PD-L2.

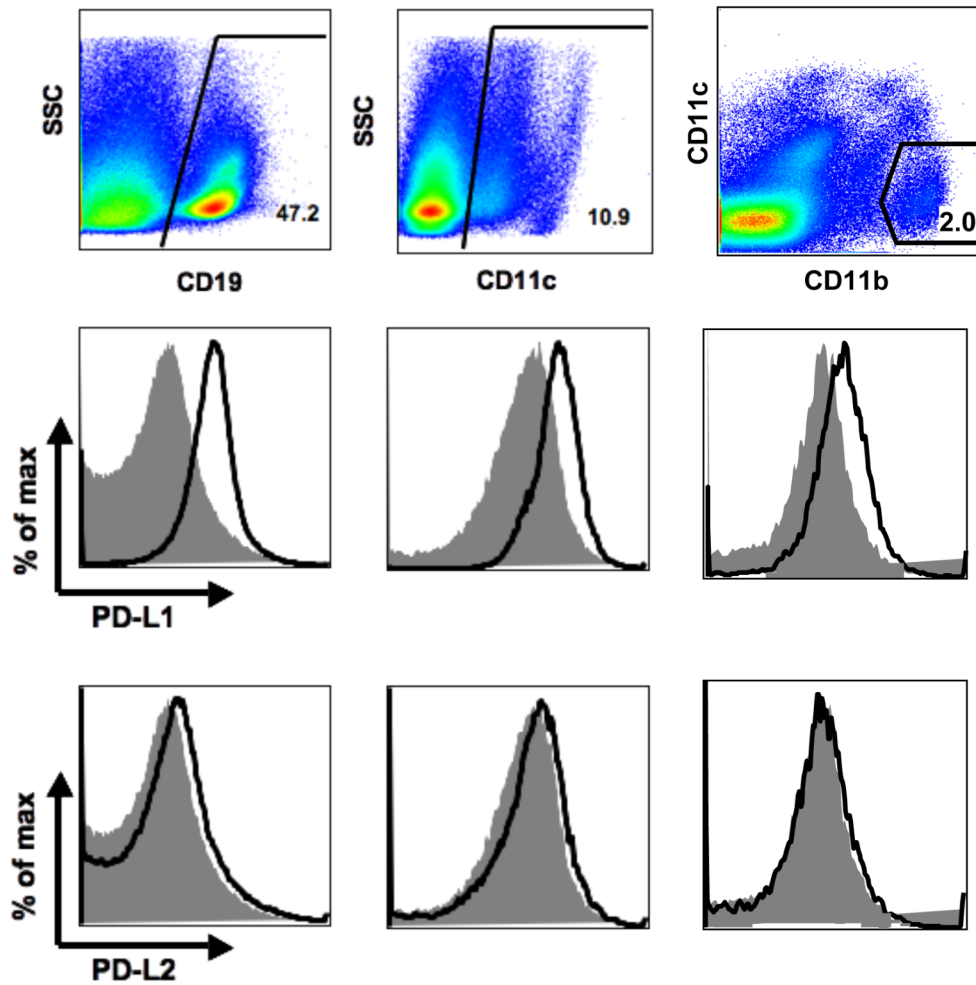
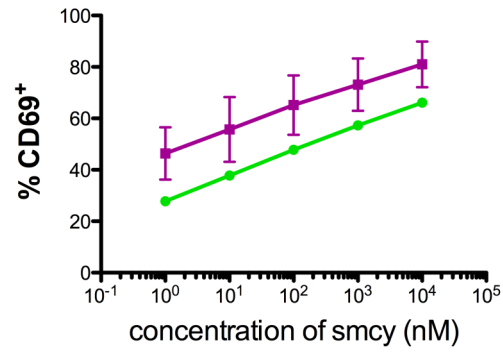


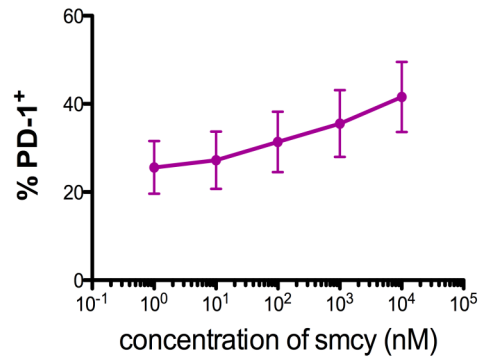
Figure 3-10: Phenotyping of B6 splenocytes. Percentage of splenocytes that are B cells (TCR β ⁻CD19⁺), DCs (TCR β ⁻CD11c⁺), and macrophages (TCR β ⁻CD11c⁻CD11b⁺). Below, histograms showing PD-L1 and PD-L2 expression for each cell type.

There were increases in CD69-expressing cells with increasing concentrations of male antigen with both $\text{HY}^{\text{cd4}}\text{F}$ and $\text{HY}^{\text{cd4}}\text{M}$ T3.70^+ DP thymocytes (**Fig 3-11A**). This indicates that the thymocytes became increasingly activated with higher concentrations of male antigen. In addition, the percentage of PD-1^+ cells in the T3.70^+ $\text{HY}^{\text{cd4}}\text{M}$ DP population increased with increasing concentration of antigen (**Fig 3-11B**). As expected, after 3h, the T3.70^+ $\text{HY}^{\text{cd4}}\text{F}$ DP thymocytes showed increasing amounts of cleaved caspase 3, and therefore apoptosis, with increasing concentrations of male antigen (**Fig 3-11C**). Surprisingly, levels of apoptosis in the bulk T3.70^+ $\text{HY}^{\text{cd4}}\text{M}$ DP thymocytes decreased slightly with increasing concentration of antigen (**Fig 3-11C**). When T3.70^+ $\text{HY}^{\text{cd4}}\text{M}$ DP PD-1^- and T3.70^+ $\text{HY}^{\text{cd4}}\text{M}$ DP PD-1^+ thymocytes were examined separately, it was revealed that the T3.70^+ $\text{HY}^{\text{cd4}}\text{M}$ DP PD-1^- thymocytes undergo increasing apoptosis with increasing amount of antigen, while, unexpectedly, the T3.70^+ $\text{HY}^{\text{cd4}}\text{M}$ DP PD-1^+ thymocytes undergo decreasing amounts of apoptosis, relative to the level of apoptosis at zero antigen (**Fig 3-11C**). Anti-PD-L1 blocking antibody at concentrations of $10\mu\text{g}/\text{mL}$ or $30\mu\text{g}/\text{mL}$ was added to the culture to block PD-1/PD-L1 interactions. Little effect was observed indicating that either PD-1 itself is not mediating the protection from apoptosis or that the antibody does not efficiently block PD-1/PD-L1 interactions *in vitro* (**Fig 3-11D**).

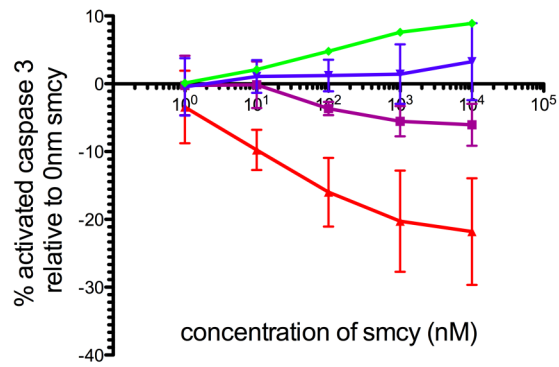
A



B



C



D

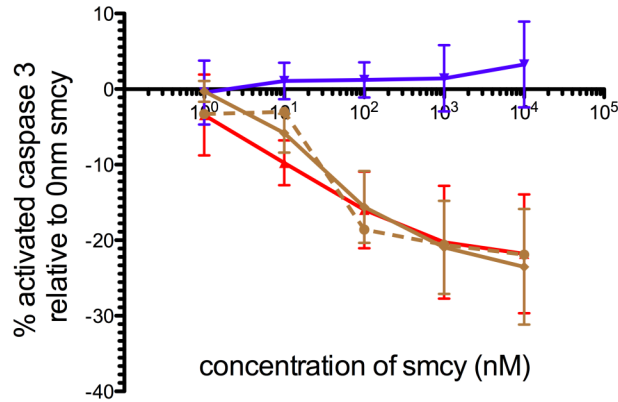


Figure 3-11: *In vitro* simulation of HY^{cd4}M and HY^{cd4}F thymocytes with B6 splenocytes pulsed at indicated concentrations of smcy. A) Percent of T3.70⁺ DP thymocytes expressing CD69. B) Percent of T3.70⁺ DP thymocytes expressing PD-1. C) Percent activated caspase 3, relative to percent activated caspase 3 at 0nM smcy, in T3.70⁺ DP thymocytes. D) Percent activated caspase 3, relative to percent activated caspase 3 at 0nM smcy, in T3.70⁺ DP thymocytes with or without addition of blocking anti-PD-L1 antibodies to the stimulation assay. T3.70⁺ HY^{cd4}F DP is in green (n=1), T3.70⁺ HY^{cd4}M bulk DP is in purple (n=4), T3.70⁺ HY^{cd4}M DP PD-1⁻ is in blue (n=4), T3.70⁺ HY^{cd4}M DP PD-1⁺ is in red (n=4), T3.70⁺ HY^{cd4}M DP PD-1⁺ with 10μg/mL anti-PD-L1 is in brown (n=3), T3.70⁺ HY^{cd4}M DP PD-1⁺ with 30μg/mL anti-PD-L1 is in dashed brown line (n=1).

However, it is important to note that only about 11% of the B6 splenocytes were DCs. This is significant because interaction with cortical dendritic cells (cDCs) has been shown to be important for inducing apoptosis of self-reactive thymocytes (112). Therefore, to establish a culture system that utilized APCs shown to be important for inducing apoptosis, DCs were cultured from B6 BM for use as APCs. The phenotype of the BM-derived DCs were CD11c⁺CD11b⁺Sirpα⁺CD8⁻, and therefore thought to be of the myeloid lineage (115) (**Fig 3-12**). Recent work has indicated that myeloid DCs found in the thymus are of extrathymic origin. They travel from the blood to the thymus where they then proliferate and increase in number, and are thought to contribute to tolerance to tissue-restricted antigens (116). The in vitro-generated BM-derived DCs expressed high levels of PD-L1 and a subset (73.3%) expressed a high level of PD-L2 (**Fig 3-12**). CD80 was highly expressed, while only 20.8% of DCs expressed high levels of CD86 (**Fig 3-13**). As expected, all the DCs expressed MHC Class I and 83.4% expressed high levels of MHC Class II (**Fig 3-13**). Only about 37.8% expressed CD40, a marker of DC activation (**Fig 3-13**). Anti-CD40 was added to the cell culture to activate the DCs. The phenotype of activated DCs was very similar to that of unstimulated DCs. There was no change in expression of Sirpα or CD8 (**Fig 3-12**). There was a slight increase in PD-L1, MHC Class I, and MHC Class II expression (**Fig 3-12, 3-13**). Anti-CD40 stimulation resulted in a slightly larger population with higher expression of PD-L2 (**Fig 3-12**), and a small population was induced to express increased levels of CD80 and CD86 (**Fig 3-13**). Surprisingly, there was only a slight increased in CD40 expression (**Fig 3-**

13). It was expected that most of the DCs would upregulate CD40 after activation, however it is possible that the anti-CD40 antibody used to activate the cells is blocking CD40.

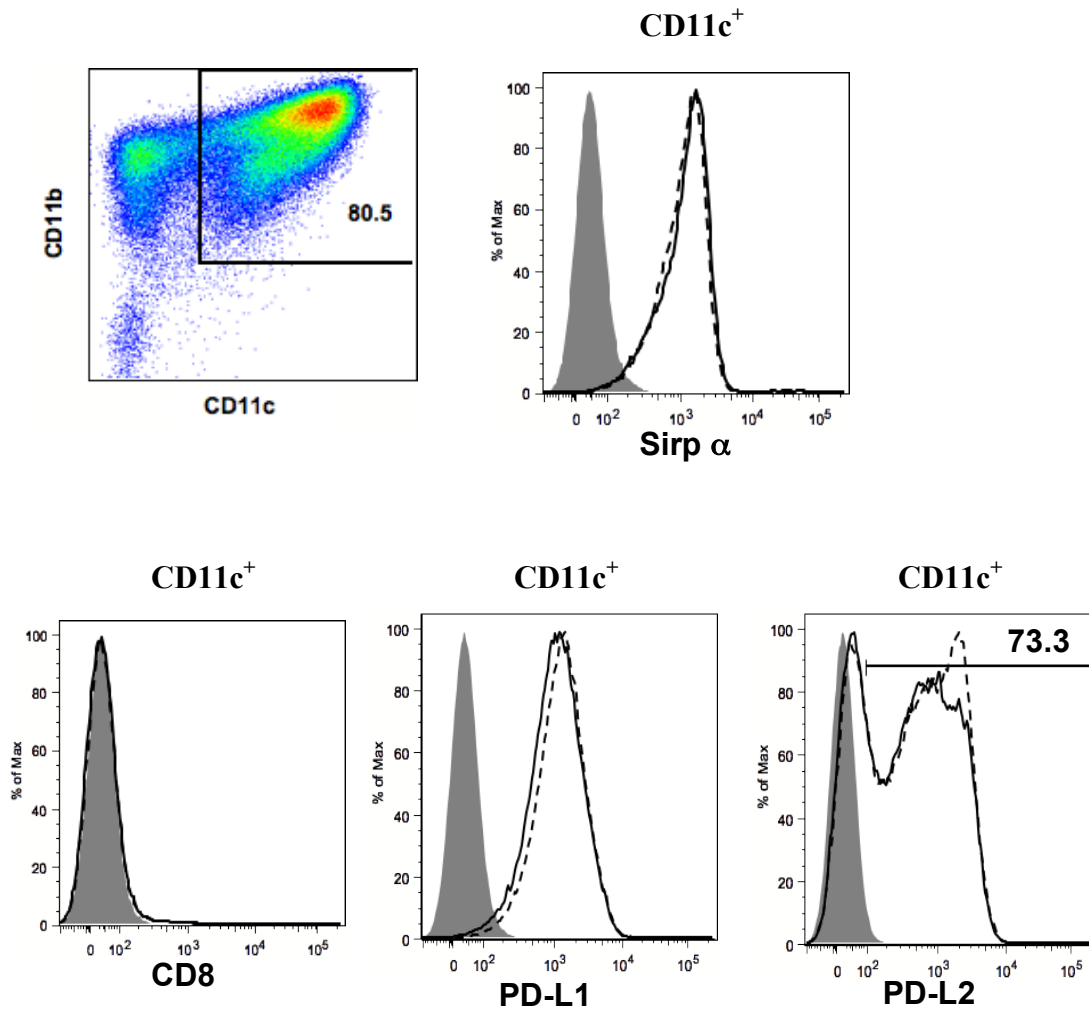


Figure 3-12: DCs generated from BM are of myeloid lineage and express PD-L1 and PD-L2. DCs were cultured from BM isolated from B6 mice and expression of CD11c, CD11b, Sirp α , CD8, PD-L1, and PD-L2 was examined, with and without overnight stimulation with anti-CD40. Unstimulated DCs = solid line, anti-CD40 stimulated DCs = dotted line. Numbers refer to percent of unstimulated DCs in gate.

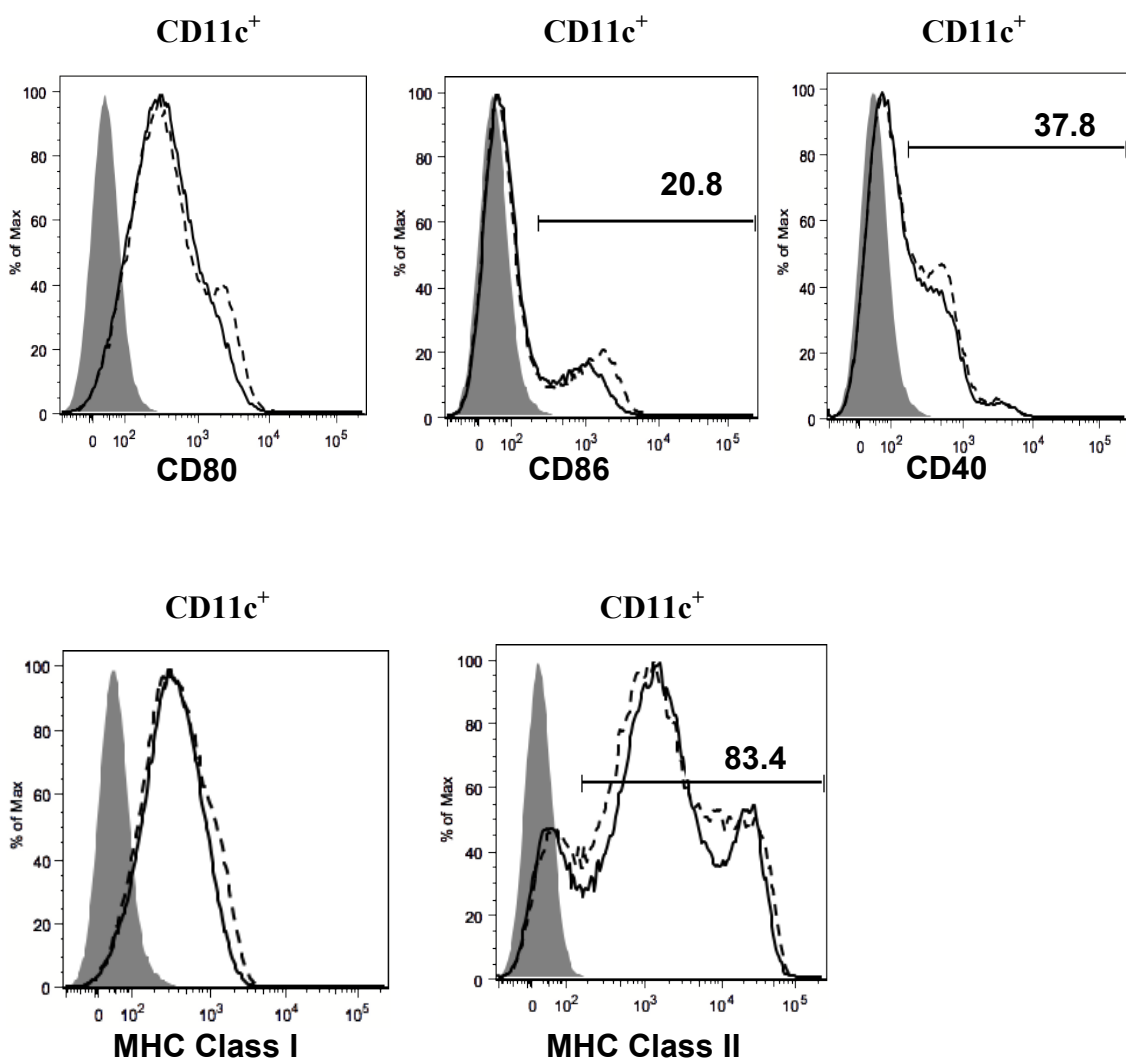
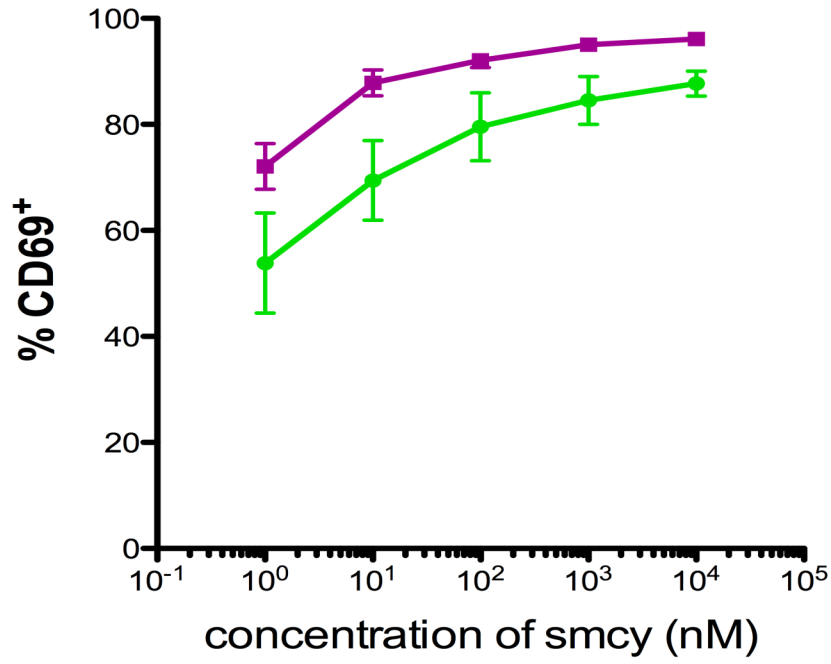


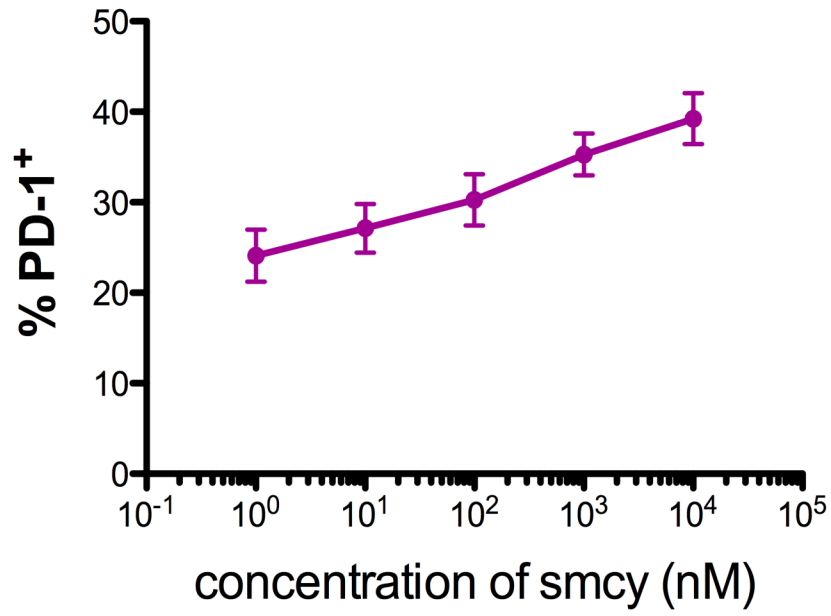
Figure 3-13: Phenotyping of BM-derived DCs. DCs were cultured from BM isolated from B6 mice and expression of CD80, CD86, CD40, MHC Class I, and MHC Class II was determined, with and without overnight stimulation with anti-CD40. Unstimulated DCs = solid line, anti-CD40 stimulated DCs = dotted line. Numbers refer to percent of unstimulated DCs in gate.

When the *in vitro* generated BM-derived DCs were used as APCs, T3.70⁺HY^{cd4}F DP thymocytes and T3.70⁺HY^{cd4}M DP PD-1⁻ thymocytes displayed an increase in caspase 3 activation with increasing concentration of smcy (**Fig 3-14C**). Increases in CD69 and PD-1 expression were also observed, as was seen with the stimulation assay using bulk splenocytes (**Fig 3-11A,B, Fig 3-14A,B**). The T3.70⁺HY^{cd4}M DP PD-1⁺ thymocytes, as they did after stimulation with bulk B6 splenocytes, seem to be protected from apoptosis, although magnitude of protection appears smaller (**Fig 3-14C**). These data suggest that PD-1 expressing thymocytes are protected from undergoing apoptosis when stimulated *in vitro* with high affinity antigen. Whether PD-1 itself mediates their protection is currently unclear.

A



B



C

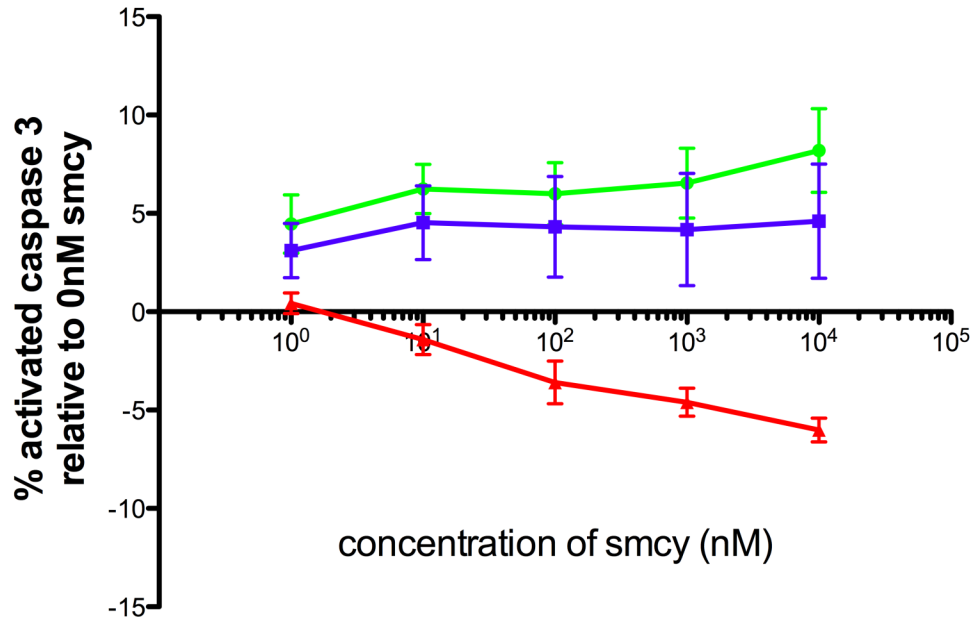


Figure 3-14: *In vitro* simulation of HY^{cd4}M and HY^{cd4}F thymocytes with BM-derived DCs at indicated concentrations of smcy. A) Percent of T3.70⁺ DP thymocytes expressing CD69. B) Percent of T3.70⁺ DP thymocytes expressing PD-1. C) Percent activated caspase 3, relative to percent activated caspase 3 at 0nM smcy, in T3.70⁺ DP thymocytes. T3.70⁺ HY^{cd4}F DP is in green, T3.70⁺ HY^{cd4}M bulk DP is in purple, T3.70⁺ HY^{cd4}M DP PD-1⁻ is in blue, and T3.70⁺ HY^{cd4}M DP PD-1⁺ is in red. n=5 for all populations.

Evaluation of factors that may protect PD-1⁺ thymocytes from apoptosis

As discussed above, it was unclear whether PD-1 was involved in mediating survival after encounter with high affinity antigen in the *in vitro* stimulation assay, or if PD-1 was simply a molecular marker of cells undergoing negative selection by a non-apoptotic mechanism. Therefore, the data generated by the previously discussed microarray (127) was re-examined to identify possible anergy factors that could contribute to this protection from apoptosis. Anergy factors were chosen because PD-1 is associated with anergy in the periphery (158), and as PD-1⁺ thymocytes are not responding to antigen, they could be anergic. Three genes with reported roles in anergy induction were selected for further study: Casitas B cell lymphoma-b (Cbl-b), early growth response gene (Egr)-2, and diacylglycerol kinase (Dgk) α .

Cbl-b

Cbl-b is a member of the Cbl family of RING-finger domain –containing E3 ubiquitin ligases and has been associated with the dampening of peripheral T cell responses (162). Cbl-b was upregulated 2.1 fold in negative selection over positive and non-selection in the microarray data mentioned above (127). To validate the gene array data, expression of Cbl-b was compared by RT-PCR using the isolated populations previously described (**Fig 3-5**). Cbl-b expression is similar between the T3.70⁺CD69⁺HY^{cd4}F DP and T3.70⁺CD69⁺HY^{cd4}M DP populations (**Fig 3-15A**). Interestingly, there is increased expression of Cbl-b in

the T3.70⁺HY^{cd4}M DP PD-1⁺ population over the T3.70⁺HY^{cd4}M DP PD-1⁻ population (p=0.0070) (**Fig 3-15A**). However, when Cbl-b was examined at the protein level using flow cytometry, there was no significant difference between the two populations (p=0.5545) (**Fig 3-15B**). To confirm the flow cytometry data, PD-1⁻ and PD-1⁺ T3.70⁺ DP thymocytes were purified, lysed, and a Western blot for Cbl-b was performed. There appears to be no difference in the level of Cbl-b protein between PD-1⁻ and PD-1⁺ thymocytes (**Fig 3-15C**).

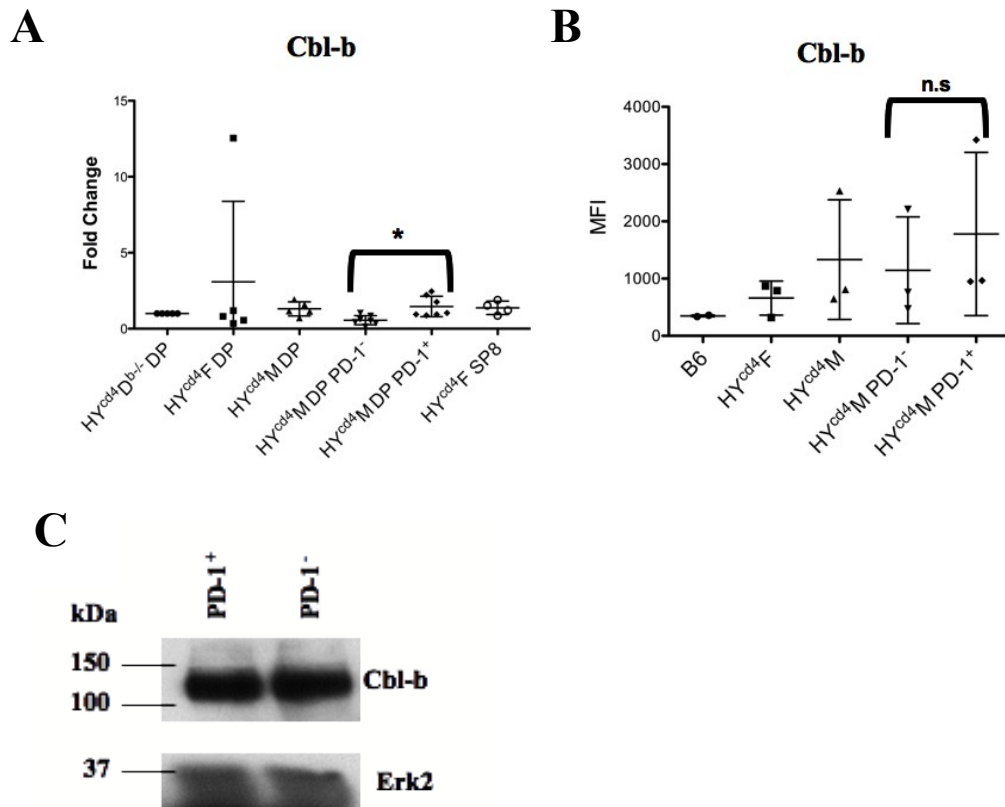


Figure 3-15: No difference in Cbl-b expression between PD-1⁻ and PD-1⁺ thymocytes. A) The $\Delta\Delta C_t$ method was used to calculate fold change with β -actin as the reference gene and T3.70⁺CD69⁻ HY^{cd4}D^{b/-} DP as the reference population. * indicates $p=0.007$, $n=5$ for T3.70⁺CD69⁻ HY^{cd4}D^{b/-} DP, T3.70⁺CD69⁺ HY^{cd4}F DP, and T3.70⁺CD69⁺ HY^{cd4}M DP. $n=7$ for T3.70⁺HY^{cd4}M DP PD-1⁻ and T3.70⁺HY^{cd4}M DP PD-1⁺ populations, and $n=4$ for T3.70⁺CD69⁺ HY^{cd4}F SP8. At least two biological replicates were used for the T3.70⁺HY^{cd4}M DP PD-1⁻ and T3.70⁺HY^{cd4}M DP PD-1⁺ populations. B) Compilation of MFI of Cbl-b expression as determined by intracellular flow cytometry. n.s.= not statistically significant. C) Lysates prepared from isolated T3.70⁺HY^{cd4}M DP PD-1⁻ and T3.70⁺HY^{cd4}M DP PD-1⁺ populations were blotting for Cbl-b and Erk2 for a loading control.

Egr-2

Egr-2 is a zinc finger transcription factor that has been identified as being important in anergy induction of peripheral T cells (163). In the microarray, *Egr-2* was induced 5 fold in positive selection over non-selection and 15 fold in negative selection over non-selection (127). Examination of *Egr-2* expression was examined by RT-PCR using the same populations as with *Cbl-b*. Expression levels were variable between replicates, but it appears that all populations upregulate *Egr-2* over the $T3.70^+ HY^{cd4}D^{b/-}$ population, and that expression of *Egr-2* is not significantly different between $T3.70^+ HY^{cd4}M DP PD-1^-$ and $PD-1^+$ thymocytes (**Fig 3-16A**).

Dgkα

Another gene examined was *Dgkα*. Although there was little change in its expression in the above mentioned microarray, it is associated with anergy through its inhibition of Ras (164). Relative expression levels of *Dgkα* between different thymocytes populations were examined as described above for *Cbl-b* and *Egr-2*. *Dgkα* appears to be downregulated in $T3.70^+ HY^{cd4}F DP$ and $T3.70^+ HY^{cd4}M DP$ populations compared to the $T3.70^+ HY^{cd4}D^{b/-}$ population (**Fig 3-16B**). There is no significant difference in *Dgkα* expression between the $T3.70^+ HY^{cd4}M DP PD-1^-$ and $PD-1^+$ populations (**Fig 3-16B**). Expression of *Dgkα* was variable between the two replicates. Taken together, these data indicate that *Cbl-b*, *Egr-2*, or *Dgkα* are not mediating the protection from apoptosis observed with $PD-1^+$ thymocytes in the *in vitro* stimulation assay.

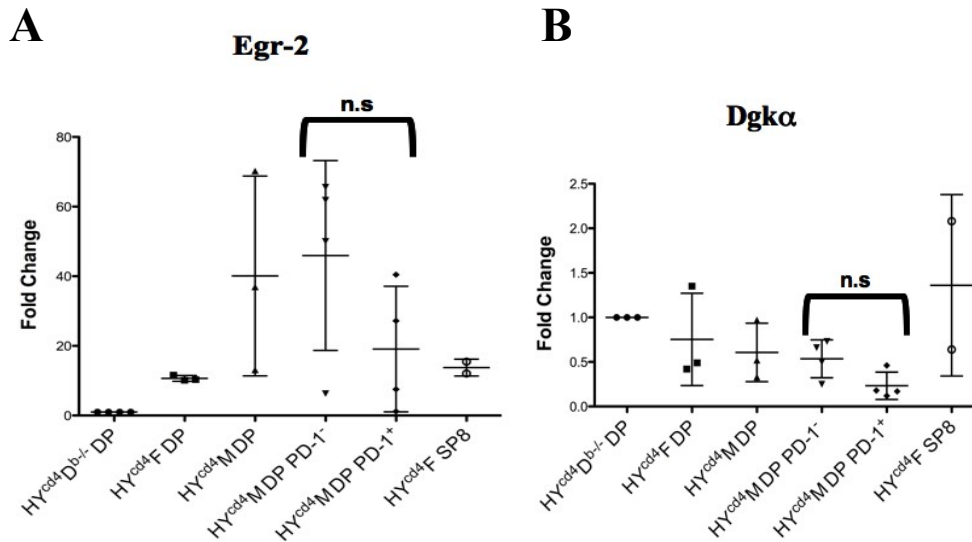


Figure 3-16: No difference in *Egr-2* or *Dgkα* expression between PD-1⁻ and PD-1⁺ thymocytes. The $\Delta\Delta C_t$ method was used to calculate fold change with β -actin as the reference gene and T3.70⁺CD69⁻HY^{cd4}D^{b/-} DP as the reference population for *Egr-2* (A) and *Dgkα* (B). n=3 for T3.70⁺CD69⁻HY^{cd4}D^{b/-} DP, T3.70⁺CD69⁺HY^{cd4}F DP, and T3.70⁺CD69⁺HY^{cd4}M DP, n=4 for T3.70⁺HY^{cd4}M DP PD-1⁻ and T3.70⁺HY^{cd4}M DP PD-1⁺ populations, and n=2 for T3.70⁺CD69⁺HY^{cd4}F SP8. At least two biological replicates were used for the T3.70⁺HY^{cd4}M DP PD-1⁻ and T3.70⁺HY^{cd4}M DP PD-1⁺ populations. n.s.= not statistically significant.

pERK

ERK is a serine/threonine mitogen activated protein kinase (MAPK) and its activation is important in signaling through the TCR (165). Recently, using an induced tolerance model, it was shown that PD-1/PD-L1 interactions in the periphery are associated with decreased levels of pERK resulting in an impairment of T cell conjugation with APCs (166). Based on this data, we predicted that T3.70⁺HY^{cd4}M DP PD-1⁻ thymocytes would exhibit increased levels of pERK over T3.70⁺HY^{cd4}M DP PD-1⁺ thymocytes. T3.70⁺HY^{cd4}M DP PD-1⁻ and T3.70⁺HY^{cd4}M DP PD-1⁺ populations were isolated by cell sorting as described previously (**Fig 3-4**). The thymocytes were then stimulated *in vitro* with smcy-pulsed BM-derived DCs and levels of ERK activation were measured. The results indicated that there was no difference in pERK levels between the two populations (**Fig 3-17**). Taken together, the above data suggest that the protection of PD-1⁺ thymocytes from apoptosis in the *in vitro* stimulation assay is not mediated by increased levels of Cbl-b, Egr-2, Dgk α , or pERK.

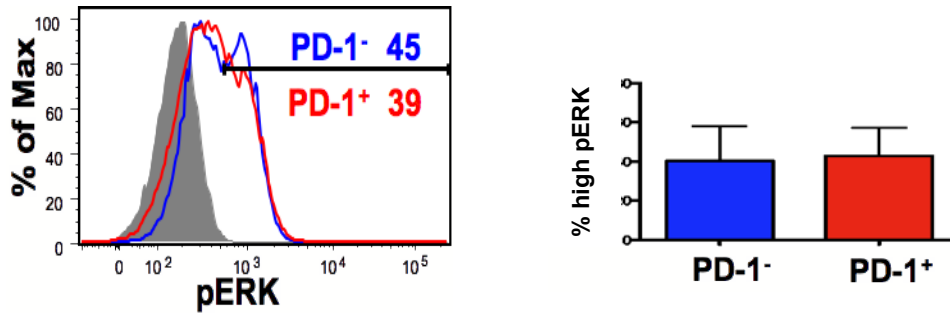


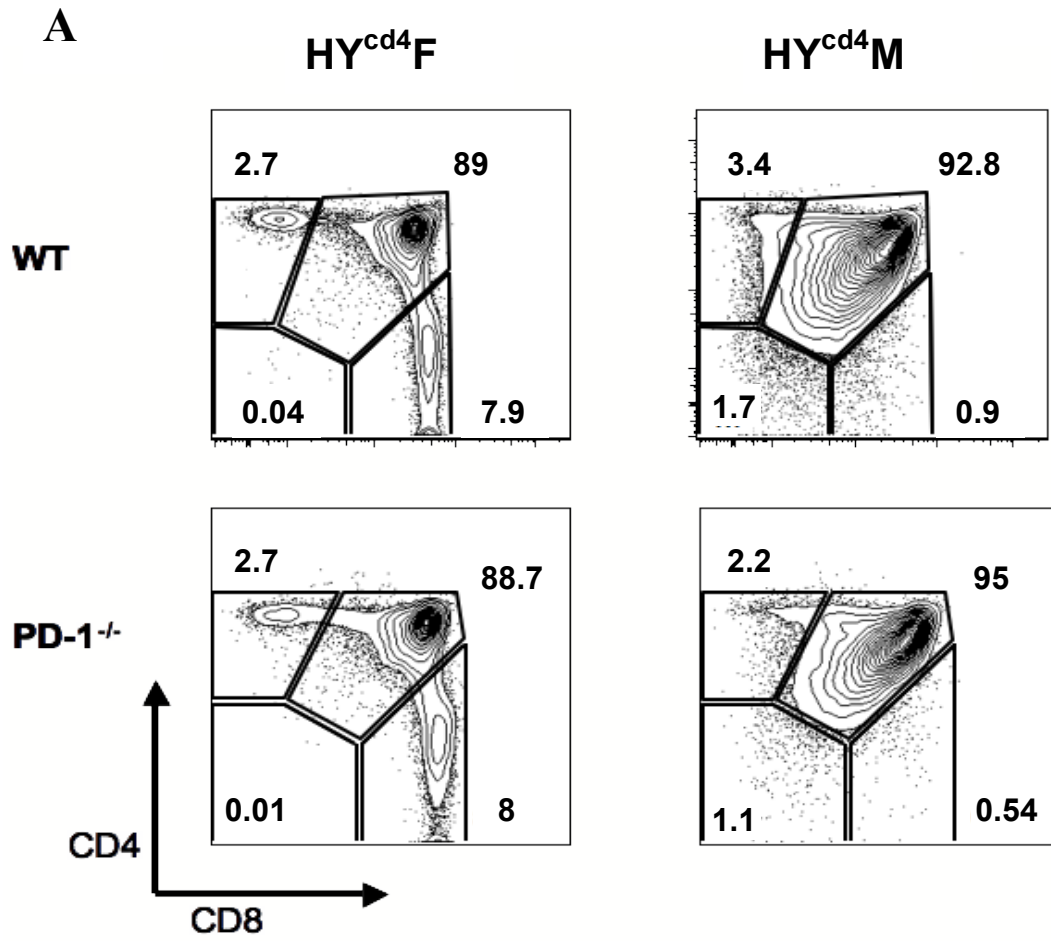
Figure 3-17: No difference in pERK expression between PD-1⁻ and PD-1⁺ thymocytes. Representative histogram (left) and compilation of percent high pERK (right) for T3.70⁺ HY^{cd4}M DP PD-1⁻ and PD-1⁺ thymocytes as determined by flow cytometry. PD-1⁻ in blue, PD-1⁺ in red. Numbers in histogram are MFI of the indicated population. T3.70⁺ HY^{cd4}M DP PD-1⁻ and PD-1⁺ thymocytes were isolated, cultured with smcy-pulsed DCs, and then stained for pERK.

Characterization of HY^{cd4} PD-1 deficient mice

Thymus

To determine whether PD-1 expression functions to directly modulate negative selection, we crossed HY^{cd4} mice to mice deficient in PD-1. These HY^{cd4}PD-1^{-/-} mice allow us to specifically determine the role of PD-1 in thymic selection. The CD4/CD8 plots of T3.70⁺ HY^{cd4}F PD-1^{-/-} thymocytes and T3.70⁺ HY^{cd4}M PD-1^{-/-} thymocytes were very similar to the HY^{cd4} PD-1 sufficient mice (**Fig 3-18A**), as were the absolute numbers of DP and SP8 thymocytes (**Fig 3-18B**), indicating that positive and negative selection still occurs in the absence of PD-1. Expression of CD24 was examined to determine the level of maturity of the T3.70⁺ DP thymocytes. HY^{cd4}F, HY^{cd4}F PD-1^{-/-}, HY^{cd4}M, and HY^{cd4}M PD-1^{-/-} had increased expression of CD24 compared to B6 DP thymocytes, indicating that they may be less mature (**Fig 3-19A**). HY^{cd4}F PD-1^{-/-} mice had slightly decreased levels of CD24 than HY^{cd4}F, suggesting that, in a model of positive selection, PD-1 deficiency results in increased maturity at the DP stage (**Fig 3-19A**). However, in the HY^{cd4}M, PD-1 sufficient and deficient T3.70⁺ DP thymocytes appeared to express similar levels of CD24 (**Fig 3-19A**). Expression of CD2, CD5, and CD69 early activation markers was also examined. B6 DP thymocytes displayed the lowest expression of CD2, CD5, and CD69, and all MFI values are displayed relative the MFI for B6 DP thymocytes (**Fig 3-19B,C,D**). As expected, T3.70⁺ HY^{cd4}F DP thymocytes had increased expression of CD2, CD5, and CD69 compared to B6 DP thymocytes, indicating that the thymocytes receive increased

signal through their TCR during positive selection (**Fig 3-19B,C,D**). Expression levels of CD2 and CD5 were similar between T3.70⁺ HY^{cd4}F DP thymocytes and T3.70⁺ HY^{cd4}F PD-1^{-/-} DP thymocytes (**Fig 3-19B,C**), while slightly higher levels of CD69 were observed in the PD-1 deficient thymocytes over the PD-1 sufficient thymocytes (**Fig 3-19D**), suggesting that the thymocytes may receive more signal in the absence of PD-1. Expression of CD2, CD5, and CD69 was higher in the T3.70⁺ HY^{cd4}M DP thymocytes than in the T3.70⁺ HY^{cd4}F DP thymocytes, confirming that a stronger signal is received during negative selection than positive selection (**Fig 3-19B,C,D**). There was slightly higher expression of CD2, CD5, and CD69 in the T3.70⁺ HY^{cd4}M PD-1^{-/-} DP thymocytes than in the T3.70⁺ HY^{cd4}M DP thymocytes, again indicating that increased signal is received in the absence of PD-1 (**Fig 3-19B,C,D**). Additionally, comparison of PD-1 levels between the mice revealed that T3.70⁺ HY^{cd4}M PD-1^{-/-}, T3.70⁺ HY^{cd4}F PD-1^{-/-}, and T3.70⁺ HY^{cd4}F DP thymocytes expressed practically no PD-1, B6 DP thymocytes expressed a low amount of PD-1, and that T3.70⁺ HY^{cd4}M DP thymocytes have two populations of cells expressing different levels of PD-1 (**Fig 3-20**). Importantly, the population previously identified as PD-1⁻ still expresses low levels of PD-1 when compared to the PD-1^{-/-}.



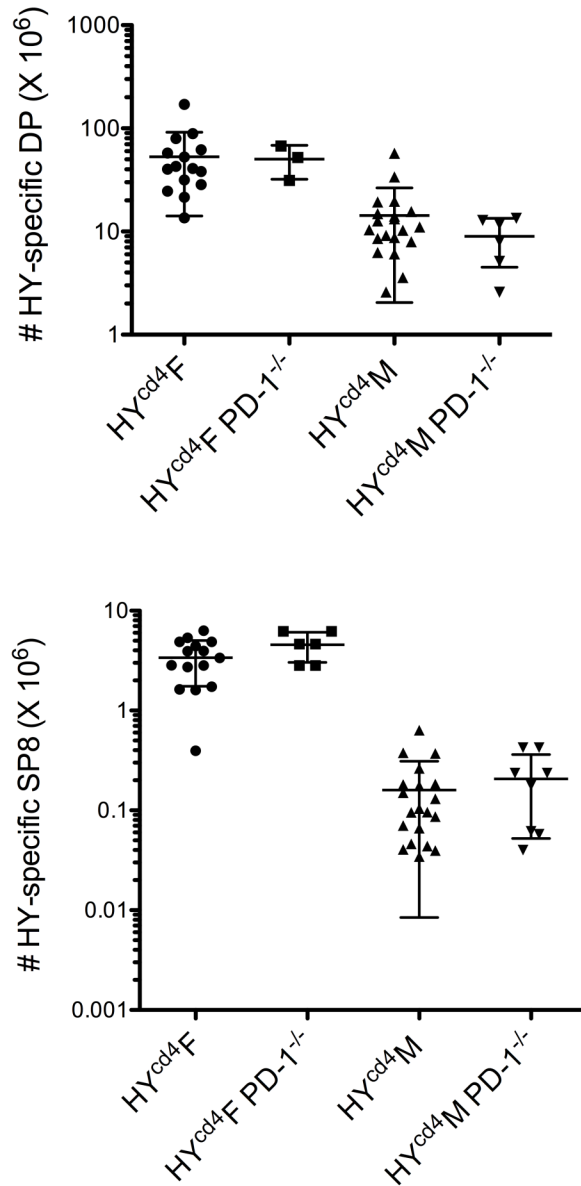
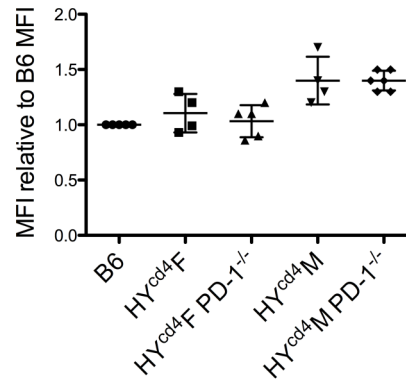
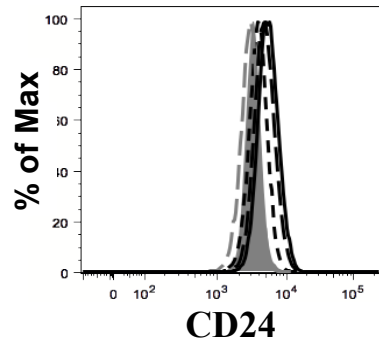
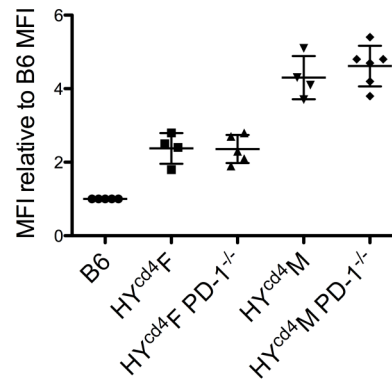
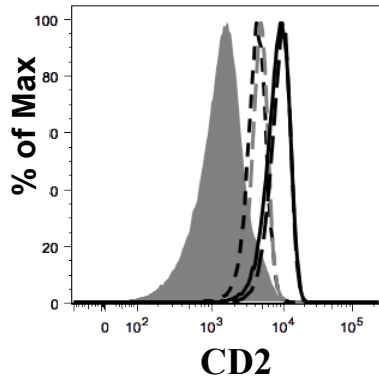
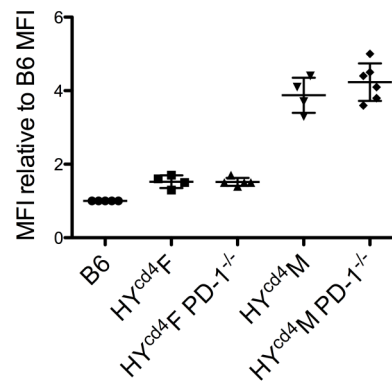
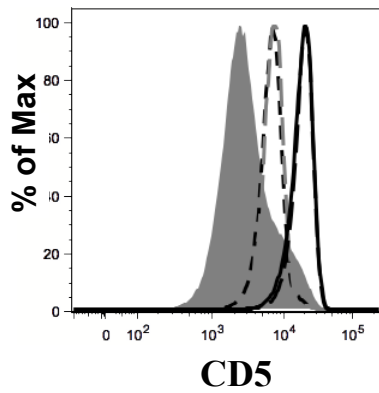
B

Figure 3-18: PD-1 deficiency does not impair negative selection. (A)

Representative CD4 by CD8 profiles of T3.70⁺ thymocytes from HY^{cd4}F, HY^{cd4}M, HY^{cd4}F PD-1^{-/-}, and HY^{cd4}M PD-1^{-/-} mice. (B) Absolute numbers of T3.70⁺ of DP and SP8 thymocytes. n=15 for HY^{cd4}F, n=3 for HY^{cd4}F PD-1^{-/-}, n=20 for HY^{cd4}M, and n=6 for HY^{cd4}M PD-1^{-/-}.

A**B****C**

D

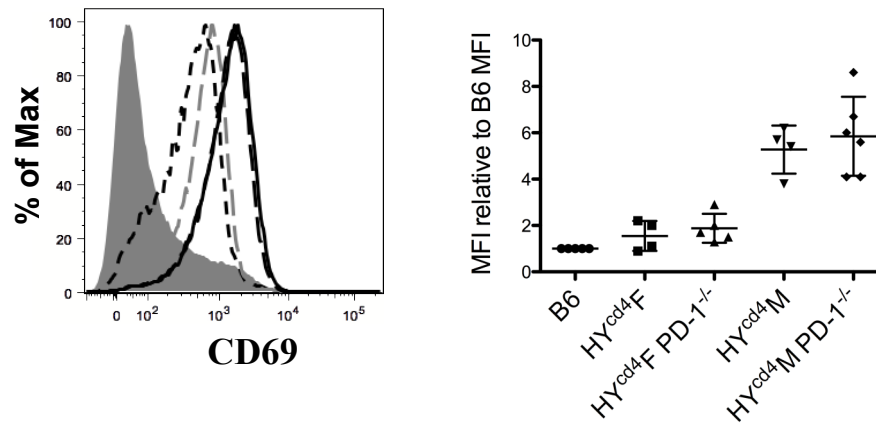


Figure 3-19: T3.70⁺ HY^{cd4}M DP thymocytes express slightly higher levels of activation markers. Representative histograms (left) and compilations of MFI relative to B6 DP (right) for CD24 (A), CD2 (B), CD5 (C), and CD69 (D). B6 DP = shaded, T3.70⁺ HY^{cd4}F DP= short dashed line, T3.70⁺ HY^{cd4}F DP PD-1^{-/-} = long dashed grey line, T3.70⁺ HY^{cd4}M DP = solid black line, T3.70⁺ HY^{cd4}M DP PD-1^{-/-} = long dashed line.

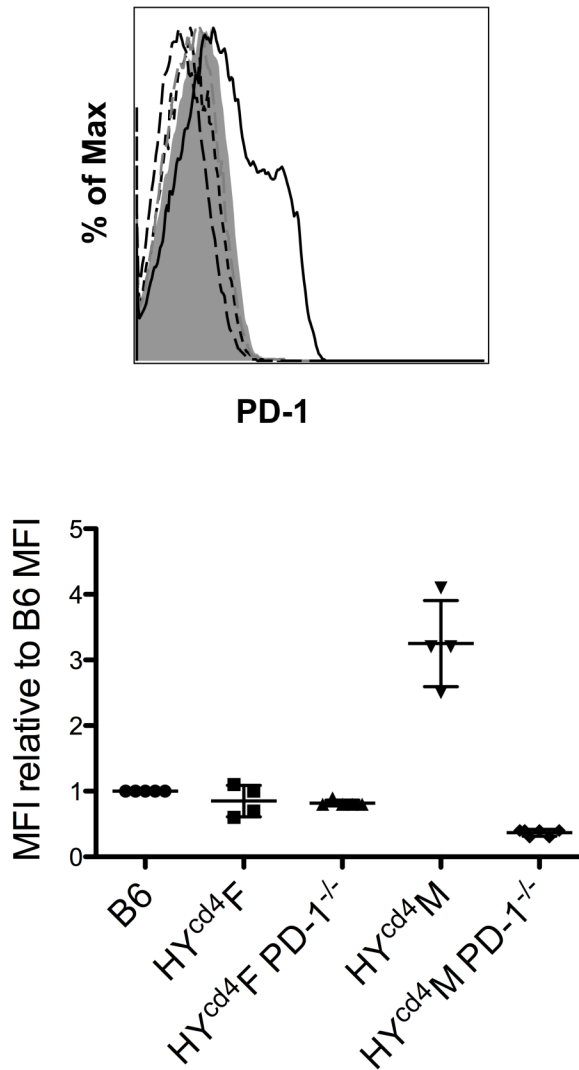
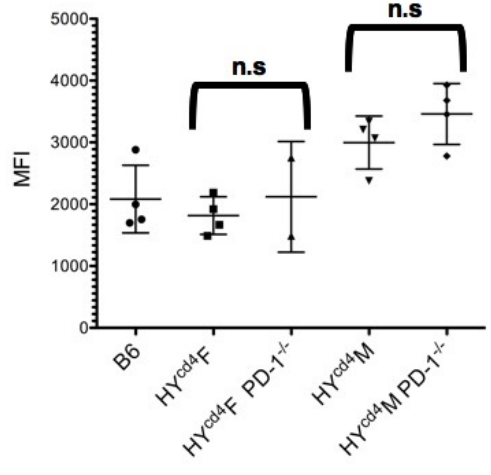
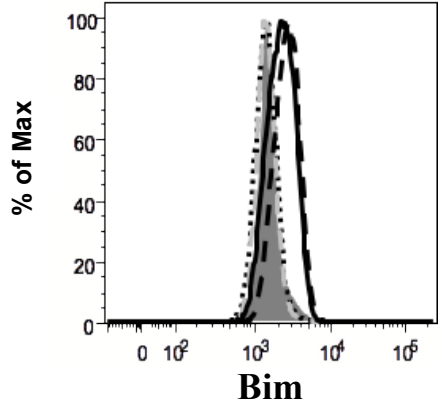


Figure 3-20: T3.70⁺ HY^{cd4}M DP PD-1⁻ thymocytes still express low levels of PD-1. Representative histogram (top) and compilation of MFI relative to B6 DP (bottom) for PD-1 expression, as determined by flow cytometry. B6 DP = shaded, T3.70⁺ HY^{cd4}F DP = short dashed line, T3.70⁺ HY^{cd4}F DP PD-1^{-/-} = long dashed grey line, T3.70⁺ HY^{cd4}M DP = solid black line, T3.70⁺ HY^{cd4}M DP PD-1^{-/-} = long dashed line.

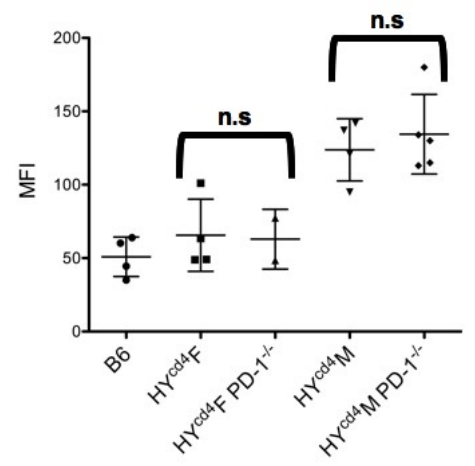
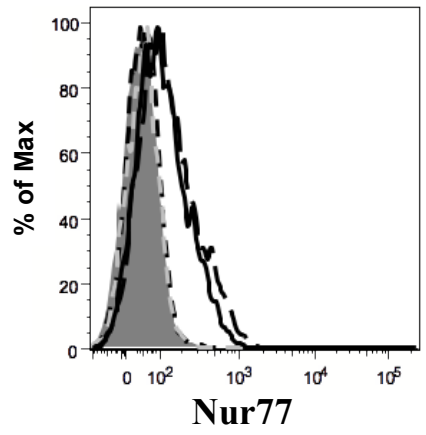
The expression of proteins important in regulating apoptosis was also compared between the PD-1 deficient and PD-1 sufficient DP thymocytes. As expected, T3.70⁺ HY^{cd4}F DP thymocytes expressed the lowest amount of Bim (**Fig 3-21A**). T3.70⁺ HY^{cd4}F PD-1^{-/-} DP thymocytes displayed variable expression of Bim (**Fig 3-21A**). As expected, T3.70⁺ HY^{cd4}M DP thymocytes expressed higher levels of Bim compared to the B6 DP thymocytes and T3.70⁺ HY^{cd4}F DP thymocytes (**Fig 3-21A**). T3.70⁺ HY^{cd4}M PD-1^{-/-} DP thymocytes exhibited higher levels of Bim than their PD-1 sufficient counterparts (**Fig 3-21A**), suggesting that there are increased levels of Bim in the absence of PD-1. B6 DP thymocytes contained the lowest amount of Nur77, T3.70⁺ HY^{cd4}F PD-1 sufficient and deficient DP thymocytes contained intermediate levels of Nur77, and T3.70⁺ HY^{cd4}M DP thymocytes, along with T3.70⁺ HY^{cd4}M PD-1^{-/-} DP thymocytes contained the highest level of Nur77 (**Fig 3-21B**). B6 DP and T3.70⁺ HY^{cd4}F DP thymocytes expressed the lowest levels of Bcl-2, T3.70⁺ HY^{cd4}F PD-1^{-/-} DP thymocytes expressed variable levels of Bcl-2, and T3.70⁺ HY^{cd4}M PD-1 sufficient and deficient thymocytes expressed higher, although variable, levels of Bcl-2 (**Fig 3-21C**). Levels of cleaved caspase 3 were also compared, as it is a more direct measure of apoptosis. As previously shown, B6 DP thymocytes and T3.70⁺ HY^{cd4}F DP thymocytes exhibited low levels of cleaved caspase 3, while T3.70⁺ HY^{cd4}M DP thymocytes contained high levels of cleaved caspase 3 (**Fig 3-1,3-22**). T3.70⁺ HY^{cd4}F PD-1^{-/-} DP thymocytes had lower levels of cleaved caspase 3 than B6 DP thymocytes and T3.70⁺ HY^{cd4}F DP thymocytes, and T3.70⁺ HY^{cd4}M PD-1^{-/-} DP thymocytes contained lower levels of cleaved caspase 3 than their PD-

1 sufficient counterparts (**Fig 3-22**). Although these results suggest that PD-1 deficiency is associated with decreased apoptosis, none of the differences between the PD-1 sufficient and PD-1 deficient populations were statistically significant.

A



B



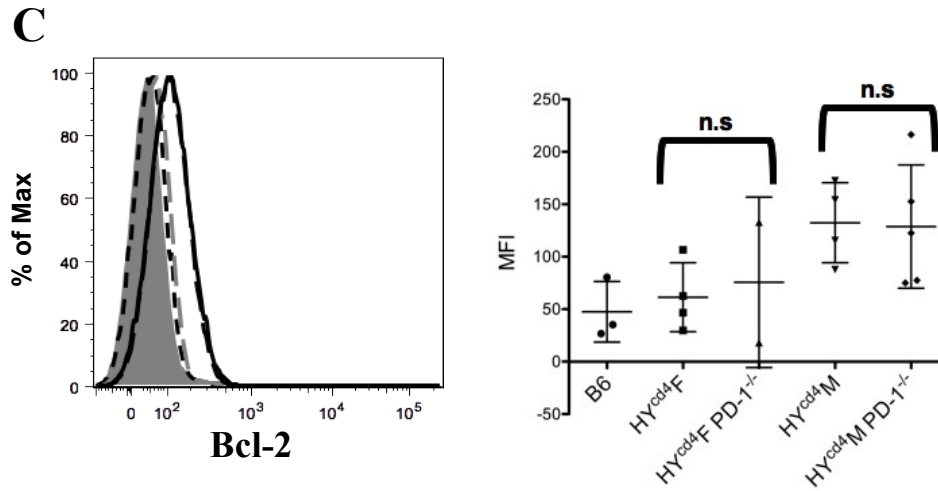


Figure 3-21: Similar levels of pro-apoptotic proteins in PD-1 sufficient and PD-1 deficient DP thymocytes. Representative histograms (top) and compilation of MFI relative to B6 DP (bottom) for Bim (A), Nur77 (B), and Bcl-2 (C), as determined by flow cytometry. B6 DP = shaded, T3.70⁺ HY^{cd4}F DP= short dashed line, T3.70⁺ HY^{cd4}F DP PD-1^{-/-} = long dashed grey line, T3.70⁺ HY^{cd4}M DP = solid black line, T3.70⁺ HY^{cd4}M DP PD-1^{-/-} = long dashed line. n.s.=not significant.

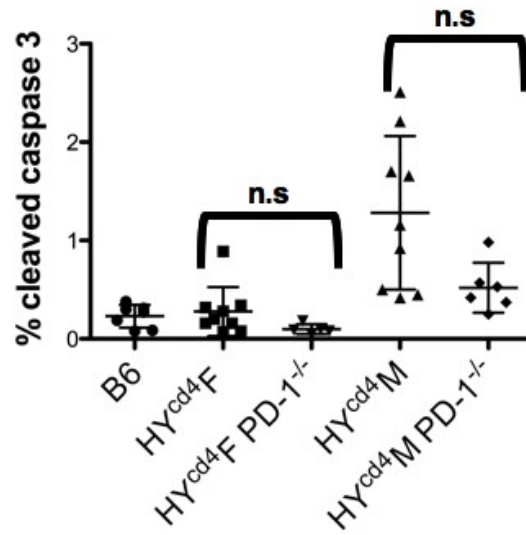
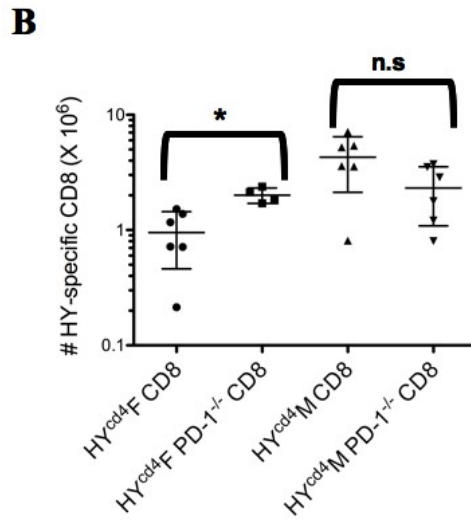
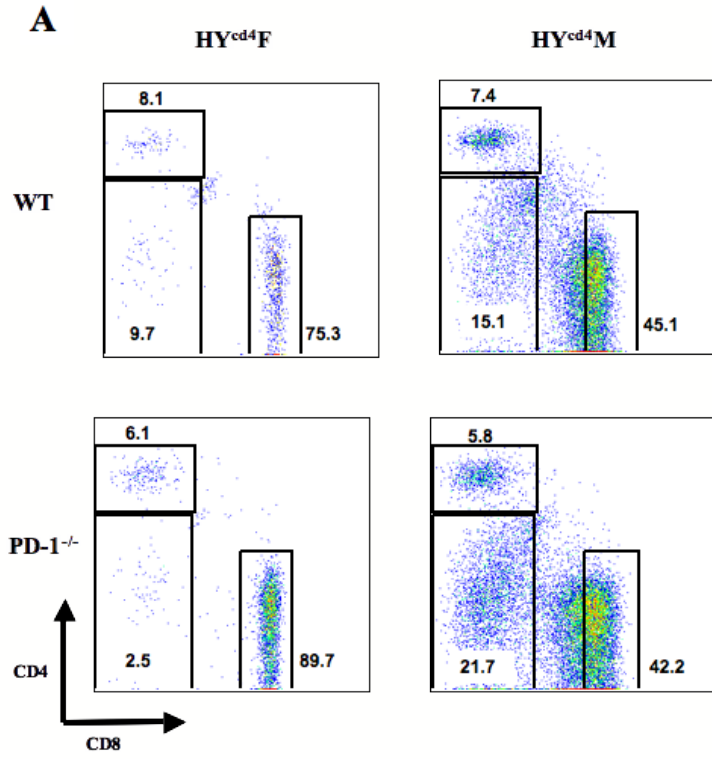


Figure 3-22: Similar levels of cleaved caspase 3 in PD-1 sufficient and PD-1 deficient DP thymocytes. Compilation of percent cleaved caspase 3 in B6 DP and T3.70⁺ HY^{cd4}F, HY^{cd4}F DP PD-1^{-/-}, HY^{cd4}M, and HY^{cd4}M DP PD-1^{-/-} DP, as determined by flow cytometry. n.s.=not significant.

Spleen

T3.70⁺ cells in the spleen of PD-1 deficient and sufficient mice were examined to determine if PD-1 deficiency affected peripheral T cell numbers. T3.70⁺ cells from HY^{cd4}F and HY^{cd4}F PD-1^{-/-}, and T3.70⁺ cells from HY^{cd4}M and HY^{cd4}M PD-1^{-/-} spleens exhibited similar CD4 by CD8 profiles (**Fig 3-23A**). However, there were increased numbers of T3.70⁺ CD8⁺ T cells in the HY^{cd4}F PD-1^{-/-} spleen over the HY^{cd4}F spleen (p=0.0053) (**Fig 3-23B**). There appeared to be slightly less T3.70⁺ CD8⁺ T cells in the male PD-1 deficient spleens compared to the male PD-1 sufficient spleens, but this difference was not significantly significant (p=0.0808) (**Fig 3-23B**). B6 CD8⁺ cells and T3.70⁺ CD8⁺ cells from male and female PD-1 sufficient and deficient mice did not express either CD69 or PD-1 (**Fig 3-23C**). There were also similar proportions of naïve, effector memory, and central memory T3.70⁺ CD8⁺ T cells in the spleen of HY^{cd4}M and HY^{cd4}M PD-1^{-/-} mice (**Fig 3-24**). Taken together, these results indicate that negative selection is not inhibited by the absence of PD-1.



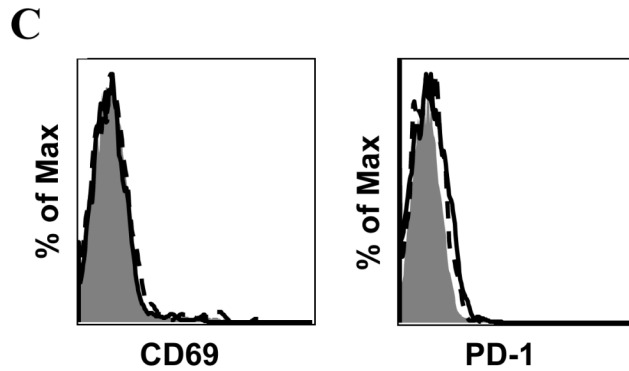


Figure 3-23: Similar numbers of T3.70⁺ CD8⁺ T cells in spleens of PD-1 deficient and sufficient mice. A) CD4/CD8 profiles of T3.70⁺ splenocytes for indicated mouse. B) Absolute numbers of T3.70⁺ CD8⁺ splenocytes, * indicates p=0.0053, n.s.= not significant. n=6 for HY^{cd4}F, HY^{cd4}M, and HY^{cd4}M PD-1^{-/-}, n=4 HY^{cd4}F PD-1^{-/-}. C) Expression of CD69 and PD-1 on DP thymocytes (B6) or T3.70⁺ DP thymocytes. B6 DP = shaded, T3.70⁺ HY^{cd4}F DP= short dashed line, T3.70⁺ HY^{cd4}F DP PD-1^{-/-} = long dashed grey line, T3.70⁺ HY^{cd4}M DP = solid black line, T3.70⁺ HY^{cd4}M DP PD-1^{-/-} = long dashed line.

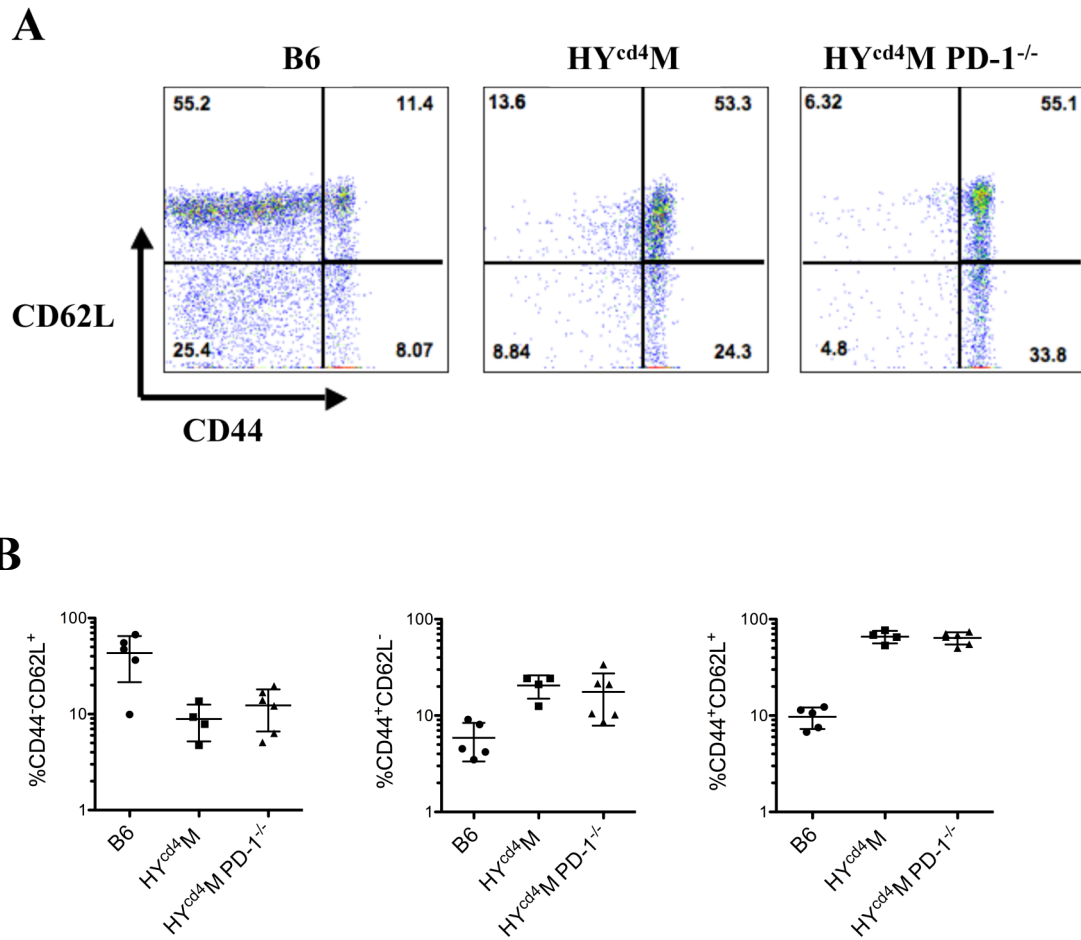


Figure 3-24: Similar proportions of naïve, effector memory, and central memory T3.70⁺ CD8⁺ T cells in HY^{cd4}M and HY^{cd4}M PD-1^{-/-} spleens. A) CD62L by CD44 plots of total CD8⁺ splenocytes (B6) or T3.70⁺ CD8⁺ splenocytes for indicated mouse. B) Proportion of naïve (CD44⁻CD62L⁺), effector memory (CD44⁺CD62L⁻), and central memory (CD44⁺CD62L⁺) CD8⁺ T cells (B6) or T3.70⁺ CD8⁺ T cells (HY^{cd4}M). n=5 for B6, n=4 for HY^{cd4}M, n=6 for HY^{cd4}M PD-1^{-/-}.

***In vitro* stimulation of thymocytes from PD-1 deficient mice**

The protection of PD-1⁺ thymocytes from apoptosis in the *in vitro* stimulation assay was not abolished when anti-PD-L1 antibody was added (**Fig 3-11D**). This does not, however, indicate that PD-1 is not important in mediating this protection, as it is possible that the antibody does not block effectively *in vitro*.

The *in vitro* stimulation assay was therefore repeated with HY^{cd4} PD-1^{-/-} mice to examine levels of apoptosis after high-affinity antigen encounter in the absence of PD-1. As expected, T3.70⁺ HY^{cd4}F, T3.70⁺ HY^{cd4}M, T3.70⁺ HY^{cd4}F PD-1^{-/-}, and T3.70⁺ HY^{cd4}M PD-1^{-/-} DP thymocytes all exhibited increases in the percentage of CD69⁺ cells with increasing concentration of male antigen (**Fig 3-25A**).

Interestingly, T3.70⁺ HY^{cd4}M PD-1^{-/-} DP thymocytes exhibited higher levels of cleaved caspase 3 than T3.70⁺ HY^{cd4}M PD-1⁺ DP thymocytes (**Fig 3-25B**).

Although the trend is not a smoothly rising curve, and the levels of cleaved caspase 3 were below that of T3.70⁺ HY^{cd4}M PD-1⁻ DP thymocytes, these results may indicate that PD-1 is somehow involved in the protection of PD-1⁺ thymocytes from apoptosis.

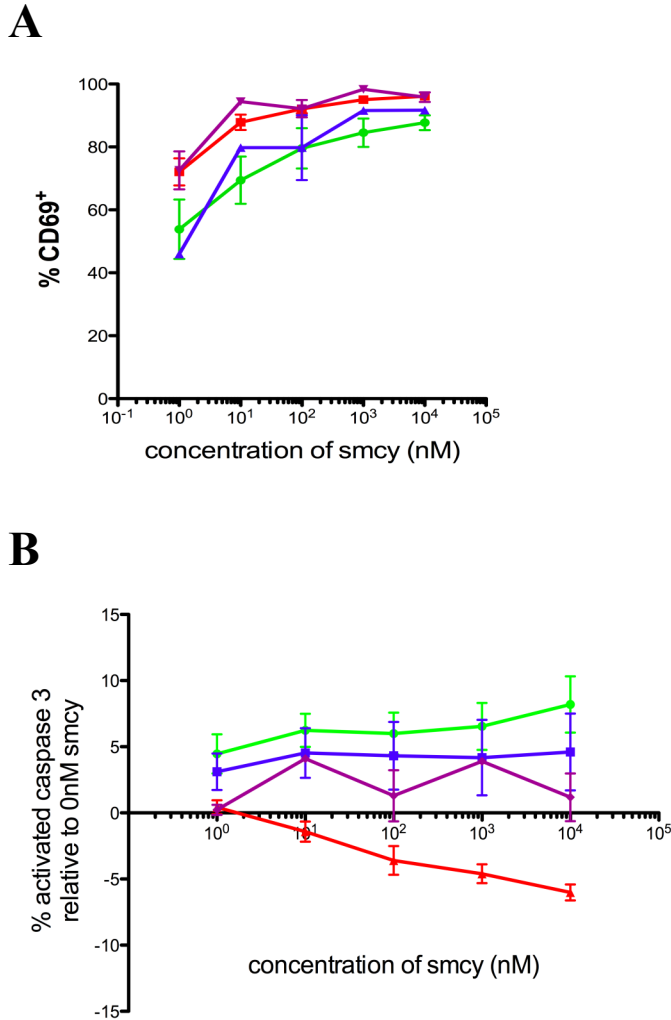


Figure 3-25: *In vitro* simulation of thymocytes from PD-1 sufficient and deficient mice with BM-derived DCs at indicated concentrations of smcy. A) Percent of T3.70⁺ DP thymocytes expressing CD69. T3.70⁺ HY^{cd4}F DP is in green, T3.70⁺ HY^{cd4}M DP is in red, T3.70⁺ HY^{cd4}F PD-1^{-/-} DP is in blue, and T3.70⁺ HY^{cd4}M PD-1^{-/-} DP is in purple. B) Percent activated caspase 3, relative to percent activated caspase 3 at 0nM smcy, in T3.70⁺ DP thymocytes. T3.70⁺ HY^{cd4}F DP is in green, T3.70⁺ HY^{cd4}M DP PD-1⁻ is in blue, T3.70⁺ HY^{cd4}M DP PD-1⁺ is in red, and T3.70⁺ HY^{cd4}M PD-1^{-/-} DP is in purple. n= 5 for HY^{cd4}F and HY^{cd4}M, n=2 for T3.70⁺ HY^{cd4}F PD-1^{-/-}, and n= 3 for HY^{cd4}M PD-1^{-/-} DP.

HY^{cd4} PD-1^{-/-} mixed BM chimeras

In order to examine PD-1 deficiency in a more physiological manner, low frequency HY^{cd4}F PD-1^{-/-} BM chimeras were generated. T cell depleted HY^{cd4}F PD-1^{-/-} BM was mixed with B6 F BM at 1:50 and injected into a lethally irradiated B6 F to examine the role of PD-1 in positive selection. Additionally, T cell depleted HY^{cd4}F PD-1^{-/-} BM was mixed with B6 M BM at 1:50 and injected into a lethally irradiated B6 M to create a situation where PD-1 deficient cells encounter their high affinity antigen. Thymocytes from the (HY^{cd4}F PD-1^{-/-} + B6 F) → B6 F chimeras were 5.2% T3.70⁺ (**Fig 3-26, left**). The T3.70⁺ thymocytes exhibited a CD4 by CD8 profile consistent with thymocytes undergoing positive selection. As expected, practically none of these thymocytes expressed PD-1 and they expressed very low levels of cleaved caspase 3. Thymocytes from the (HY^{cd4}F PD-1^{-/-} + B6 M) → B6 M chimeras were 0.9% T3.70⁺ (**Fig 3-26, right**). The T3.70⁺ thymocytes exhibited a CD4 by CD8 profile consistent with thymocytes undergoing negative selection. As with the (HY^{cd4}F PD-1^{-/-} + B6 F) → B6 F chimeras, a low proportion of T3.70⁺ cells expressed PD-1. Additionally, as expected, T3.70⁺ thymocytes from the (HY^{cd4}F PD-1^{-/-} + B6 M) → B6 M chimeras expressed about 10 fold more cleaved caspase 3 than the T3.70⁺ thymocytes from the (HY^{cd4}F PD-1^{-/-} + B6 F) → B6 F chimeras, confirming that they are undergoing apoptosis. Thus, taken together, it can be concluded that both positive selection and negative selection continue to occur in the absence of PD-1.

(HY^{cd4}F PD-1^{-/-}
+ B6F) → B6F

(HY^{cd4}F PD-1^{-/-}
+ B6M) → B6M

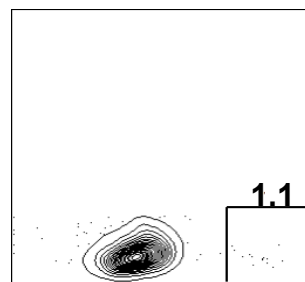
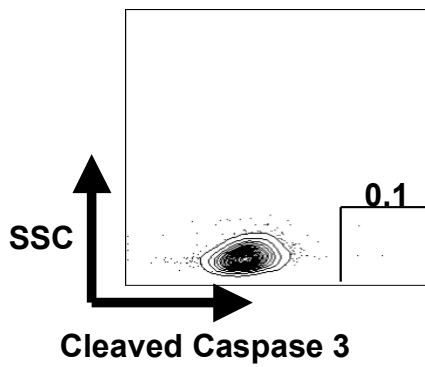
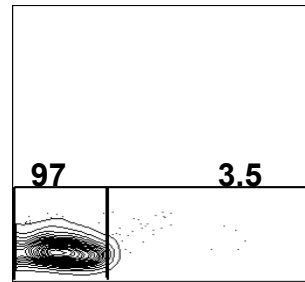
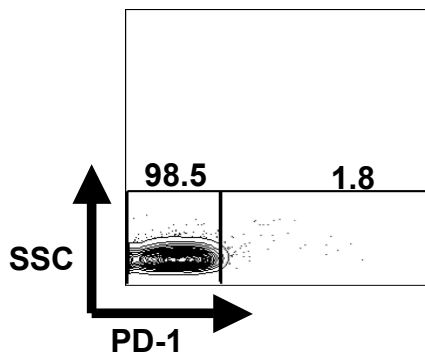
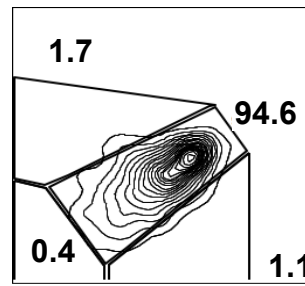
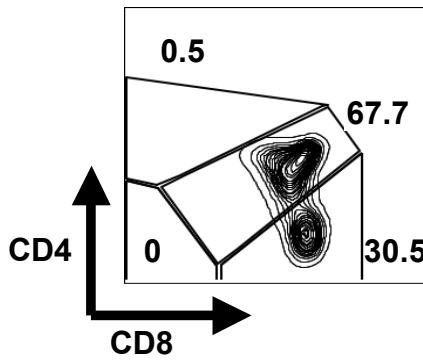
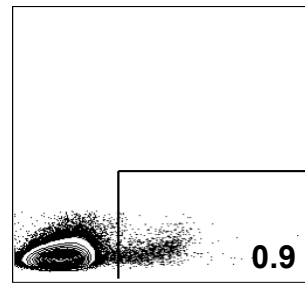
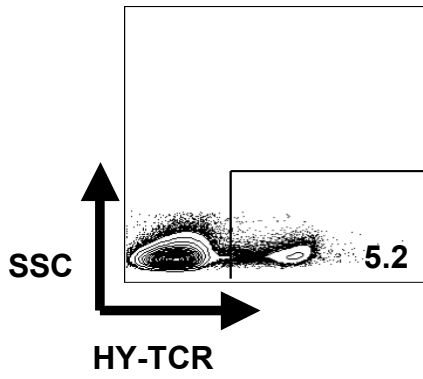


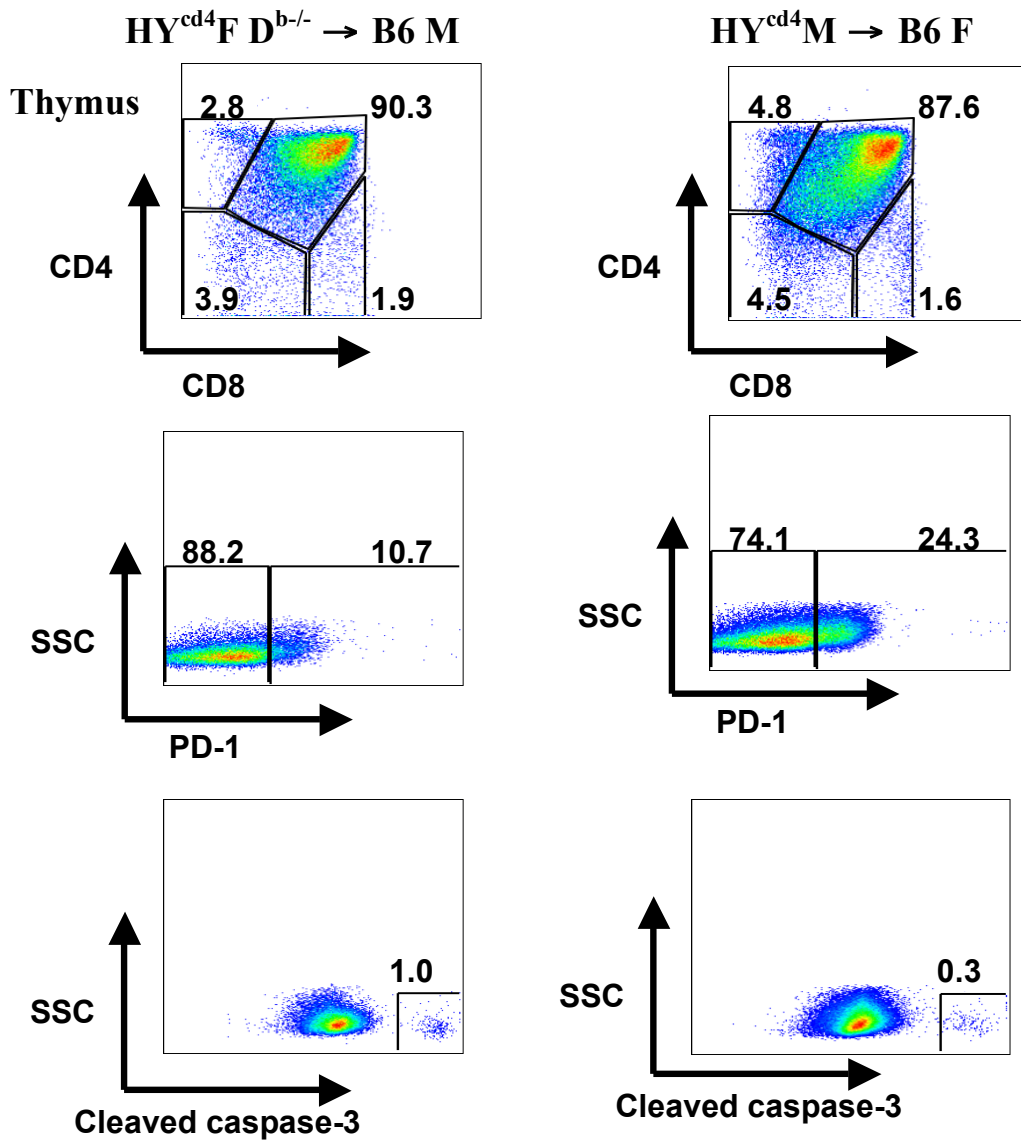
Figure 3-26: Low frequency HY^{cd4} PD-1^{-/-} mixed BM chimeras. T cell depleted HY^{cd4}F PD-1^{-/-} BM was mixed with either B6 F BM at 1:50 and injected into a lethally irradiated B6 F (left), or B6 M BM at 1:50 and injected into a lethally irradiated B6 M (right). Frequency of T3.70⁺ thymocytes, CD4 by CD8 thymic profiles, expression of PD-1, and levels of cleaved caspase 3 of the T3.70⁺ thymocytes were examined by flow cytometry.

Characterization of chimeras in which high-affinity antigen presentation is restricted to either hematopoietically derived cells or TECs

It has recently been shown that the type of APC encountered in the thymus during negative selection influences the fate of thymocytes. Thymocytes that encounter high-affinity antigen presented by hematopoietically derived cells, such as DCs, undergo immediate apoptosis, while high-affinity antigen presented by thymic epithelial cells (TECs) induce low levels of caspase 3 activation and upregulate PD-1 (112). We attempted to replicate these results by creating chimeras in which presentation of male antigen was restricted to either TECs or hematopoietically derived cells. To restrict presentation to TECs, HY^{cd4}F D^{b/-} BM was injected into lethally irradiated B6 M mice (**Fig 3-27A, left**). Presentation of male antigen was restricted to hematopoietically derived cells by injecting HY^{cd4}M BM into lethally irradiated B6 F mice (**Fig 3-27A, right**). The results were unexpected, as they contradicted what had been previously published. T3.70⁺ DP thymocytes that encountered male antigen presented by TECs expressed lower levels of PD-1 and higher levels of cleaved caspase 3 than those thymocytes that encountered high affinity antigen expressed on hematopoietically derived cells (**Fig 3-27A**). However, it is important to note that the chimeras were very ill due to high doses of radiation, and this may account for the conflicting results. Both sets of chimeras contained T3.70⁺ cells in the spleen (**Fig 3-27B**). Interestingly, T3.70⁺ cells that developed in thymi in which male antigen was restricted to hematopoietically derived cells had lower expression of CD8 and an increased

proportion of CD4⁻CD8⁻ cells compared to those T3.70⁺ cells that were presented male antigen by TECs (**Fig 3-27B**). This significance of these results are not yet clear, and, as mentioned above, may not represent a physiologically situation.

A



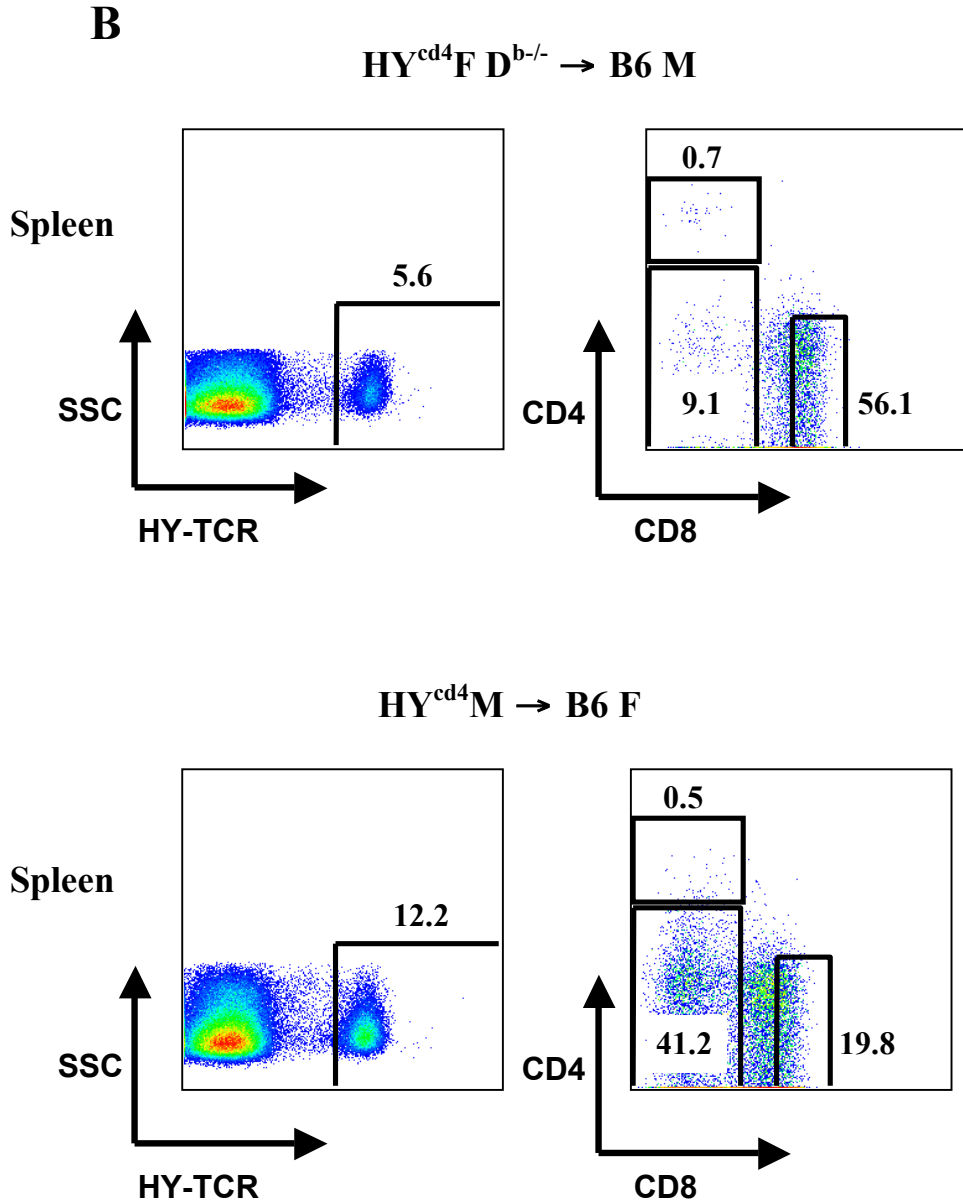


Figure 3-27: Restriction of male antigen presentation to thymic epithelial cells or to hematopoietically derived cells. T cell depleted HY^{cd4}F D^{b/-} BM was injected into a lethally irradiated B6 M to create an environment where male antigen is only presented by TECs (left). Additionally, T cell depleted HY^{cd4}M BM was injected into a lethally irradiated B6 F to create an environment where

male antigen is only presented by hematopoietically derived cells (right). A) CD4 by CD8 thymic profiles, expression of PD-1, and levels of cleaved caspase 3 of T3.70⁺ thymocytes were examined by flow cytometry. B) Proportion of T3.70⁺ cells in the spleen and CD4 by CD8 thymic profiles, were determined using flow cytometry.

Chapter 4: Discussion

Peripheral T3.70⁺ T cells in the HY^{cd4} male and female mouse

The above experiments characterized the role of PD-1 in negative selection using the HY^{cd4} mouse model of thymic development. The HY^{cd4} model is more physiologically relevant than other TCR transgenic mice models because of the appropriate timing of the HY-TCR α chain and use of endogenous self-antigen as the cognate antigen (122). As the CD4/CD8 thymic profiles and levels of cleaved caspase 3 indicate that negative selection is occurring in the thymus of HY^{cd4} male mice (**Fig 3-1**), it was surprising to observe a considerable population of T3.70⁺ CD8⁺ T cells in the spleen (**Fig 3-2**). Intriguingly, these T cells exhibit decreased expression of CD8 (**Fig 3-2**). The same phenomenon is observed in the traditional in the HY male as well (152). It is possible that these T cells are derived from a few self-reactive thymocytes that escape clonal deletion by having decreased expression of CD8, thereby decreasing the amount of signal. These cells can proliferate extensively once they enter the periphery due to the abundance of their cognate antigen. A large proportion of the T3.70⁺ CD8 T cells in the male are CD44⁺ (**Fig 3-3**), and this suggests that they have encountered antigen. An alternative explanation for the decreased CD8 expression of male T3.70⁺ T cells is a negative feedback mechanism known as co-receptor tuning. Co-receptor tuning occurs when a strong signal through the TCR results in decreased IL-7R expression and IL-7 signaling, which leads to decreased

expression of the CD8 co-receptor (72). Co-receptor tuning is thought to be involved in preventing auto-reactivity in self-reactive peripheral T cells.

PD-1 expression is upregulated in peripheral T cells in response to continued exposure to antigen (158). As T3.70⁺ peripheral T cells in the male will be constantly encountering their cognate antigen, it is puzzling that they do not express PD-1 (**Fig 3-4**); particularly since 20-40% of DP thymocytes in the HY^{cd4}M express PD-1 (**Fig 3-4**). One possibility is that PD-1⁺ thymocytes are not exiting the thymus. However, this is somewhat unlikely, as both PD-1⁻ and PD-1⁺ thymocytes have similar expression of KLF2 (**Fig 3-7D**), a transcription factor important in thymic egress (92). Ontogeny studies or RTE tracking could confirm that both PD-1⁺ and PD-1⁻ are entering the periphery.

Conversely, the relatively low numbers of T3.70⁺ CD8⁺ T cells in the HY^{cd4} female spleen (**Fig 3-2**) were also somewhat unexpected. We speculate that the numbers are low because the T3.70⁺ cells are poor homeostatic competitors for a variety of reasons. Since the ligand that the HY-TCR recognizes in female mice for positive selection is unknown, and it is possible that the expression of this ligand is minimal. It has been shown that interaction with positively selecting ligands is important for homeostatic proliferation in the periphery (155, 156). In addition, based on CD5 expression levels, the HY-TCR has low affinity for this unknown ligand, making it less likely to undergo homeostatic proliferation (148).

It is important to note that it is not known if the T3.70⁺ peripheral T cells in the male are functional. Although overt autoimmune disease has not been observed in the HY^{cd4} male, these mice have not been examined for the presence of autoantibodies, nor has tissue histology been performed to look for lymphocyte infiltration. In addition, these mice are generally euthanized within 6 months, before the development of late-onset autoimmunity would be apparent. Further work should determine if the T3.70⁺ T cells in the HY^{cd4} male periphery are functional. If PD-1 expressing cells do exit the thymus, it is possible that PD-1 could be downregulated upon entry into peripheral lymphoid organs. This could be determined through ontogeny studies or RTE tracking. In this case, autoimmune disease could be prevented by upregulation of other co-inhibitory molecules such as cytotoxic T lymphocyte antigen 4 (CTLA-4) (167). It would be interesting to examine expression levels of CTLA-4 in PD-1 sufficient and deficient HY^{cd4}M mice.

While the HY^{cd4} mouse model is an excellent tool with which to study thymic selection events, there are many features of the peripheral immune system that are perplexing and we do not understand at this moment. Specifically, it would be of significant interest to determine if the T3.70⁺ T cells in HY^{cd4} male mice are functional. This information could aid our understanding of the mechanisms of peripheral tolerance.

Gene expression profiles of PD-1⁻ and PD-1⁺ thymocytes

Bim and Nur77, known mediators of clonal deletion, were expressed at similar levels between PD-1⁻ and PD-1⁺ thymocytes, with slightly increased expression in the PD-1⁺ thymocytes. This was found at both the mRNA level (**Fig 3-6A,B**) and protein level (**Fig 3-8A,B**). However, Bcl-2 expression was significantly increased in PD-1⁺ thymocytes over PD-1⁻ thymocytes (**Fig 3-8C**). Thymocyte apoptosis versus survival is thought to be controlled by pro- and anti-apoptotic members of the Bcl-2 family (168), and increased levels of Bcl-2 may account for the longer survival of PD-1⁺ thymocytes compared to PD-1⁻ thymocytes in a BrdU time course assay (112). Interestingly, although Bcl-2 is generally considered an anti-apoptotic protein, it has also been demonstrated that Nur77 converts Bcl-2 to a pro-apoptotic form. Winoto and Thompson found that TCR stimulation of thymocytes leads to the association of Nur77 with Bcl-2, as well as a conformational change in Bcl-2, exposing the pro-apoptotic Bcl-2 homology-3 (BH3) domain (98). The results of this study do not support this scenario as there is increased expression of both Nur77 and Bcl-2 in the PD-1⁺ thymocytes, but they are similarly apoptotic compared to PD-1⁻ thymocytes (**Fig 3-6B, Fig 3-8B,C, Fig 3-9**). However, it would be interesting to compare Bcl-2 -BH3 exposure in PD-1⁻ versus PD-1⁺ thymocytes.

Similar expression patterns of Gadd45 β in PD-1⁻ and PD-1⁺ thymocytes were also observed (**Fig 3-6C**). Gadd45 β has been found to be upregulated in microarray analysis using various models of negative selection (128, 161), and Gadd45 β

deficiency increases susceptibility to autoimmune disease (169). The role of Gadd45 β in negative selection is unclear but it may be involved in regulating MAPK signaling (170). Work is currently in progress to examine the role of Gadd45 β in thymocyte selection in the HY^{cd4} model.

Expression of 2610019F03Rik, a newly identified gene that was identified as being associated with positive selection in microarray analysis (127), was found to be downregulated in negative selection, but was less downregulated in PD-1⁻ thymocytes compared to PD-1⁺ thymocytes (**Fig 3-7A**). This could be due to the fact that PD-1⁺ cells see signal longer than PD-1⁻ cells, as shown by the longer survival of PD-1⁺ cells in a 5-bromo-2-deoxyuridine (BrdU) assay (112), and therefore they have more time to downregulate 2610019F03Rik. The role of 2610019F03Rik in T cell biology, let alone thymocyte selection, is completely unknown at this point, but based on gene expression patterns could be involved in positive selection. Expression of CCR7, which is induced after positive selection and mediates migration from the cortex to the medulla (49), was expressed similarly between PD-1⁻ and PD-1⁺ thymocytes (**Fig 3-7C**), implying that both have the same capability to move into the medulla.

Collectively, it appears that PD-1⁻ and PD-1⁺ thymocytes have similar abilities to undergo apoptosis, migrate from the cortex to the medulla, and enter the periphery. However, comparison of PD-1 expression in HY^{cd4}PD-1^{-/-} mice and HY^{cd4}PD-1^{+/+} mice revealed that “PD-1⁻” thymocytes in HY^{cd4}PD-1^{+/+} mice

actually express low levels of PD-1 (**Fig 3-20**). RT-PCR should be re-performed using the HY^{cd4}PD-1^{-/-} populations that are truly PD-1 deficient to compare gene expression between thymocytes sufficient and deficient in PD-1. For example, KLF2 is downregulated slightly less in PD-1^{low} thymocytes than in PD-1⁺ thymocytes (**Fig 3-7D**). It would be interesting to see if this difference in expression level is more significant when comparing PD-1⁺ thymocytes to thymocytes that are truly PD-1⁻.

Mechanism of negative selection of PD-1⁺ thymocytes

HY^{cd4}M PD-1⁺ DP thymocytes underwent decreasing apoptosis with increased concentration of antigen in the *in vitro* stimulation assay (**Fig 3-11, 3-14**). The increased expression of CD69 and PD-1 indicates that these cells are recognizing antigen and becoming activated, so why are they not undergoing apoptosis? When peripheral T cells get activated they undergo proliferation and increase cytokine production. Anergy is functional non-responsiveness, a lack of proliferation and decreased production of cytokines (171). DP thymocytes do not proliferate or release cytokines when they are activated with their cognate antigen, instead they undergo apoptosis. As the PD-1⁺ thymocytes are not undergoing apoptosis it is possible that they are anergic.

The factors important in anergy are still being elucidated, but it is thought that signaling through nuclear factor of activated T cells (NFAT) is important. It has been shown that cyclosporine A, which inhibits NFAT signaling, can prevent

anergy induction (172) and that T cells deficient in NFAT-1 cannot be induced to undergo anergy (173). Interestingly, some of the downstream targets of NFAT signaling are early growth response gene (Egr)2, Egr3, diacylglycerol kinase (DGK) α , and Casitas B-cell lymphoma-b (Cbl-b) (164, 173-175) (**Fig 4-1**). Egr2 and Egr3 are zinc finger transcription factors that may regulate DGK α expression (171). DGK α , inhibits Ras activation, which inhibits activation of ERK and JNK (164). In addition, overexpression of Egr2 and Egr3 leads to increased expression of Cbl-b (176). Another target of NFAT is PD-1. Inhibiting NFAT signaling through cyclosporine A or mutating the consensus binding site of NFAT abolishes PD-1 expression (177). Interestingly, Fife et al found that PD-1/PD-L1 interactions in the periphery are associated with decreased levels of ERK activation (166).

Expression levels of Egr2, DGK α , Cbl-b, and pERK were found to be similar between PD-1⁻ and PD-1⁺ thymocytes (**Fig 3-15, 3-16, 3-17**), although as mentioned above, expression of these genes could be re-examined using thymocytes from HY^{cd4}PD-1^{-/-} mice to compare expression levels between PD-1⁺ thymocytes and thymocytes that are truly PD-1 deficient.

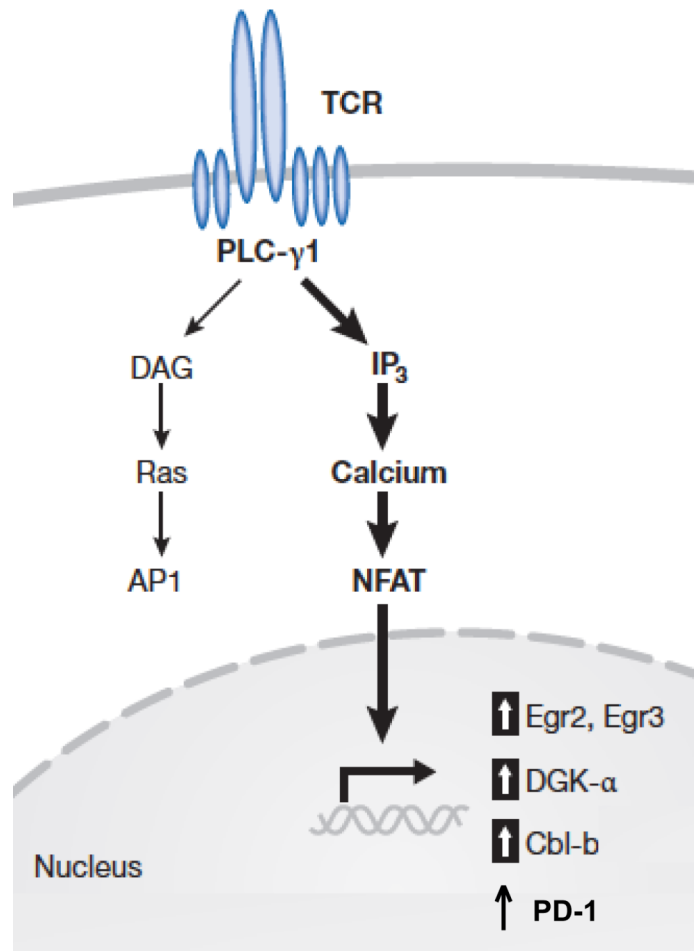


Figure 4-1: NFAT signaling is associated with anergy induction. Some of the factors identified to be downstream of NFAT signaling are early growth response gene (Egr)2, Egr3, diacylglycerol kinase (DGK) α , Casitas B-cell lymphoma-b (Cbl-b), and Programmed death-1 (PD-1). *Modified from Zheng, Y. et al. 2008. EMBO reports 9, 50-55.*

Given the limited changes in gene expression of anergy factors, there are at least two possibilities for how PD-1 expression regulates negative selection. PD-1 either has an active role in negative selection or is just a marker of cells undergoing negative selection by a different mechanism. PD-1 has been shown to inhibit phosphorylation of CD3 ζ , zeta-chain-associated protein kinase 70 (ZAP-70), and protein kinase C theta (PKC θ), likely through recruitment of SHP-1/SHP-2 (178). Differences in phosphorylation of these membrane-proximal signaling molecules should be compared between PD-1⁻ and PD-1⁺ thymocytes.

HY^{cd4}PD-1 deficient mice

There is slightly higher expression of activation markers on the HY^{cd4}PD-1^{-/-} DP thymocytes than on the HY^{cd4}PD-1^{+/+} DP thymocytes indicating that thymocytes are receiving a higher intensity signal in the absence of PD-1 (**Fig 3-19**). This is consistent with the role of PD-1 as a co-inhibitory molecule. It is possible that negative selection could be more efficient in the absence of PD-1 as a result of increased signal through the TCR. To determine this, chimeras with mixed PD-1 deficient and PD-1 sufficient BM could be generated and a BrdU pulse-chase assay could be performed to track the lifespan of PD-1⁻ and PD-1⁺ thymocytes.

In support of the possibility of increased efficiency of negative selection in PD-1 deficient mice, increased levels of cleaved caspase 3 were detected in the mixed BM chimeras where PD-1⁻ thymocytes were present at a low precursor frequency (**Fig 3-26**). An alternative explanation for increased efficiency of negative

selection with a decreased precursor frequency is decreased competition for negatively selecting ligands, as happens with positive selection (179). Further experiments are required to distinguish between these possibilities.

Collectively, by generating $\text{HY}^{\text{cd4}}\text{PD-1}^{-/-}$ mice, we now have a tool to be able to directly assess the role of PD-1 in negative selection. Differences in negative selection between PD-1^+ and PD-1^- thymocytes would support the idea the PD-1 plays an active role in regulating negative selection, while no difference would suggest that PD-1 is simply upregulated on older thymocytes that received a high affinity signal.

Antigen-presentation restricted chimeras

Based on previously published results we predicted that the chimeras in which male-antigen presentation was restricted to the hematopoietically-derived cells would exhibit low PD-1 expression and high levels of cleaved caspase 3, and that chimeras in which male-antigen presentation was restricted to epithelial cells would have high expression of PD-1 but low levels of cleaved caspase 3 (112). However, the results were not as expected. In fact, they were opposite: there was higher expression of PD-1 and lower levels of cleaved caspase 3 when male-antigen was presented only by hematopoietically-derived cells, and lower levels of PD-1 and higher levels of cleaved caspase 3 when male antigen was only presented by epithelial cells (**Fig 3-27**). These unexpected results could be a side effect of an overdose of radiation. Alternatively, it could also be due to an

increased precursor frequency as McCaughtry et al used mixed BM chimeras.

This experiment will be repeated with a lower dose of radiation and mixed BM chimeras with a low precursor frequency.

In conclusion, these experiments indicate PD-1 is upregulated in the HY^{cd4} model of negative selection. PD-1⁺ and PD-1⁻ thymocytes appear to be capable of undergoing apoptosis to the same extent, however PD-1⁺ thymocytes are protected from apoptosis when stimulated with male antigen *in vitro*. The mechanism and physiological relevance of this protection is unknown and future work comparing membrane-proximal signaling following TCR stimulation between PD-1⁻ and PD-1⁺ thymocytes, as well as examination of PD-1 deficient thymocytes should contribute to our understanding of the role of PD-1 in thymic development.

Literature Cited

1. Brooks, J. T., J. E. Kaplan, K. K. Holmes, C. Benson, A. Pau, and H. Masur. 2009. HIV-associated opportunistic infections--going, going, but not gone: the continued need for prevention and treatment guidelines. *Clin Infect Dis* 48:609-611.
2. Buckley, R. H. 2004. Molecular defects in human severe combined immunodeficiency and approaches to immune reconstitution. *Annual review of immunology* 22:625-655.
3. Chaplin, D. D. Overview of the immune response. *The Journal of allergy and clinical immunology* 125:S3-23.
4. Lanier, L. L. 2005. NK cell recognition. *Annual review of immunology* 23:225-274.
5. Donskoy, E., and I. Goldschneider. 1992. Thymocytopoiesis is maintained by blood-borne precursors throughout postnatal life. A study in parabiotic mice. *J Immunol* 148:1604-1612.
6. Lind, E. F., S. E. Prockop, H. E. Porritt, and H. T. Petrie. 2001. Mapping precursor movement through the postnatal thymus reveals specific microenvironments supporting defined stages of early lymphoid development. *The Journal of experimental medicine* 194:127-134.
7. Bhandoola, A., H. von Boehmer, H. T. Petrie, and J. C. Zuniga-Pflucker. 2007. Commitment and developmental potential of extrathymic and

- intrathymic T cell precursors: plenty to choose from. *Immunity* 26:678-689.
8. Schwarz, B. A., A. Sambandam, I. Maillard, B. C. Harman, P. E. Love, and A. Bhandoola. 2007. Selective thymus settling regulated by cytokine and chemokine receptors. *J Immunol* 178:2008-2017.
 9. Wallis, V. J., E. Leuchars, S. Chwalinski, and A. J. Davies. 1975. On the sparse seeding of bone marrow and thymus in radiation chimaeras. *Transplantation* 19:2-11.
 10. Kadish, J. L., and R. S. Basch. 1976. Hematopoietic thymocyte precursors. I. Assay and kinetics of the appearance of progeny. *The Journal of experimental medicine* 143:1082-1099.
 11. Zubkova, I., H. Mostowski, and M. Zaitseva. 2005. Up-regulation of IL-7, stromal-derived factor-1 alpha, thymus-expressed chemokine, and secondary lymphoid tissue chemokine gene expression in the stromal cells in response to thymocyte depletion: implication for thymus reconstitution. *J Immunol* 175:2321-2330.
 12. Madri, J. A., and D. Graesser. 2000. Cell migration in the immune system: the evolving inter-related roles of adhesion molecules and proteinases. *Developmental immunology* 7:103-116.
 13. Rossi, F. M., S. Y. Corbel, J. S. Merzaban, D. A. Carlow, K. Gossens, J. Duenas, L. So, L. Yi, and H. J. Ziltener. 2005. Recruitment of adult thymic progenitors is regulated by P-selectin and its ligand PSGL-1. *Nature immunology* 6:626-634.

14. Scimone, M. L., I. Aifantis, I. Apostolou, H. von Boehmer, and U. H. von Andrian. 2006. A multistep adhesion cascade for lymphoid progenitor cell homing to the thymus. *Proceedings of the National Academy of Sciences of the United States of America* 103:7006-7011.
15. Ruiz, P., M. V. Wiles, and B. A. Imhof. 1995. Alpha 6 integrins participate in pro-T cell homing to the thymus. *European journal of immunology* 25:2034-2041.
16. Lepique, A. P., S. Palencia, H. Irjala, and H. T. Petrie. 2003. Characterization of vascular adhesion molecules that may facilitate progenitor homing in the post-natal mouse thymus. *Clinical & developmental immunology* 10:27-33.
17. Robertson, P., T. K. Means, A. D. Luster, and D. T. Scadden. 2006. CXCR4 and CCR5 mediate homing of primitive bone marrow-derived hematopoietic cells to the postnatal thymus. *Experimental hematology* 34:308-319.
18. Uehara, S., A. Grinberg, J. M. Farber, and P. E. Love. 2002. A role for CCR9 in T lymphocyte development and migration. *J Immunol* 168:2811-2819.
19. Krueger, A., S. Willenzon, M. Lyszkiewicz, E. Kremmer, and R. Forster. CC chemokine receptor 7 and 9 double-deficient hematopoietic progenitors are severely impaired in seeding the adult thymus. *Blood* 115:1906-1912.

20. Zlotoff, D. A., A. Sambandam, T. D. Logan, J. J. Bell, B. A. Schwarz, and A. Bhandoola. CCR7 and CCR9 together recruit hematopoietic progenitors to the adult thymus. *Blood* 115:1897-1905.
21. Johnston, B., and E. C. Butcher. 2002. Chemokines in rapid leukocyte adhesion triggering and migration. *Seminars in immunology* 14:83-92.
22. Wu, L., P. W. Kincade, and K. Shortman. 1993. The CD44 expressed on the earliest intrathymic precursor population functions as a thymus homing molecule but does not bind to hyaluronate. *Immunology letters* 38:69-75.
23. Godfrey, D. I., J. Kennedy, T. Suda, and A. Zlotnik. 1993. A developmental pathway involving four phenotypically and functionally distinct subsets of CD3-CD4-CD8- triple-negative adult mouse thymocytes defined by CD44 and CD25 expression. *J Immunol* 150:4244-4252.
24. Ara, T., M. Itoi, K. Kawabata, T. Egawa, K. Tokoyoda, T. Sugiyama, N. Fujii, T. Amagai, and T. Nagasawa. 2003. A role of CXC chemokine ligand 12/stromal cell-derived factor-1/pre-B cell growth stimulating factor and its receptor CXCR4 in fetal and adult T cell development in vivo. *J Immunol* 170:4649-4655.
25. Plotkin, J., S. E. Prockop, A. Lepique, and H. T. Petrie. 2003. Critical role for CXCR4 signaling in progenitor localization and T cell differentiation in the postnatal thymus. *J Immunol* 171:4521-4527.

26. Griffith, A. V., M. Fallahi, H. Nakase, M. Gosink, B. Young, and H. T. Petrie. 2009. Spatial mapping of thymic stromal microenvironments reveals unique features influencing T lymphoid differentiation. *Immunity* 31:999-1009.
27. Porritt, H. E., L. L. Rumfelt, S. Tabrizifard, T. M. Schmitt, J. C. Zuniga-Pflucker, and H. T. Petrie. 2004. Heterogeneity among DN1 prothymocytes reveals multiple progenitors with different capacities to generate T cell and non-T cell lineages. *Immunity* 20:735-745.
28. Porritt, H. E., K. Gordon, and H. T. Petrie. 2003. Kinetics of steady-state differentiation and mapping of intrathymic-signaling environments by stem cell transplantation in nonirradiated mice. *The Journal of experimental medicine* 198:957-962.
29. Rodewald, H. R., M. Ogawa, C. Haller, C. Waskow, and J. P. DiSanto. 1997. Pro-thymocyte expansion by c-kit and the common cytokine receptor gamma chain is essential for repertoire formation. *Immunity* 6:265-272.
30. Stanley, P., and C. J. Guidos. 2009. Regulation of Notch signaling during T- and B-cell development by O-fucose glycans. *Immunological reviews* 230:201-215.
31. Hozumi, K., C. Mailhos, N. Negishi, K. Hirano, T. Yahata, K. Ando, S. Zuklys, G. A. Hollander, D. T. Shima, and S. Habu. 2008. Delta-like 4 is indispensable in thymic environment specific for T cell development. *The Journal of experimental medicine* 205:2507-2513.

32. Koch, U., E. Fiorini, R. Benedito, V. Besseyrias, K. Schuster-Gossler, M. Pierres, N. R. Manley, A. Duarte, H. R. Macdonald, and F. Radtke. 2008. Delta-like 4 is the essential, nonredundant ligand for Notch1 during thymic T cell lineage commitment. *The Journal of experimental medicine* 205:2515-2523.
33. Misslitz, A., O. Pabst, G. Hintzen, L. Ohl, E. Kremmer, H. T. Petrie, and R. Forster. 2004. Thymic T cell development and progenitor localization depend on CCR7. *The Journal of experimental medicine* 200:481-491.
34. Wilson, A., W. Held, and H. R. MacDonald. 1994. Two waves of recombinase gene expression in developing thymocytes. *The Journal of experimental medicine* 179:1355-1360.
35. Capone, M., R. D. Hockett, Jr., and A. Zlotnik. 1998. Kinetics of T cell receptor beta, gamma, and delta rearrangements during adult thymic development: T cell receptor rearrangements are present in CD44(+)CD25(+) Pro-T thymocytes. *Proceedings of the National Academy of Sciences of the United States of America* 95:12522-12527.
36. Livak, F., M. Tourigny, D. G. Schatz, and H. T. Petrie. 1999. Characterization of TCR gene rearrangements during adult murine T cell development. *J Immunol* 162:2575-2580.
37. Schlissel, M. S., S. D. Durum, and K. Muegge. 2000. The interleukin 7 receptor is required for T cell receptor gamma locus accessibility to the V(D)J recombinase. *The Journal of experimental medicine* 191:1045-1050.

38. Prockop, S. E., S. Palencia, C. M. Ryan, K. Gordon, D. Gray, and H. T. Petrie. 2002. Stromal cells provide the matrix for migration of early lymphoid progenitors through the thymic cortex. *J Immunol* 169:4354-4361.
39. Benz, C., K. Heinzl, and C. C. Bleul. 2004. Homing of immature thymocytes to the subcapsular microenvironment within the thymus is not an absolute requirement for T cell development. *European journal of immunology* 34:3652-3663.
40. Irving, B. A., F. W. Alt, and N. Killeen. 1998. Thymocyte development in the absence of pre-T cell receptor extracellular immunoglobulin domains. *Science (New York, N.Y)* 280:905-908.
41. Yamasaki, S., E. Ishikawa, M. Sakuma, K. Ogata, K. Sakata-Sogawa, M. Hiroshima, D. L. Wiest, M. Tokunaga, and T. Saito. 2006. Mechanistic basis of pre-T cell receptor-mediated autonomous signaling critical for thymocyte development. *Nature immunology* 7:67-75.
42. Kreslavsky, T., A. I. Garbe, A. Krueger, and H. von Boehmer. 2008. T cell receptor-instructed alphabeta versus gammadelta lineage commitment revealed by single-cell analysis. *The Journal of experimental medicine* 205:1173-1186.
43. Witt, C. M., S. Raychaudhuri, B. Schaefer, A. K. Chakraborty, and E. A. Robey. 2005. Directed migration of positively selected thymocytes visualized in real time. *PLoS biology* 3:e160.

44. Alam, S. M., P. J. Travers, J. L. Wung, W. Nasholds, S. Redpath, S. C. Jameson, and N. R. Gascoigne. 1996. T-cell-receptor affinity and thymocyte positive selection. *Nature* 381:616-620.
45. Surh, C. D., and J. Sprent. 1994. T-cell apoptosis detected in situ during positive and negative selection in the thymus. *Nature* 372:100-103.
46. van Meerwijk, J. P., S. Marguerat, R. K. Lees, R. N. Germain, B. J. Fowlkes, and H. R. MacDonald. 1997. Quantitative impact of thymic clonal deletion on the T cell repertoire. *The Journal of experimental medicine* 185:377-383.
47. Lauritsen, J. P., S. Kurella, S. Y. Lee, J. M. Lefebvre, M. Rhodes, J. Alberola-Ila, and D. L. Wiest. 2008. Egr2 is required for Bcl-2 induction during positive selection. *J Immunol* 181:7778-7785.
48. Kurobe, H., C. Liu, T. Ueno, F. Saito, I. Ohigashi, N. Seach, R. Arakaki, Y. Hayashi, T. Kitagawa, M. Lipp, R. L. Boyd, and Y. Takahama. 2006. CCR7-dependent cortex-to-medulla migration of positively selected thymocytes is essential for establishing central tolerance. *Immunity* 24:165-177.
49. Ueno, T., F. Saito, D. H. Gray, S. Kuse, K. Hieshima, H. Nakano, T. Kakiuchi, M. Lipp, R. L. Boyd, and Y. Takahama. 2004. CCR7 signals are essential for cortex-medulla migration of developing thymocytes. *The Journal of experimental medicine* 200:493-505.
50. McNeil, L. K., T. K. Starr, and K. A. Hogquist. 2005. A requirement for sustained ERK signaling during thymocyte positive selection in vivo.

Proceedings of the National Academy of Sciences of the United States of America 102:13574-13579.

51. Sugawara, T., T. Moriguchi, E. Nishida, and Y. Takahama. 1998. Differential roles of ERK and p38 MAP kinase pathways in positive and negative selection of T lymphocytes. *Immunity* 9:565-574.
52. Rincon, M., A. Whitmarsh, D. D. Yang, L. Weiss, B. Derijard, P. Jayaraj, R. J. Davis, and R. A. Flavell. 1998. The JNK pathway regulates the In vivo deletion of immature CD4(+)CD8(+) thymocytes. *The Journal of experimental medicine* 188:1817-1830.
53. Sabapathy, K., T. Kallunki, J. P. David, I. Graef, M. Karin, and E. F. Wagner. 2001. c-Jun NH2-terminal kinase (JNK)1 and JNK2 have similar and stage-dependent roles in regulating T cell apoptosis and proliferation. *The Journal of experimental medicine* 193:317-328.
54. Bevan, M. J. 1977. In a radiation chimaera, host H-2 antigens determine immune responsiveness of donor cytotoxic cells. *Nature* 269:417-418.
55. Benoist, C., and D. Mathis. 1989. Positive selection of the T cell repertoire: where and when does it occur? *Cell* 58:1027-1033.
56. Cosgrove, D., S. H. Chan, C. Waltzinger, C. Benoist, and D. Mathis. 1992. The thymic compartment responsible for positive selection of CD4+ T cells. *International immunology* 4:707-710.
57. Honey, K., T. Nakagawa, C. Peters, and A. Rudensky. 2002. Cathepsin L regulates CD4+ T cell selection independently of its effect on invariant

- chain: a role in the generation of positively selecting peptide ligands. *The Journal of experimental medicine* 195:1349-1358.
58. Nakagawa, T., W. Roth, P. Wong, A. Nelson, A. Farr, J. Deussing, J. A. Villadangos, H. Ploegh, C. Peters, and A. Y. Rudensky. 1998. Cathepsin L: critical role in Ii degradation and CD4 T cell selection in the thymus. *Science (New York, N.Y)* 280:450-453.
59. Nitta, T., S. Murata, K. Sasaki, H. Fujii, A. M. Ripen, N. Ishimaru, S. Koyasu, K. Tanaka, and Y. Takahama. Thymoproteasome shapes immunocompetent repertoire of CD8+ T cells. *Immunity* 32:29-40.
60. Murata, S., K. Sasaki, T. Kishimoto, S. Niwa, H. Hayashi, Y. Takahama, and K. Tanaka. 2007. Regulation of CD8+ T cell development by thymus-specific proteasomes. *Science (New York, N.Y)* 316:1349-1353.
61. Singer, A., S. Adoro, and J. H. Park. 2008. Lineage fate and intense debate: myths, models and mechanisms of CD4- versus CD8-lineage choice. *Nature reviews* 8:788-801.
62. Itano, A., and E. Robey. 2000. Highly efficient selection of CD4 and CD8 lineage thymocytes supports an instructive model of lineage commitment. *Immunity* 12:383-389.
63. Wiest, D. L., L. Yuan, J. Jefferson, P. Benveniste, M. Tsokos, R. D. Klausner, L. H. Glimcher, L. E. Samelson, and A. Singer. 1993. Regulation of T cell receptor expression in immature CD4+CD8+ thymocytes by p56lck tyrosine kinase: basis for differential signaling by

- CD4 and CD8 in immature thymocytes expressing both coreceptor molecules. *The Journal of experimental medicine* 178:1701-1712.
64. Itano, A., P. Salmon, D. Kioussis, M. Tolaini, P. Corbella, and E. Robey. 1996. The cytoplasmic domain of CD4 promotes the development of CD4 lineage T cells. *The Journal of experimental medicine* 183:731-741.
65. Yasutomo, K., C. Doyle, L. Miele, C. Fuchs, and R. N. Germain. 2000. The duration of antigen receptor signalling determines CD4⁺ versus CD8⁺ T-cell lineage fate. *Nature* 404:506-510.
66. Brugnera, E., A. Bhandoola, R. Cibotti, Q. Yu, T. I. Guinter, Y. Yamashita, S. O. Sharrow, and A. Singer. 2000. Coreceptor reversal in the thymus: signaled CD4⁺8⁺ thymocytes initially terminate CD8 transcription even when differentiating into CD8⁺ T cells. *Immunity* 13:59-71.
67. Sawada, S., J. D. Scarborough, N. Killeen, and D. R. Littman. 1994. A lineage-specific transcriptional silencer regulates CD4 gene expression during T lymphocyte development. *Cell* 77:917-929.
68. Siu, G., A. L. Wurster, D. D. Duncan, T. M. Soliman, and S. M. Hedrick. 1994. A transcriptional silencer controls the developmental expression of the CD4 gene. *The EMBO journal* 13:3570-3579.
69. Feik, N., I. Bilic, J. Tinhofer, B. Unger, D. R. Littman, and W. Ellmeier. 2005. Functional and molecular analysis of the double-positive stage-specific CD8 enhancer E8III during thymocyte development. *J Immunol* 174:1513-1524.

70. Ellmeier, W., M. J. Sunshine, K. Losos, F. Hatam, and D. R. Littman. 1997. An enhancer that directs lineage-specific expression of CD8 in positively selected thymocytes and mature T cells. *Immunity* 7:537-547.
71. Sarafova, S. D., B. Erman, Q. Yu, F. Van Laethem, T. Guinter, S. O. Sharrow, L. Feigenbaum, K. F. Wildt, W. Ellmeier, and A. Singer. 2005. Modulation of coreceptor transcription during positive selection dictates lineage fate independently of TCR/coreceptor specificity. *Immunity* 23:75-87.
72. Park, J. H., S. Adoro, P. J. Lucas, S. D. Sarafova, A. S. Alag, L. L. Doan, B. Erman, X. Liu, W. Ellmeier, R. Bosselut, L. Feigenbaum, and A. Singer. 2007. 'Coreceptor tuning': cytokine signals transcriptionally tailor CD8 coreceptor expression to the self-specificity of the TCR. *Nature immunology* 8:1049-1059.
73. Yu, Q., J. H. Park, L. L. Doan, B. Erman, L. Feigenbaum, and A. Singer. 2006. Cytokine signal transduction is suppressed in preselection double-positive thymocytes and restored by positive selection. *The Journal of experimental medicine* 203:165-175.
74. Peschon, J. J., P. J. Morrissey, K. H. Grabstein, F. J. Ramsdell, E. Maraskovsky, B. C. Gliniak, L. S. Park, S. F. Ziegler, D. E. Williams, C. B. Ware, J. D. Meyer, and B. L. Davison. 1994. Early lymphocyte expansion is severely impaired in interleukin 7 receptor-deficient mice. *The Journal of experimental medicine* 180:1955-1960.

75. Hernandez-Hoyos, G., M. K. Anderson, C. Wang, E. V. Rothenberg, and J. Alberola-Ila. 2003. GATA-3 expression is controlled by TCR signals and regulates CD4/CD8 differentiation. *Immunity* 19:83-94.
76. Wang, L., K. F. Wildt, J. Zhu, X. Zhang, L. Feigenbaum, L. Tessarollo, W. E. Paul, B. J. Fowlkes, and R. Bosselut. 2008. Distinct functions for the transcription factors GATA-3 and ThPOK during intrathymic differentiation of CD4(+) T cells. *Nature immunology* 9:1122-1130.
77. Nawijn, M. C., R. Ferreira, G. M. Dingjan, O. Kahre, D. Drabek, A. Karis, F. Grosveld, and R. W. Hendriks. 2001. Enforced expression of GATA-3 during T cell development inhibits maturation of CD8 single-positive cells and induces thymic lymphoma in transgenic mice. *J Immunol* 167:715-723.
78. He, X., X. He, V. P. Dave, Y. Zhang, X. Hua, E. Nicolas, W. Xu, B. A. Roe, and D. J. Kappes. 2005. The zinc finger transcription factor Th-POK regulates CD4 versus CD8 T-cell lineage commitment. *Nature* 433:826-833.
79. Sun, G., X. Liu, P. Mercado, S. R. Jenkinson, M. Kypriotou, L. Feigenbaum, P. Galera, and R. Bosselut. 2005. The zinc finger protein cKrox directs CD4 lineage differentiation during intrathymic T cell positive selection. *Nature immunology* 6:373-381.
80. Taniuchi, I., M. Osato, T. Egawa, M. J. Sunshine, S. C. Bae, T. Komori, Y. Ito, and D. R. Littman. 2002. Differential requirements for Runx

proteins in CD4 repression and epigenetic silencing during T lymphocyte development. *Cell* 111:621-633.

81. Sato, T., S. Ohno, T. Hayashi, C. Sato, K. Kohu, M. Satake, and S. Habu. 2005. Dual functions of Runx proteins for reactivating CD8 and silencing CD4 at the commitment process into CD8 thymocytes. *Immunity* 22:317-328.
82. Setoguchi, R., M. Tachibana, Y. Naoe, S. Muroi, K. Akiyama, C. Tezuka, T. Okuda, and I. Taniuchi. 2008. Repression of the transcription factor Th-POK by Runx complexes in cytotoxic T cell development. *Science (New York, N.Y)* 319:822-825.
83. Woolf, E., C. Xiao, O. Fainaru, J. Lotem, D. Rosen, V. Negreanu, Y. Bernstein, D. Goldenberg, O. Brenner, G. Berke, D. Levanon, and Y. Groner. 2003. Runx3 and Runx1 are required for CD8 T cell development during thymopoiesis. *Proceedings of the National Academy of Sciences of the United States of America* 100:7731-7736.
84. Kohu, K., T. Sato, S. Ohno, K. Hayashi, R. Uchino, N. Abe, M. Nakazato, N. Yoshida, T. Kikuchi, Y. Iwakura, Y. Inoue, T. Watanabe, S. Habu, and M. Satake. 2005. Overexpression of the Runx3 transcription factor increases the proportion of mature thymocytes of the CD8 single-positive lineage. *J Immunol* 174:2627-2636.
85. Adachi, S., T. Kuwata, M. Miyaike, and M. Iwata. 2001. Induction of CCR7 expression in thymocytes requires both ERK signal and Ca(2+)

- signal. *Biochemical and biophysical research communications* 288:1188-1193.
86. McCaughy, T. M., M. S. Wilken, and K. A. Hogquist. 2007. Thymic emigration revisited. *The Journal of experimental medicine* 204:2513-2520.
87. Gabor, M. J., D. I. Godfrey, and R. Scollay. 1997. Recent thymic emigrants are distinct from most medullary thymocytes. *European journal of immunology* 27:2010-2015.
88. Matloubian, M., C. G. Lo, G. Cinamon, M. J. Lesneski, Y. Xu, V. Brinkmann, M. L. Allende, R. L. Proia, and J. G. Cyster. 2004. Lymphocyte egress from thymus and peripheral lymphoid organs is dependent on S1P receptor 1. *Nature* 427:355-360.
89. Schwab, S. R., J. P. Pereira, M. Matloubian, Y. Xu, Y. Huang, and J. G. Cyster. 2005. Lymphocyte sequestration through S1P lyase inhibition and disruption of S1P gradients. *Science (New York, N.Y)* 309:1735-1739.
90. Shioh, L. R., D. B. Rosen, N. Brdickova, Y. Xu, J. An, L. L. Lanier, J. G. Cyster, and M. Matloubian. 2006. CD69 acts downstream of interferon-alpha/beta to inhibit S1P1 and lymphocyte egress from lymphoid organs. *Nature* 440:540-544.
91. Feng, C., K. J. Woodside, B. A. Vance, D. El-Khoury, M. Canelles, J. Lee, R. Gress, B. J. Fowlkes, E. W. Shores, and P. E. Love. 2002. A potential role for CD69 in thymocyte emigration. *International immunology* 14:535-544.

92. Carlson, C. M., B. T. Endrizzi, J. Wu, X. Ding, M. A. Weinreich, E. R. Walsh, M. A. Wani, J. B. Lingrel, K. A. Hogquist, and S. C. Jameson. 2006. Kruppel-like factor 2 regulates thymocyte and T-cell migration. *Nature* 442:299-302.
93. Kappler, J. W., N. Roehm, and P. Marrack. 1987. T cell tolerance by clonal elimination in the thymus. *Cell* 49:273-280.
94. Newton, K., A. W. Harris, M. L. Bath, K. G. Smith, and A. Strasser. 1998. A dominant interfering mutant of FADD/MORT1 enhances deletion of autoreactive thymocytes and inhibits proliferation of mature T lymphocytes. *The EMBO journal* 17:706-718.
95. Bouillet, P., J. F. Purton, D. I. Godfrey, L. C. Zhang, L. Coultas, H. Puthalakath, M. Pellegrini, S. Cory, J. M. Adams, and A. Strasser. 2002. BH3-only Bcl-2 family member Bim is required for apoptosis of autoreactive thymocytes. *Nature* 415:922-926.
96. Kuang, A. A., D. Cado, and A. Winoto. 1999. Nur77 transcription activity correlates with its apoptotic function in vivo. *European journal of immunology* 29:3722-3728.
97. Rajpal, A., Y. A. Cho, B. Yelent, P. H. Koza-Taylor, D. Li, E. Chen, M. Whang, C. Kang, T. G. Turi, and A. Winoto. 2003. Transcriptional activation of known and novel apoptotic pathways by Nur77 orphan steroid receptor. *The EMBO journal* 22:6526-6536.
98. Thompson, J., and A. Winoto. 2008. During negative selection, Nur77 family proteins translocate to mitochondria where they associate with Bcl-

- 2 and expose its proapoptotic BH3 domain. *The Journal of experimental medicine* 205:1029-1036.
99. McGargill, M. A., J. M. Derbinski, and K. A. Hogquist. 2000. Receptor editing in developing T cells. *Nature immunology* 1:336-341.
100. Roberts, J. L., S. O. Sharrow, and A. Singer. 1990. Clonal deletion and clonal anergy in the thymus induced by cellular elements with different radiation sensitivities. *The Journal of experimental medicine* 171:935-940.
101. Ramsdell, F., T. Lantz, and B. J. Fowlkes. 1989. A nondeletional mechanism of thymic self tolerance. *Science (New York, N.Y)* 246:1038-1041.
102. Hu, Q., A. Sader, J. C. Parkman, and T. A. Baldwin. 2009. Bim-mediated apoptosis is not necessary for thymic negative selection to ubiquitous self-antigens. *J Immunol* 183:7761-7767.
103. Anderson, M. S., E. S. Venanzi, L. Klein, Z. Chen, S. P. Berzins, S. J. Turley, H. von Boehmer, R. Bronson, A. Dierich, C. Benoist, and D. Mathis. 2002. Projection of an immunological self shadow within the thymus by the aire protein. *Science (New York, N.Y)* 298:1395-1401.
104. Aaltonen, J., P. Björnses, J. Perheentupa, N. Horelli-Kuitunen, A. Palotie, L. Peltonen, S. Y. Lee, F. Francis, S. Henning, C. Thiel, H. Leharach, and M. Yaspo. 1997. An autoimmune disease, APECED, caused by mutations in a novel gene featuring two PHD-type zinc-finger domains. *Nature genetics* 17:399-403.

105. Capone, M., P. Romagnoli, F. Beermann, H. R. MacDonald, and J. P. van Meerwijk. 2001. Dissociation of thymic positive and negative selection in transgenic mice expressing major histocompatibility complex class I molecules exclusively on thymic cortical epithelial cells. *Blood* 97:1336-1342.
106. Allison, J., A. Mullbacher, K. Cox, G. Morahan, R. Boyd, R. Scollay, R. V. Blanden, and J. F. Miller. 1990. Selection of the T-cell repertoire in transgenic mice expressing a transplantation antigen in distinct thymus subsets. *Proceedings* 241:170-178.
107. Goldman, K. P., C. S. Park, M. Kim, P. Matzinger, and C. C. Anderson. 2005. Thymic cortical epithelium induces self tolerance. *European journal of immunology* 35:709-717.
108. Mayerova, D., and K. A. Hogquist. 2004. Central tolerance to self-antigen expressed by cortical epithelial cells. *J Immunol* 172:851-856.
109. Bonomo, A., and P. Matzinger. 1993. Thymus epithelium induces tissue-specific tolerance. *The Journal of experimental medicine* 177:1153-1164.
110. Hoffmann, M. W., W. R. Heath, D. Ruschmeyer, and J. F. Miller. 1995. Deletion of high-avidity T cells by thymic epithelium. *Proceedings of the National Academy of Sciences of the United States of America* 92:9851-9855.
111. Schonrich, G., F. Momburg, G. J. Hammerling, and B. Arnold. 1992. Anergy induced by thymic medullary epithelium. *European journal of immunology* 22:1687-1691.

112. McCaughy, T. M., T. A. Baldwin, M. S. Wilken, and K. A. Hogquist. 2008. Clonal deletion of thymocytes can occur in the cortex with no involvement of the medulla. *The Journal of experimental medicine* 205:2575-2584.
113. Janeway, C. A., P. Travers, M. Walport, and M. J. Schlomchik. 2001. *Immunobiology*. Garland Science, New York.
114. Gallegos, A. M., and M. J. Bevan. 2004. Central tolerance to tissue-specific antigens mediated by direct and indirect antigen presentation. *The Journal of experimental medicine* 200:1039-1049.
115. Wu, L., and K. Shortman. 2005. Heterogeneity of thymic dendritic cells. *Seminars in immunology* 17:304-312.
116. Li, J., J. Park, D. Foss, and I. Goldschneider. 2009. Thymus-homing peripheral dendritic cells constitute two of the three major subsets of dendritic cells in the steady-state thymus. *The Journal of experimental medicine* 206:607-622.
117. Ladi, E., T. A. Schwickert, T. Chtanova, Y. Chen, P. Herzmark, X. Yin, H. Aaron, S. W. Chan, M. Lipp, B. Roysam, and E. A. Robey. 2008. Thymocyte-dendritic cell interactions near sources of CCR7 ligands in the thymic cortex. *J Immunol* 181:7014-7023.
118. Smith, C. A., G. T. Williams, R. Kingston, E. J. Jenkinson, and J. J. Owen. 1989. Antibodies to CD3/T-cell receptor complex induce death by apoptosis in immature T cells in thymic cultures. *Nature* 337:181-184.

119. Swat, W., L. Ignatowicz, H. von Boehmer, and P. Kisielow. 1991. Clonal deletion of immature CD4+8+ thymocytes in suspension culture by extrathymic antigen-presenting cells. *Nature* 351:150-153.
120. Brewer, J. A., O. Kanagawa, B. P. Sleckman, and L. J. Muglia. 2002. Thymocyte apoptosis induced by T cell activation is mediated by glucocorticoids in vivo. *J Immunol* 169:1837-1843.
121. Martin, S., and M. J. Bevan. 1997. Antigen-specific and nonspecific deletion of immature cortical thymocytes caused by antigen injection. *European journal of immunology* 27:2726-2736.
122. Baldwin, T. A., M. M. Sandau, S. C. Jameson, and K. A. Hogquist. 2005. The timing of TCR alpha expression critically influences T cell development and selection. *The Journal of experimental medicine* 202:111-121.
123. Tabrizifard, S., A. Oлару, J. Plotkin, M. Fallahi-Sichani, F. Livak, and H. T. Petrie. 2004. Analysis of transcription factor expression during discrete stages of postnatal thymocyte differentiation. *J Immunol* 173:1094-1102.
124. Egerton, M., K. Shortman, and R. Scollay. 1990. The kinetics of immature murine thymocyte development in vivo. *International immunology* 2:501-507.
125. Terrence, K., C. P. Pavlovich, E. O. Matechak, and B. J. Fowlkes. 2000. Premature expression of T cell receptor (TCR)alphabeta suppresses TCRgammadelta gene rearrangement but permits development of

- gammadelta lineage T cells. *The Journal of experimental medicine* 192:537-548.
126. Hogquist, K. A., T. A. Baldwin, and S. C. Jameson. 2005. Central tolerance: learning self-control in the thymus. *Nature reviews* 5:772-782.
127. Baldwin, T. A., and K. A. Hogquist. 2007. Transcriptional analysis of clonal deletion in vivo. *J Immunol* 179:837-844.
128. Schmitz, I., L. K. Clayton, and E. L. Reinherz. 2003. Gene expression analysis of thymocyte selection in vivo. *International immunology* 15:1237-1248.
129. Zucchelli, S., P. Holler, T. Yamagata, M. Roy, C. Benoist, and D. Mathis. 2005. Defective central tolerance induction in NOD mice: genomics and genetics. *Immunity* 22:385-396.
130. Ishida, Y., Y. Agata, K. Shibahara, and T. Honjo. 1992. Induced expression of PD-1, a novel member of the immunoglobulin gene superfamily, upon programmed cell death. *The EMBO journal* 11:3887-3895.
131. Liang, S. C., Y. E. Latchman, J. E. Buhlmann, M. F. Tomczak, B. H. Horwitz, G. J. Freeman, and A. H. Sharpe. 2003. Regulation of PD-1, PD-L1, and PD-L2 expression during normal and autoimmune responses. *European journal of immunology* 33:2706-2716.
132. Keir, M. E., M. J. Butte, G. J. Freeman, and A. H. Sharpe. 2008. PD-1 and its ligands in tolerance and immunity. *Annual review of immunology* 26:677-704.

133. Barber, D. L., E. J. Wherry, D. Masopust, B. Zhu, J. P. Allison, A. H. Sharpe, G. J. Freeman, and R. Ahmed. 2006. Restoring function in exhausted CD8 T cells during chronic viral infection. *Nature* 439:682-687.
134. Nishimura, H., M. Nose, H. Hiai, N. Minato, and T. Honjo. 1999. Development of lupus-like autoimmune diseases by disruption of the PD-1 gene encoding an ITIM motif-carrying immunoreceptor. *Immunity* 11:141-151.
135. Nishimura, H., T. Okazaki, Y. Tanaka, K. Nakatani, M. Hara, A. Matsumori, S. Sasayama, A. Mizoguchi, H. Hiai, N. Minato, and T. Honjo. 2001. Autoimmune dilated cardiomyopathy in PD-1 receptor-deficient mice. *Science (New York, N.Y)* 291:319-322.
136. Prokunina, L., C. Castillejo-Lopez, F. Oberg, I. Gunnarsson, L. Berg, V. Magnusson, A. J. Brookes, D. Tentler, H. Kristjansdottir, G. Grondal, A. I. Bolstad, E. Svenungsson, I. Lundberg, G. Sturfelt, A. Jonssen, L. Truedsson, G. Lima, J. Alcocer-Varela, R. Jonsson, U. B. Gyllensten, J. B. Harley, D. Alarcon-Segovia, K. Steinsson, and M. E. Alarcon-Riquelme. 2002. A regulatory polymorphism in PDCD1 is associated with susceptibility to systemic lupus erythematosus in humans. *Nature genetics* 32:666-669.
137. Prokunina, L., L. Padyukov, A. Bennet, U. de Faire, B. Wiman, J. Prince, L. Alfredsson, L. Klareskog, and M. Alarcon-Riquelme. 2004. Association of the PD-1.3A allele of the PDCD1 gene in patients with rheumatoid

- arthritis negative for rheumatoid factor and the shared epitope. *Arthritis and rheumatism* 50:1770-1773.
138. Nielsen, C., D. Hansen, S. Husby, B. B. Jacobsen, and S. T. Lillevang. 2003. Association of a putative regulatory polymorphism in the PD-1 gene with susceptibility to type 1 diabetes. *Tissue antigens* 62:492-497.
139. Ishida, M., Y. Iwai, Y. Tanaka, T. Okazaki, G. J. Freeman, N. Minato, and T. Honjo. 2002. Differential expression of PD-L1 and PD-L2, ligands for an inhibitory receptor PD-1, in the cells of lymphohematopoietic tissues. *Immunology letters* 84:57-62.
140. Yamazaki, T., H. Akiba, H. Iwai, H. Matsuda, M. Aoki, Y. Tanno, T. Shin, H. Tsuchiya, D. M. Pardoll, K. Okumura, M. Azuma, and H. Yagita. 2002. Expression of programmed death 1 ligands by murine T cells and APC. *J Immunol* 169:5538-5545.
141. Fife, B. T., I. Guleria, M. Gubbels Bupp, T. N. Eagar, Q. Tang, H. Bour-Jordan, H. Yagita, M. Azuma, M. H. Sayegh, and J. A. Bluestone. 2006. Insulin-induced remission in new-onset NOD mice is maintained by the PD-1-PD-L1 pathway. *The Journal of experimental medicine* 203:2737-2747.
142. Sharpe, A. H., and G. J. Freeman. 2002. The B7-CD28 superfamily. *Nature reviews* 2:116-126.
143. Shlapatska, L. M., S. V. Mikhalap, A. G. Berdova, O. M. Zelensky, T. J. Yun, K. E. Nichols, E. A. Clark, and S. P. Sidorenko. 2001. CD150 association with either the SH2-containing inositol phosphatase or the

- SH2-containing protein tyrosine phosphatase is regulated by the adaptor protein SH2D1A. *J Immunol* 166:5480-5487.
144. Okazaki, T., A. Maeda, H. Nishimura, T. Kurosaki, and T. Honjo. 2001. PD-1 immunoreceptor inhibits B cell receptor-mediated signaling by recruiting src homology 2-domain-containing tyrosine phosphatase 2 to phosphotyrosine. *Proceedings of the National Academy of Sciences of the United States of America* 98:13866-13871.
145. Chemnitz, J. M., R. V. Parry, K. E. Nichols, C. H. June, and J. L. Riley. 2004. SHP-1 and SHP-2 associate with immunoreceptor tyrosine-based switch motif of programmed death 1 upon primary human T cell stimulation, but only receptor ligation prevents T cell activation. *J Immunol* 173:945-954.
146. Keir, M. E., Y. E. Latchman, G. J. Freeman, and A. H. Sharpe. 2005. Programmed death-1 (PD-1):PD-ligand 1 interactions inhibit TCR-mediated positive selection of thymocytes. *J Immunol* 175:7372-7379.
147. Mick, V. E., T. K. Starr, T. M. McCaughtry, L. K. McNeil, and K. A. Hogquist. 2004. The regulated expression of a diverse set of genes during thymocyte positive selection in vivo. *J Immunol* 173:5434-5444.
148. Kieper, W. C., J. T. Burghardt, and C. D. Surh. 2004. A role for TCR affinity in regulating naive T cell homeostasis. *J Immunol* 172:40-44.
149. Blank, C., I. Brown, R. Marks, H. Nishimura, T. Honjo, and T. F. Gajewski. 2003. Absence of programmed death receptor 1 alters thymic

- development and enhances generation of CD4/CD8 double-negative TCR-transgenic T cells. *J Immunol* 171:4574-4581.
150. Nishimura, H., N. Minato, T. Nakano, and T. Honjo. 1998. Immunological studies on PD-1 deficient mice: implication of PD-1 as a negative regulator for B cell responses. *International immunology* 10:1563-1572.
151. Nikolic, T., M. F. de Bruijn, M. B. Lutz, and P. J. Leenen. 2003. Developmental stages of myeloid dendritic cells in mouse bone marrow. *International immunology* 15:515-524.
152. Kisielow, P., H. Bluthmann, U. D. Staerz, M. Steinmetz, and H. von Boehmer. 1988. Tolerance in T-cell-receptor transgenic mice involves deletion of nonmature CD4+8+ thymocytes. *Nature* 333:742-746.
153. Dhanji, S., M. T. Chow, and H. S. Teh. 2006. Self-antigen maintains the innate antibacterial function of self-specific CD8 T cells in vivo. *J Immunol* 177:138-146.
154. Dhanji, S., S. J. Teh, D. Oble, J. J. Priatel, and H. S. Teh. 2004. Self-reactive memory-phenotype CD8 T cells exhibit both MHC-restricted and non-MHC-restricted cytotoxicity: a role for the T-cell receptor and natural killer cell receptors. *Blood* 104:2116-2123.
155. Ebert, P. J., S. Jiang, J. Xie, Q. J. Li, and M. M. Davis. 2009. An endogenous positively selecting peptide enhances mature T cell responses and becomes an autoantigen in the absence of microRNA miR-181a. *Nature immunology* 10:1162-1169.

156. Lo, W. L., N. J. Felix, J. J. Walters, H. Rohrs, M. L. Gross, and P. M. Allen. 2009. An endogenous peptide positively selects and augments the activation and survival of peripheral CD4+ T cells. *Nature immunology* 10:1155-1161.
157. Oehen, S., and K. Brduscha-Riem. 1998. Differentiation of naive CTL to effector and memory CTL: correlation of effector function with phenotype and cell division. *J Immunol* 161:5338-5346.
158. Sharpe, A. H., E. J. Wherry, R. Ahmed, and G. J. Freeman. 2007. The function of programmed cell death 1 and its ligands in regulating autoimmunity and infection. *Nature immunology* 8:239-245.
159. Agata, Y., A. Kawasaki, H. Nishimura, Y. Ishida, T. Tsubata, H. Yagita, and T. Honjo. 1996. Expression of the PD-1 antigen on the surface of stimulated mouse T and B lymphocytes. *International immunology* 8:765-772.
160. Calnan, B. J., S. Szychowski, F. K. Chan, D. Cado, and A. Winoto. 1995. A role for the orphan steroid receptor Nur77 in apoptosis accompanying antigen-induced negative selection. *Immunity* 3:273-282.
161. Liston, A., K. Hardy, Y. Pittelkow, S. R. Wilson, L. E. Makaroff, A. M. Fahrner, and C. C. Goodnow. 2007. Impairment of organ-specific T cell negative selection by diabetes susceptibility genes: genomic analysis by mRNA profiling. *Genome biology* 8:R12.
162. Jeon, M. S., A. Atfield, K. Venuprasad, C. Krawczyk, R. Sarao, C. Elly, C. Yang, S. Arya, K. Bachmaier, L. Su, D. Bouchard, R. Jones, M.

- Gronski, P. Ohashi, T. Wada, D. Bloom, C. G. Fathman, Y. C. Liu, and J. M. Penninger. 2004. Essential role of the E3 ubiquitin ligase Cbl-b in T cell anergy induction. *Immunity* 21:167-177.
163. Harris, J. E., K. D. Bishop, N. E. Phillips, J. P. Mordes, D. L. Greiner, A. A. Rossini, and M. P. Czech. 2004. Early growth response gene-2, a zinc-finger transcription factor, is required for full induction of clonal anergy in CD4+ T cells. *J Immunol* 173:7331-7338.
164. Zha, Y., R. Marks, A. W. Ho, A. C. Peterson, S. Janardhan, I. Brown, K. Praveen, S. Stang, J. C. Stone, and T. F. Gajewski. 2006. T cell anergy is reversed by active Ras and is regulated by diacylglycerol kinase- α . *Nature immunology* 7:1166-1173.
165. Starr, T. K., S. C. Jameson, and K. A. Hogquist. 2003. Positive and negative selection of T cells. *Annual review of immunology* 21:139-176.
166. Fife, B. T., K. E. Pauken, T. N. Eagar, T. Obu, J. Wu, Q. Tang, M. Azuma, M. F. Krummel, and J. A. Bluestone. 2009. Interactions between PD-1 and PD-L1 promote tolerance by blocking the TCR-induced stop signal. *Nature immunology* 10:1185-1192.
167. Walunas, T. L., D. J. Lenschow, C. Y. Bakker, P. S. Linsley, G. J. Freeman, J. M. Green, C. B. Thompson, and J. A. Bluestone. 1994. CTLA-4 can function as a negative regulator of T cell activation. *Immunity* 1:405-413.

168. Strasser, A., H. Puthalakath, L. A. O'Reilly, and P. Bouillet. 2008. What do we know about the mechanisms of elimination of autoreactive T and B cells and what challenges remain. *Immunology and cell biology* 86:57-66.
169. Liu, L., E. Tran, Y. Zhao, Y. Huang, R. Flavell, and B. Lu. 2005. Gadd45 beta and Gadd45 gamma are critical for regulating autoimmunity. *The Journal of experimental medicine* 202:1341-1347.
170. Lu, B., A. F. Ferrandino, and R. A. Flavell. 2004. Gadd45beta is important for perpetuating cognate and inflammatory signals in T cells. *Nature immunology* 5:38-44.
171. Zheng, Y., Y. Zha, and T. F. Gajewski. 2008. Molecular regulation of T-cell anergy. *EMBO reports* 9:50-55.
172. Vanier, L. E., and G. J. Prud'homme. 1992. Cyclosporin A markedly enhances superantigen-induced peripheral T cell deletion and inhibits anergy induction. *The Journal of experimental medicine* 176:37-46.
173. Macian, F., F. Garcia-Cozar, S. H. Im, H. F. Horton, M. C. Byrne, and A. Rao. 2002. Transcriptional mechanisms underlying lymphocyte tolerance. *Cell* 109:719-731.
174. Hsiao, H. W., W. H. Liu, C. J. Wang, Y. H. Lo, Y. H. Wu, S. T. Jiang, and M. Z. Lai. 2009. Deltex1 is a target of the transcription factor NFAT that promotes T cell anergy. *Immunity* 31:72-83.
175. Heissmeyer, V., F. Macian, S. H. Im, R. Varma, S. Feske, K. Venuprasad, H. Gu, Y. C. Liu, M. L. Dustin, and A. Rao. 2004. Calcineurin imposes T

cell unresponsiveness through targeted proteolysis of signaling proteins.
Nature immunology 5:255-265.

176. Safford, M., S. Collins, M. A. Lutz, A. Allen, C. T. Huang, J. Kowalski, A. Blackford, M. R. Horton, C. Drake, R. H. Schwartz, and J. D. Powell. 2005. Egr-2 and Egr-3 are negative regulators of T cell activation. *Nature immunology* 6:472-480.
177. Oestreich, K. J., H. Yoon, R. Ahmed, and J. M. Boss. 2008. NFATc1 regulates PD-1 expression upon T cell activation. *J Immunol* 181:4832-4839.
178. Sheppard, K. A., L. J. Fitz, J. M. Lee, C. Benander, J. A. George, J. Wooters, Y. Qiu, J. M. Jussif, L. L. Carter, C. R. Wood, and D. Chaudhary. 2004. PD-1 inhibits T-cell receptor induced phosphorylation of the ZAP70/CD3zeta signalosome and downstream signaling to PKCtheta. *FEBS letters* 574:37-41.
179. Wong, P., A. W. Goldrath, and A. Y. Rudensky. 2000. Competition for specific intrathymic ligands limits positive selection in a TCR transgenic model of CD4+ T cell development. *J Immunol* 164:6252-6259.

Appendix I: shRNA knock-down of Bim isoforms

Introduction

Bcl-2 interacting mediator of cell death (Bim (Bcl2l11)) is a proapoptotic member of the Bcl-2 family. It is essential for clonal deletion of self-reactive thymocytes in negative selection (1). Alternative splicing creates different isoforms. The 3 main isoforms are Bim extra long (Bim_{EL}), Bim long (Bim_L), and Bim short (Bim_S) (2). Bim_{EL}, the most abundant of the isoforms, is the least potent and can be phosphorylated post-translationally by the MAPKs ERK and JNK (3). Bim_L is more abundant and potent than Bim_{EL} and can be regulated by JNK phosphorylation (3). Bim_S is the least abundant and most potent isoform and is not thought to be subject to post-translational regulation (3). The relative proapoptotic potency of the different isoforms is thought to be due to phosphorylation. The importance of the individual isoforms in clonal deletion is unknown, and the objective of this project is to determine the relevance of each isoform by using shRNAs to knock-down individual isoforms. Three different types of shRNAs are needed. One to knock-down all the isoforms of Bim (Bim_{pan}), one to knock down Bim_{EL}, allowing expression of only the Bim_L and Bim_S isoforms, and one to knock-down Bim_{EL} and Bim_L, allowing expression of the Bim_S isoform only. These shRNAs will be expressed via a lentivirus vector. Lentiviral-transduced HY^{cd4}M BM will be injected into an irradiated recipient and clonal deletion in the absence of the various isoforms will be examined.

Materials and Methods

shRNA design and cloning

The shRNAs were constructed using the cloning strategy found on the Tronolab website (http://tronolab.epfl.ch/webdav/site/tronolab/shared/protocols/cloning_strategies.html) (**Fig 1A**) to target specific isoforms of Bim (**Fig 2**). The sequences of the shRNAs are listed in **Table 1**. The shRNAs were cloned into the pLVTHM plasmid downstream of the H1 polymerase III promoter, between the MluI and ClaI restriction enzyme sites (**Fig 1B**). pLVTHM containing shRNAs were cloned into Escherichia coli DH5 α and screened for the presence of recombinant plasmid. The presence of the shRNA was confirmed by sequencing. See **Table 2** for shRNAs not yet tested.

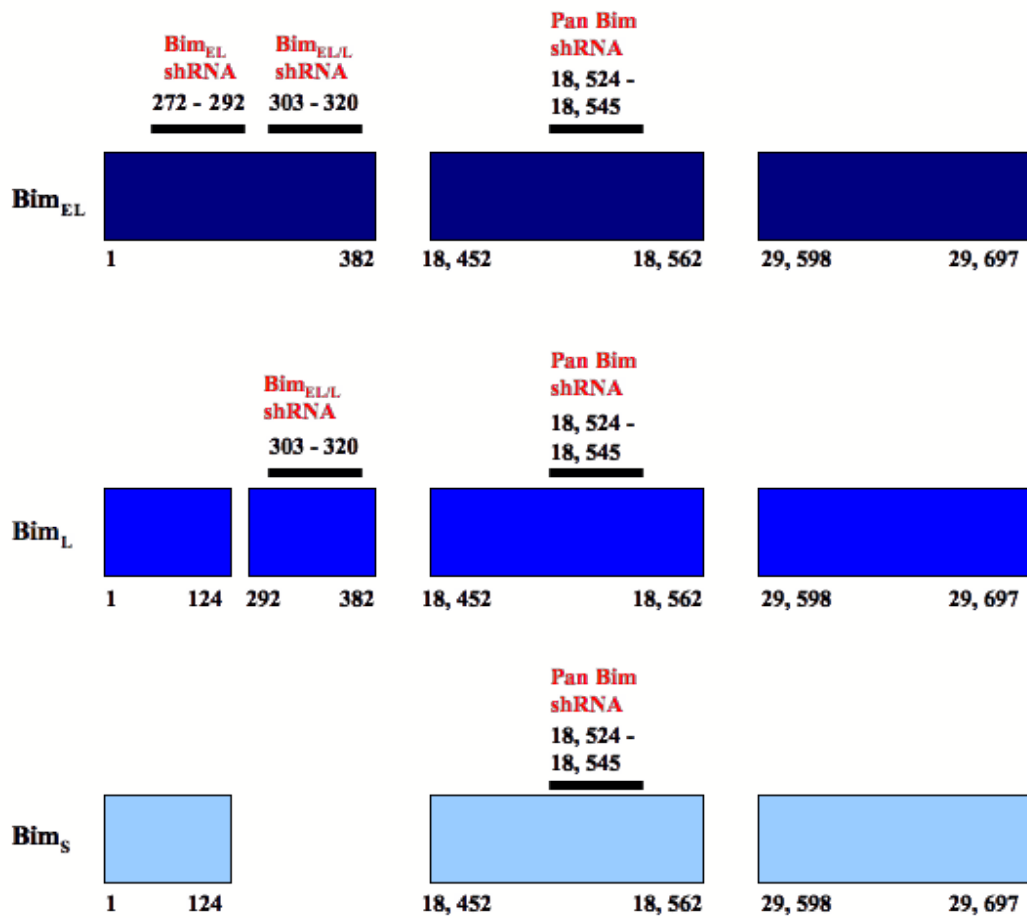


Figure 2: Alternative splicing of the Bcl2l11 gene produces Bim_{EL}, Bim_L, and Bim_S isoforms. shRNAs used (see Table 1) are indicated. Pan Bim shRNA targets all three isoforms, Bim_{EL/L} shRNA targets Bim_{EL} and Bim_L isoforms, and Bim_{EL} shRNA targets the Bim_{EL} isoform only. Numbers refer to base pairs within the genomic sequence.

Table 1: Sequences of shRNAs used. MluI and ClaI restriction enzyme sites indicated in red and purple, respectively, hairpin loop indicated in green, transcription termination signal indicated in blue. Target refers to base pairs within genomic sequence (see **Fig 2**).

Name	Sequence (5' to 3')	Target	Reference
MluI-panBim-ClaI-A	CGCGTCCCCGGATCGGAGACGAGTTCAACGTTCAA GAGACGTTGAACTCGTCTCCGATCCTTTTGGAAAT	18,524- 18,545	
MluI-panBim-ClaI-B	CGATTTCCAAAAAGGATCGGAGACGAGTTCAACGT CTCTTGAACTGAACTCGTCTCCGATCCGGGGA	18,524- 18,545	
MluI-BimEL1-ClaI-A	CGCGTCCCCGGTATTTCTCTTTTGACACAGTTCAAGAG ACTGTGTCAAAGAGAAATACCTTTTGGAAAT	272-292	(4)
MluI-BimEL1-ClaI-B	CGATTTCCAAAAAGGTATTTCTCTTTTGACACAGTCTC TTGAACTGTGTCAAAGAGAAATACCGGGGA	272-292	(4)
MluI-BimEL/L-ClaI-A	CGCGTCCCCCAGCACCCATGAGTTGTGATTCAAGAG ATCACAACATCATGGGTGCTGTTTTGGAAAT	303-320	(5)
MluI-BimEL/L-ClaI-B	CGATTTCCAAAAACAGCACCCATGAGTTGTGATCTC TTGAATCACAACATCATGGGTGCTGGGGGA	303-320	(5)

Table 2: Sequences of shRNAs to be tested. MluI and ClaI restriction enzyme sites indicated in red and purple, respectively, hairpin loop indicated in green, transcription termination signal indicated in blue. Target refers to base pairs within genomic sequence (see **Fig 2**).

Name	Sequence (5' to 3')	Target
MluI-panBim_2-ClaI-A	CGCGTCCCCTGACAGAGAAGGTGGACAATCAAGAG ATTGTCCACCTTCTCTGTCATTTTGGAAAT	36-54
MluI-panBim_2-ClaI-B	CGATTTCCAAAAATGACAGAGAAGGTGGACAATCTC TTGAATTGTCCACCTTCTCTGTCCAGGGGA	36-54
MluI-panBim_3-ClaI-A	CGCGTCCCCGAGACGAGTTCAACGAAATCAAGAG ATTCGTTGAACTCGTCTCCTTTTGGAAAT	18, 529-18, 549
MluI-panBim_3-ClaI-B	CGATTTCCAAAAAGGAGACGAGTTCAACGAAATCTC TTGAATTT CGTTGAACTCGTCTCCGGGGA	18, 529-18, 549
MluI-panBim_4-ClaI-A	CGCGTCCCCAAGGAGGGTGTGTTGCAAATCAAGAG ATTTGCAAACACCCTCCTGTTTTGGAAAT	18, 554-18, 562, 29, 598- 29, 609
MluI-panBim_4-ClaI-B	CGATTTCCAAAAACAAGGAGGGTGTGTTGCAAATCTCT TGAATTTGCAAACACCCTCCTGGGGGA	18, 554-18, 562, 29, 598- 29, 609
MluI-EL/L_2-ClaI-A	CGCGTCCCCGCACCCATGAGTTGTGACATCAAGAGA TGCACAACATCATGGGTGCTTTTTGGAAAT	304-323
MluI-EL/L_2-ClaI-B	CGATTTCCAAAAAGCACCCATGAGTTGTGACATCTCT TGAATGTCACAACATCATGGGTGCGGGGA	304-323
MluI-EL_3-ClaI-A	CGCGTCCCCAGGTAATCCCGACGGCGAATCAAGAG ATTCGCCGTCGGGATTACCTTTTTGGAAAT	123-141
MluI-EL_3-ClaI-B	CGATTTCCAAAAAGGTAATCCCGACGGCGAATCTCT TGAATTCGCCGTCGGGATTACCTGGGGA	123-141
MluI-EL_4-ClaI-A	CGCGTCCCCGGGTATTTCTCTTTTGACATCAAGAGA TGTCAAAGAGAAATACCCTTTTGGAAAT	271-289
MluI-EL_4-ClaI-B	CGATTTCCAAAAAGGGTATTTCTCTTTTGACATCTCTT GAATGTCAAAGAGAAATACCCGGGGA	271-289

Lentivirus production

Lentiviral vectors were generated in 293T cells as per the following protocol. 2.5×10^6 293T cells were cultured per 100mm plate, with 2 plates for each construct. The following day, the cells were transfected by using calcium-phosphate precipitation. 20 μ g of the transfer vector (pLVTHM with shRNA cloned in), 15 μ g of psPax2 (the packaging plasmid), 6 μ g of pMD2.G (the envelope plasmid) were mixed together. Water was added to 0.5mL, then 0.5mL of 2X HBS (280 mM NaCl, 10.2 mM KCl, 1.4 mM Na₂HPO₄, 42 mM Hepes, and 11.1 mM glucose), and 20 μ L of 2.5M CaCl₂ was added. The solution was then incubated at room temperature for 25 min and then added to the 293T cells. Media was changed to serum-free opti-MEM 7h later. Two days later the media was collected, spun down at 3,000 rpm for 5 min at room temperature and filtered through a 0.22 μ m filter. The lentiviral constructs were then titrated as described by the Tronolab protocol (http://tronolab.epfl.ch/webdav/site/tronolab/shared/protocols/protocols_LVtitration.html) except that 50,000 cells were plated out and cells were transduced with lentivirus by 1:6 serial dilutions. Lentiviral concentrations were determined by examining the serial dilutions for GFP expression and calculated using dilutions where 1-10% of the cells are GFP⁺.

Cell culture

293T cells were obtained from Dr. Tom Hobman (University of Alberta) and were cultured in DM10 (DMEM + 10% FCS + 5mM HEPES + 50U(mg)/mL

penicillin/streptomycin + 2mM L-glutamine + 50mM 2-mercaptoethanol + 50mg/mL gentamicin sulfate). EL4 hCAR cells were obtained from Dr. James DeGregori (University of Colorado) and were cultured in RP10 (RPMI + 10% FCS + 5mM HEPES + 50U(mg)/mL penicillin/streptomycin + 2mM L-glutamine + 50mM 2-mercaptoethanol + 50mg/mL gentamicin sulfate). NIH 3T3 were obtained from Dr. Hanne Ostergaard (University of Alberta) and were cultured in RP10.

Flow cytometry

EL4, 293T, and NIH 3T3 cells infected with lentivirus expressing pLVTHM + shRNAs were harvested, resuspended in FACS buffer (PBS, 1% FBS, 0.02% sodium azide (pH 7.2)) and cell events collected with a FACS Calibur or FACS Canto to determine GFP expression. For Bim staining, cells were fixed with the BD Cytofix/Cytoperm™ Fixation/Permeabilization Kit, stained at 1:200 with anti-Bim_{S/EL/L} (10B12, Alexis Biochemicals), washed twice with FACS buffer, and stained at 1:200 with anti-rat antibody (Invitrogen). Cell events were collected using FACS Canto and FlowJo software was used for data analysis.

RT-PCR

The following primers were used: Bim_Pan_JP-F1 (CGAGTTCAACGAAACTT ACACAA), Bim_Pan_JP-R2 (TCAATGCCTTCTCCATACCA), Baldwin/BimEL-F1(CGGTCCTCCAGTGGGTATTT), Baldwin/BimEL-R1

(AGGACTTGGGGTTTGTGTTG), Baldwin/BimL-F1 (ACAGAACCGCAAGA CAGGAG), Baldwin/BimL-R1 (GCACTG AGATAGTGGTTGAAGG), Baldwin/BimS-F1 (CCTTCTGATGTAAGTTCTGAGTG TG), Baldwin/BimS-R1 (ATGGAAGCTTGCGGTTCTGTC), Baldwin/Nur77-L1 (GGCATGGTGAA GGAAGTTGT), and Baldwin/Nur77-R1 (TGAGGGAAGTGAGAAGATTGGT).

RNA was extracted from 293T and NIH 3T3 cells transfected with pLVTHM + shRNAs using the Qiagen RNeasy Mini kit and cDNA was synthesized using the SuperScript III first-strand cDNA synthesis kit (Invitrogen). Quantitative RT-PCR was performed using the Power SYBR Green kit (Applied Biosystems) and the 7900 HT Fast real-time PCR system (Applied Biosystems) or the Eppendorf Mastercycler[®] ep realplex² S. Relative gene expression levels were determined via the $\Delta\Delta$ cycle threshold (C_T) method with uninfected NIH 3T3 cells as the reference population and β -actin as the reference gene.

Western Blot

Cells were lysed in 1% Triton X-100 in PBS, and 1×10^6 cell equivalents were loaded into a 12% resolving SDS-PAGE gel. The gel ran at 150V and was then transferred to an Immobilon P membrane overnight at 30V. The membrane was blocked for 8h in 5% skim milk. The membrane was blotted with Bim/BOD polyclonal antibody (Assay Designs) diluted 1:4,000 in 5% skim milk overnight at 4 °C. The blot was washed 5 times for 5min each in TBS-T and then blotted

with HRP-conjugated goat-anti-rabbit (Jackson ImmunoResearch) diluted 1:10,000 in 5% skin milk for 3h at room temperature. The blot was again washed, then developed using SuperSignal® West Pico Chemiluminescent Substrate (ThermoScientific) and a KODAK M35A X-OMAT Processor. The membrane was incubated in a 55 °C water bath with stripping buffer (0.1M β -mercaptoethanol, Tris pH 6.8, 2% SDS) for 30 min and then re-probed as described above with anti-calnexin (Cell Signaling) at 1:4,000 or 1:10,000 overnight, and HRP-conjugated goat-anti-rabbit (Jackson ImmunoResearch) at 1:10 000 for 2h.

Results

Infection efficiency of EL4, 293T, and NIH 3T3 cells

EL4 cells were infected with the lentiviral constructs at multiplicities of infection (m.o.i.s) of 1, 5 and 15. Five days later, flow cytometry was performed to examine infection by GFP expression and cell lysates were prepared for western blot. There were very few GFP⁺ cells, even at a m.o.i. of 15, indicating that EL4 cells were not being readily infected (**Fig 3**). Next, we tested infection of 293T cells. Again, five days following infection with lentivirus a low percentage of GFP⁺ cells were observed. Therefore, we doubly infected 293T cells by infecting at a m.o.i. of 15 on day one and a m.o.i. of 11 the following day. Four days later, 80.7% of the cells infected with lentivirus expressing Pan Bim shRNA were GFP⁺, 77.2% of the cells infected with lentivirus expressing Bim_{EL/L} shRNA were GFP⁺, and 81.9% of the cells infected with lentivirus expressing Bim_{EL} shRNA were GFP⁺ (**Fig 4**). GFP⁺ cells were purified by FACS and put back into culture. One week later, cells infected with lentivirus expressing Pan Bim shRNA were 77.5% GFP⁺, cells infected with lentivirus expressing Bim_{EL/L} shRNA were 79.9% GFP⁺, and cells infected with lentivirus expressing Bim_{EL} shRNA were 83.7% GFP⁺. Five days later cells infected with lentivirus expressing Pan Bim shRNA were 77% GFP⁺, cells infected with lentivirus expressing Bim_{EL/L} shRNA were 83% GFP⁺, and cells infected with lentivirus expressing Bim_{EL} shRNA were 85.5% GFP⁺. Cell lysates from these stably expressing cell lines were utilized for western blot and RNA was extracted for RT-PCR. Since the lentivirus is

replication defective, the infected cells were stably transduced and did not appear to be at a competitive disadvantage with respect to survival or proliferation.

Although 293T cells can be infected with the lentivirus, they are a human cell line and the shRNAs target murine Bim. Therefore, NIH 3T3 cells, a mouse fibroblast cell line, were infected. NIH 3T3 cells were infected with lentivirus expressing Pan Bim shRNA and Bim_{EL} shRNA at a m.o.i. of 15 two days in a row. One week later, cells infected with lentivirus expressing Pan Bim shRNA were 67.9% GFP⁺, and cells infected with lentivirus expressing Bim_{EL} shRNA were 80.2% GFP⁺. After two weeks, cells were 65.4% GFP⁺ and 78.1% GFP⁺, respectively. After three weeks, GFP⁺ cells were purified by FACS and RNA was extracted for RT-PCR.

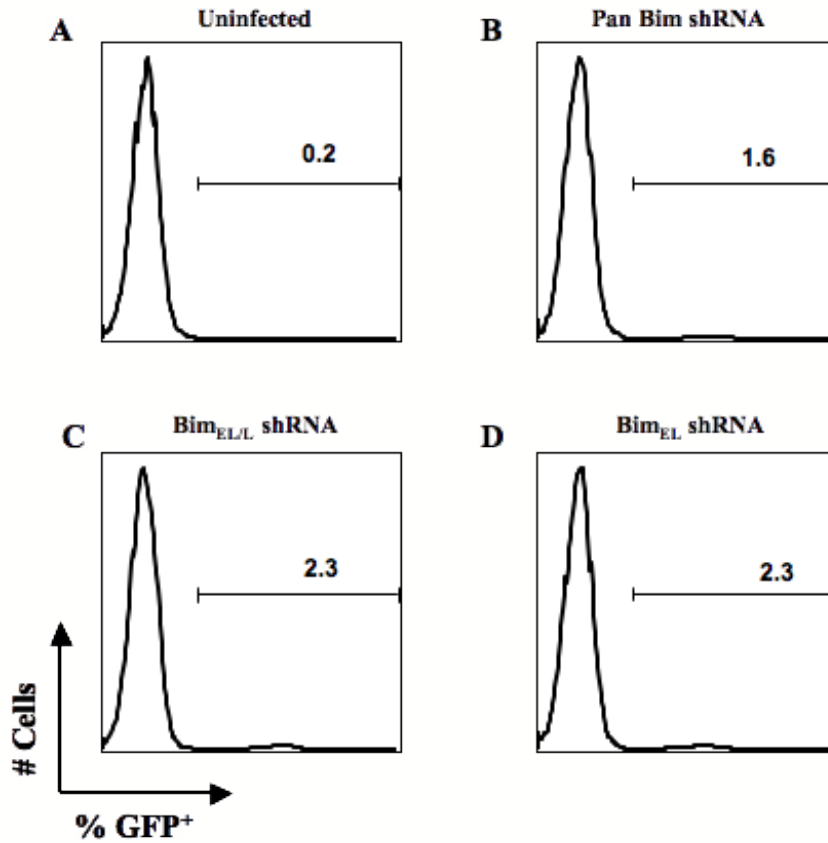


Figure 3: The lentivirus does not infect EL4 cells. A) uninfected. B) lentivirus expressing Pan Bim shRNA C) lentivirus expressing Bim_{EL/L} shRNA, D) lentivirus expressing Bim_{EL} shRNA. Multiplicity of infection (m.o.i.) is 15 for all infections. Expression of shRNAs is indicated by GFP expression.

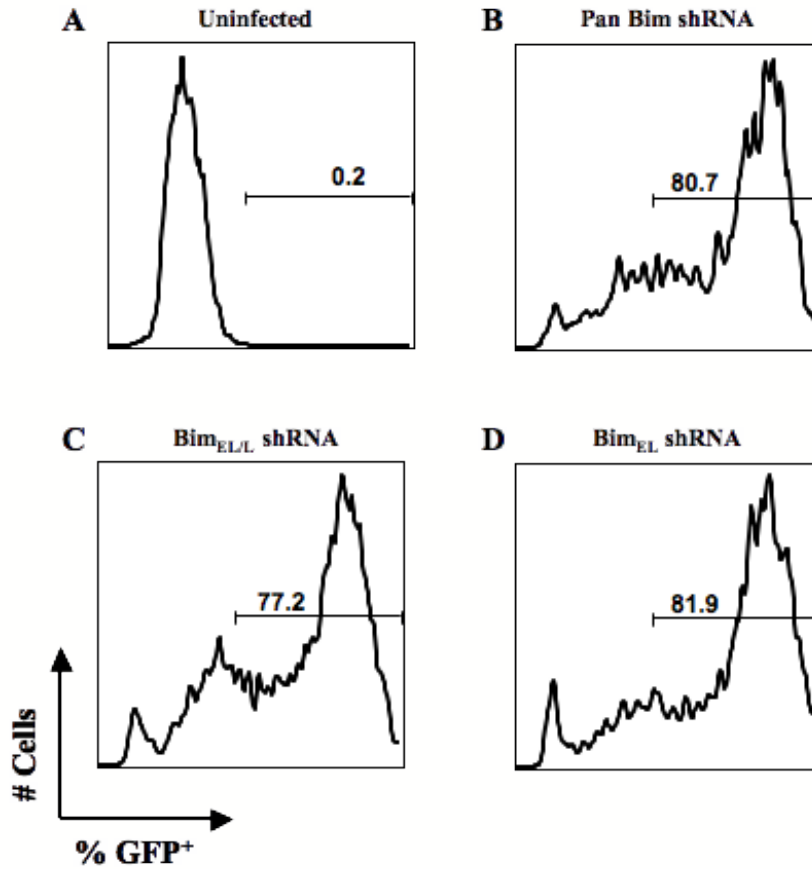


Figure 4: Double infections of 293T cells. A) uninfected. B) lentivirus expressing Pan Bim shRNA C) lentivirus expressing Bim_{EL/L} shRNA, D) lentivirus expressing Bim_{EL} shRNA. Multiplicity of infection (m.o.i.) is 15 for first injection, m.o.i.= 11 for second infection. Cells harvested and stained after 4 days in culture Expression of shRNAs is indicated by GFP expression.

Evaluation of knock-down by intracellular staining

Knock-down of Bim in infected NIH 3T3 cells was examined by intracellular staining for Bim using an antibody that recognizes all Bim isoforms. In one experiment, cells infected with lentivirus expressing the Pan Bim shRNA expressed 29% less Bim than the uninfected cells, while cells infected with lentivirus expressing the Bim_{EL} shRNA expressed more Bim than the uninfected cells (**Fig 5A**). However, a later experiment showed 14.5% and 7.8% knock-down in cells expressing Pan Bim shRNA and Bim_{EL} shRNA, respectively (**Fig 5B**). Thus, it appears that Pan Bim shRNA may be able to reduce Bim expression, and Bim_{EL} shRNA may be knocking-down Bim_{EL}. However, using this strategy, it is impossible to know which Bim isoform is being knocked down in this experiment, and consistent results were not obtained.

In both experiments, 97-99% of the cells were GFP⁺. This demonstrates that a high percentage of GFP⁺ cells does not correlate with a large amount of knock-down. This could be because shRNAs provide variably efficiency of knock-down. It could also be because expression of GFP does not necessarily equal expression of the shRNAs.

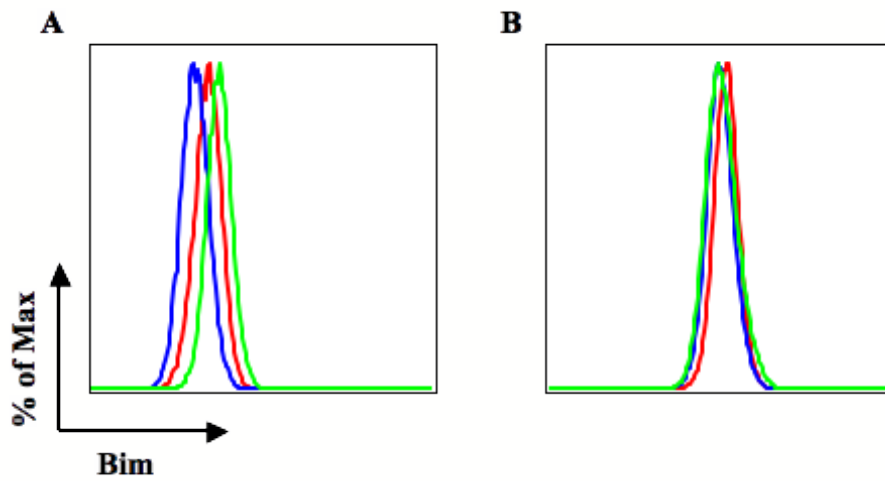


Figure 5: Bim knock-down in infected NIH 3T3 cells. Red = uninfected, blue = infected with lentivirus expressing Pan Bim shRNA, green = infected with lentivirus expressing Bim_{EL} shRNA. A) and B) are from two separate experiments.

Evaluation of knock-down by Western Blot

Bim_{EL} is only isoform that can be visualized by western blot in 293T cells (**Fig 6**).

In one experiment it appeared that Pan Bim shRNA was knocking down Bim_{EL}

but that Bim_{EL/L} shRNA and Bim_{EL} shRNA are not knocking down Bim_{EL} (**Fig**

6A). However, a subsequent western blot showed no Bim knock-down for any of

the shRNAs tested (**Fig 6B**).

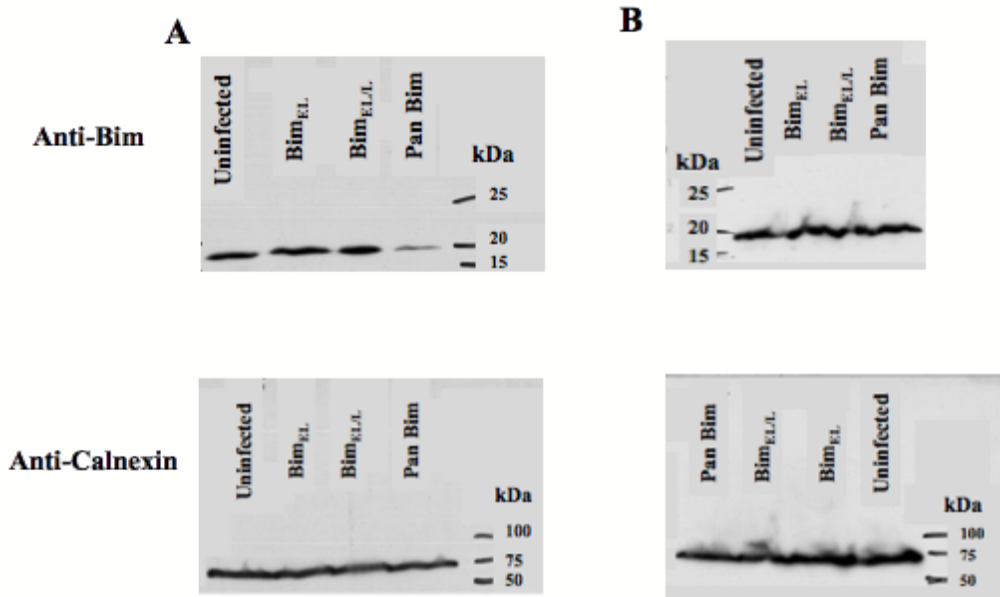


Figure 6: Western Blot of Bim knock-down in 293T infected cells. A) Top: Primary antibody = anti-Bim at 1:4000 overnight. Secondary antibody = goat anti-rabbit at 1:10 000 for 3h. Exposed for 10s. Bottom: Primary antibody = anti-calnexin at 1:4000 overnight. Secondary antibody = goat anti-rabbit at 1:10 000 for 2h. Exposed for 3s. B) Top: Same as in (A). Bottom: Primary antibody = anti-calnexin at 1:10 000 overnight. Secondary antibody = goat anti-rabbit at 10 000 for 2h. Exposed for 5s.

Evaluation of knock-down by RT-PCR

To examine the amount of Bim transcript in the knock-down cell lines, RT-PCR was performed on cDNA generated from RNA isolated from NIH 3T3 cells infected with lentivirus expressing Pan Bim and Bim_{EL} shRNAs. Gene expression is displayed relative to expression in uninfected NIH 3T3 cells. Expression of Pan Bim shRNA and Bim_{EL} shRNA both decreased total expression of the Bim isoforms, with more decreased expression observed with Pan Bim shRNA (**Fig 7A**). This indicates that both Pan Bim and Bim_{EL} shRNAs are knocking-down Bim to some extent. A similar trend is observed when expression of the Bim_{EL} isoform is specifically examined (**Fig 7B**). As expected, Pan Bim shRNA appears to knock-down Bim_{EL}, Bim_L, and Bim_S (**Fig 7 B,C,D**). However, expression of Bim_{EL} shRNA also decreases expression of the Bim_L isoform in one experiment, indicating that the Bim_{EL} shRNA may not be specifically targeting Bim_{EL} (**Fig 7C**).

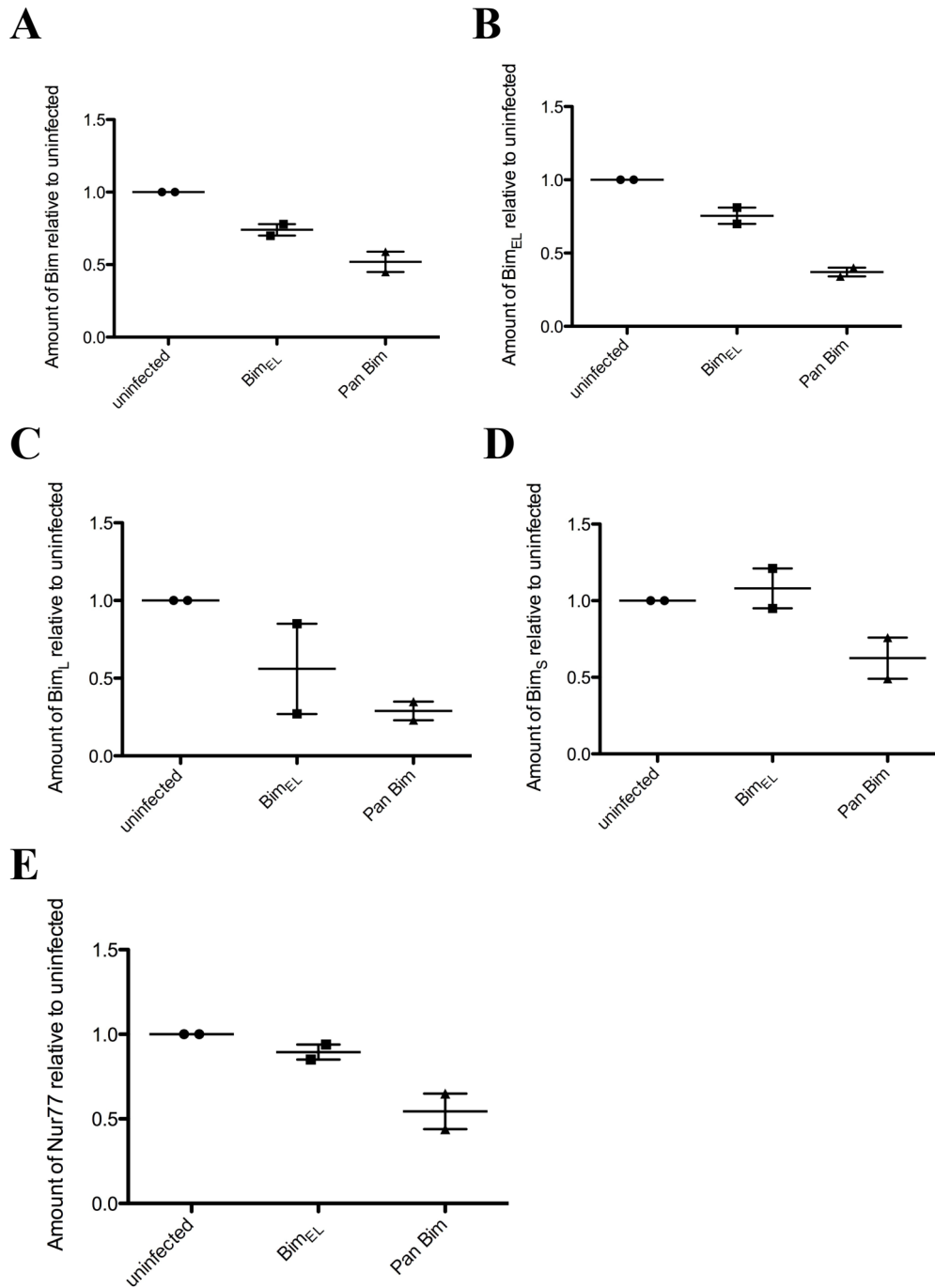


Figure 7: Nonspecific knock-down by Bim shRNAs. RNA was extracted from uninfected NIH 3T3 cells and NIH 3T3 cells infected with lentivirus expressing Bim_{EL} and Pan Bim shRNA. Knock-down of A) all isoforms of Bim, B) Bim_{EL}, C) Bim_L, D) Bim_S, and E) Nur77 relative to uninfected cells.

Discussion

The shRNAs appear to be knocking down Bim isoforms non-specifically. This is puzzling, as the shRNAs should be isoform specific (**Fig 2**). However, although some of the shRNAs were designed from published siRNA sequences, the same sequence may not knock-down when expressed as part of a hairpin. Often many shRNAs are tested before successful knock-down is obtained and many more shRNAs will be tested (**Table 2**). The ability to knock-down individual isoforms of Bim will be very useful in determining the role of Bim in negative selection.

Literature Cited

1. Bouillet, P., J. F. Purton, D. I. Godfrey, L. C. Zhang, L. Coultas, H. Puthalakath, M. Pellegrini, S. Cory, J. M. Adams, and A. Strasser. 2002. BH3-only Bcl-2 family member Bim is required for apoptosis of autoreactive thymocytes. *Nature* 415:922-926.
2. O'Connor, L., A. Strasser, L. A. O'Reilly, G. Hausmann, J. M. Adams, S. Cory, and D. C. Huang. 1998. Bim: a novel member of the Bcl-2 family that promotes apoptosis. *The EMBO journal* 17:384-395.
3. Ley, R., K. E. Ewings, K. Hadfield, and S. J. Cook. 2005. Regulatory phosphorylation of Bim: sorting out the ERK from the JNK. *Cell death and differentiation* 12:1008-1014.
4. Becker, E. B., J. Howell, Y. Kodama, P. A. Barker, and A. Bonni. 2004. Characterization of the c-Jun N-terminal kinase-BimEL signaling pathway in neuronal apoptosis. *J Neurosci* 24:8762-8770.
5. Abrams, M. T., N. M. Robertson, K. Yoon, and E. Wickstrom. 2004. Inhibition of glucocorticoid-induced apoptosis by targeting the major splice variants of BIM mRNA with small interfering RNA and short hairpin RNA. *The Journal of biological chemistry* 279:55809-55817.

Appendix II: Id3, Runx3, and CCR7 gene expression in HY^{cd4}M and HY^{cd4}F Bim sufficient and deficient thymocytes¹

Materials and Methods

Cell Sorting

Cells were stained for cell surface antigens at 20 X 10⁶ cells/mL in FACS buffer. HY^{cd4}F T3.70⁺CD4⁺CD8⁺CD69⁺, HY^{cd4}F T3.70⁺CD8⁺CD69⁺, HY^{cd4}M T3.70⁺CD4⁺CD8⁺CD69⁺, HY^{cd4}F Bim^{-/-} T3.70⁺CD4⁺CD8⁺CD69⁺, and HY^{cd4}M Bim^{-/-} T3.70⁺CD4⁺CD8⁺CD69⁺ thymocytes were purified on the FACS Aria.

Quantitative reverse-transcriptase PCR

Total RNA was isolated using the Qiagen RNeasy Mini kit and cDNA was synthesized using the SuperScript III first-strand cDNA synthesis kit (Invitrogen). Quantitative RT-PCR was performed using the Power SYBR Green kit (Applied Biosystems) and the 7900 HT Fast real-time PCR system (Applied Biosystems). Gene expression is given as a percentage of β -actin expression. The following primer sequences were used. β -actin: forward: 5'CTAAGGCCAACCGTGAA AAG-3', reverse: 5'-ACCAGAGGCATACAGGGACA-3', Id3: forward: 5'-TGT

¹ A version of this chapter has been published. Hu, Q., A. Sader, J. C. Parkman, and T. A. Baldwin. 2009. Bim-mediated apoptosis is not necessary for thymic negative selection to ubiquitous self-antigens. *J Immunol* 183:7761-7767.

CATAGACTACATCCTCGACCTT-3', reverse: 5'-GCAAAAGCTCCTCTTGT
CCTT-3', Runx3: forward: 5'-ACCGTGTTACCAACCCTAC-3', reverse: 5'-
GCCTT GGTCTGGTCTTCTATCT-3', CCR7: forward: 5' – CAGGGAAACCCA
GGAAAAAC – 3', reverse: 5' – CCTCATCTTGGCAGA AGCAC – 3'.

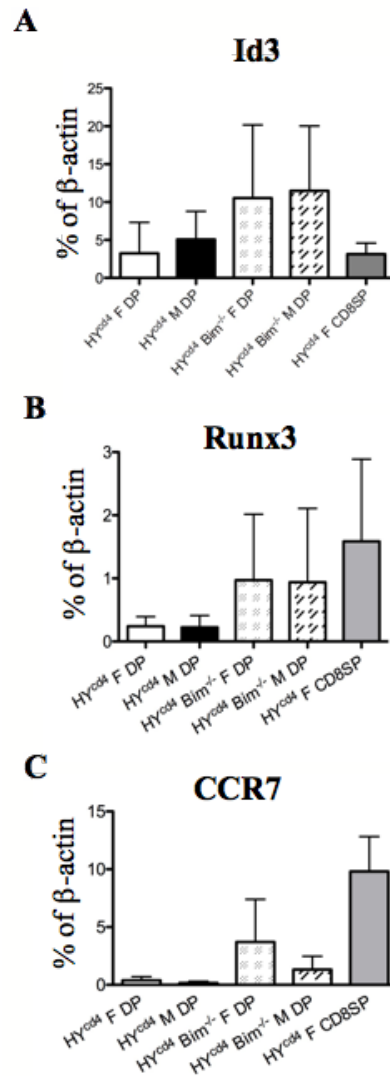


Figure 1: Expression of Id3, Runx3, and CCR7 in Bim sufficient and deficient thymocytes. Expression of Id3 (A), Runx3 (B), and CCR7 (C) in HY^{cd4}F DP, HY^{cd4}M DP, HY^{cd4}F Bim^{-/-} DP, HY^{cd4}M Bim^{-/-} DP, and HY^{cd4}F CD8SP thymocytes populations, as determined by RT-PCR. Expression is given as a percentage of β -actin expression. n=4 for all populations.

Acknowledgements

Alyssa Sader and Troy A. Baldwin performed the cell sorting and RNA extraction.